博士論文

Functional analysis of P450 monooxygenases responsible for production of highly functional secondary metabolites in Actinomycetes

（放線菌二次代謝産物の高機能化を司る P450 モノオキシゲナーゼの機能解明）

手島 愛子

広島大学大学院先端物質科学研究科

2021 年 3 月

目次

1. 主論文

Functional analysis of P450 monooxygenases responsible for production of highly functional secondary metabolites in Actinomycetes
(放線菌二次代謝産物の高機能化を司る P450 モノオキシゲナーゼの機能解明)
手島 愛子

2. 公表論文

(1) Functional analysis of P450 monooxygenase SrrO in the biosynthesis of butenolide-type signaling molecules in *Streptomyces rochei*
Aiko Teshima, Nozomi Hadae, Naoto Tsuda, and Kenji Arakawa
Biomolecules, 10(9), 1237 (2020).
DOI : 10.3390/biom10091237

(2) Substrate specificity of two cytochrome P450 monooxygenases involved in lankamycin biosynthesis
Aiko Teshima, Hisashi Kondo, Yu Tanaka, Yosi Nindita, Yuya Misaki, Yuji Konaka, Yasuhiro Itakura, Tsugumi Tonokawa, Haruyasu Kinashi, and Kenji Arakawa
Bioscience, Biotechnology, and Biochemistry, 85(1), 115-125 (2021).
DOI : 10.1093/bbb/zbaa063

3. 参考論文

(1) The genome sequence of *Streptomyces rochei* 7434AN4, which carries a linear chromosome and three characteristic linear plasmids.
Yosi Nindita, Zhisheng Cao, Amirudin Akhmad Fauzi, Aiko Teshima, Yuya Misaki, Rukman Muslimin, Yingjie Yang, Yuh Shiwa, Hirofumi Yoshikawa, Michihira Tagami, Alexander Lezhava, Jun Ishikawa, Makoto Kuroda, Tsuyoshi Sekizuka, Kuninobu Inada, Haruyasu Kinashi, and Kenji Arakawa
Scientific Reports, 9, 10973 (2019).
DOI : 10.1038/s41598-019-47406-y

主論文

Contents

General introduction

Secondary metabolites including antibiotics are assembled by multiple enzymes that coordinate their unique structures with a variety of biological activities. The cytochrome P450 enzymes (P450s) form a superfamily of heme-containing enzymes that are responsible for oxidation of secondary metabolites (Figure 1) [**1**]. They are widely spread in all Kingdom including animals, fungi, bacteria, and plants.

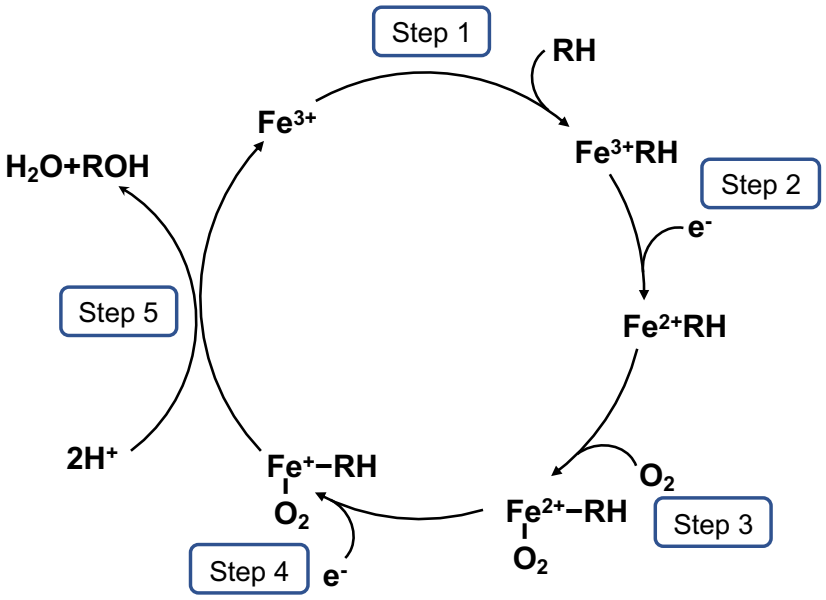

Figure 1. The catalytic cycle of cytochrome P450 [1]. Fe^{3+}: Heme iron in oxidized P450 (trivalent ion), Fe^{2+}: Heme iron in reduced P450 (divalent ion), RH : substrate, ROH : hydroxylated substrate (reaction product). Step 1; Binding of substrate to active site, changes the conformation of the enzyme. Step 2; Transfer of an electron from NAD(P)H. Step 3; Binding of O_2 to the heme iron. Step 4; Transfer of a second electron, reducing dioxygen to a negatively charged peroxy group. Step 5; The peroxy group sis rapidly protonated twice, releasing one molecule of water, forming a highly reactive iron(V)-oxo species. R-H in the active site reacts with the highly reactive iron(V)-oxo species, releasing a hydroxylated product.

Genes encoding cytochrome P450s are not usually abundant in microbe, but *Streptomyces* and *Mycobacteria* genomes have relatively large numbers of P450 genes (Table 1) [**2**]; they are presumably involved in the biosynthesis of secondary metabolites.

Table 1. Number of P450 genes on various microbial genomes [2]

Scientific name	Number of P450
Saccharomyces cerevisiae	3
Mycobacterium tuberculosis	20
Bacillus subtilis	9
Synechocystis	2
Escherichia coli	0
Streptomyces coelicolor	18
Sulfolobus salfataricus	1

Streptomyces produce a various type of secondary metabolites including antibiotics, anti-parasitic agents, herbicides, and immunosuppressants. According to genome sequence analysis, *Streptomyces coelicolor* A3(2) has 18 P450 genes, *Streptomyces avermitilis* has 33; *Streptomyces scabies* has 25; *Streptomyces peucetius* has 21; *Streptomyces hygroscopicus* has 7; and *Saccharopolyspora erythraea* has 22, within their chromosome sequences [**3**].

Streptomyces P450s exhibit a variety of functional diversity in natural product biosynthetic pathways and in xenobiotic degradation (Figure 2) [**4**]. Most *Streptomyces* P450 enzymes associate with electron-recycling redox partners such as

ferredoxin/ferredoxin reductase, and they flexibly accept heterologous redox partners in other *Streptomyces* species [**5**] (Figure 3).

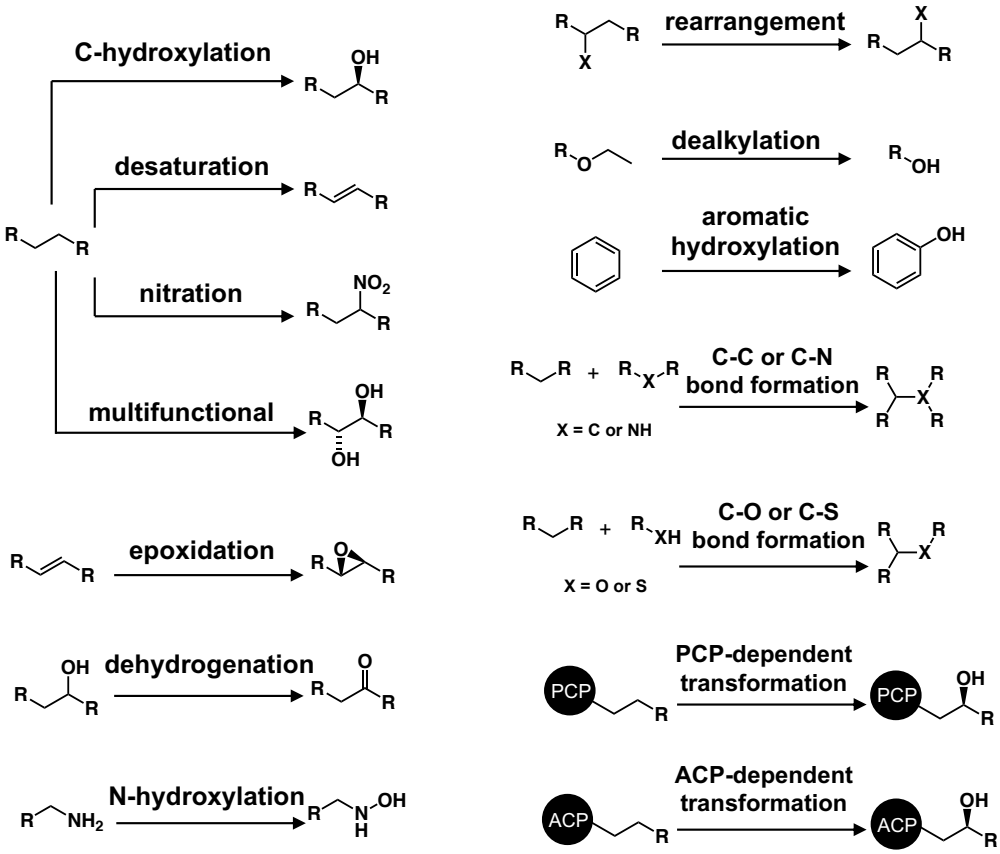

Figure 2. The functional diversity of P450s in *Streptomyces* [4]

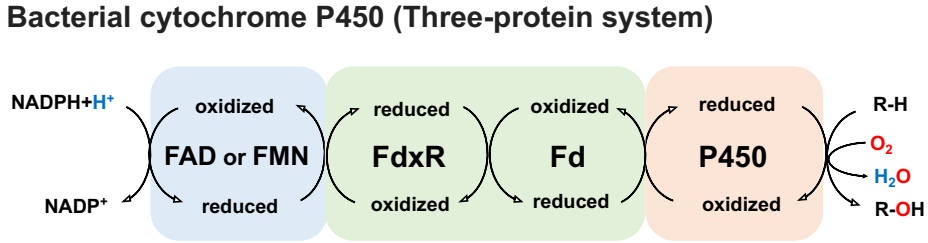

Figure 3. Classification of P450 systems in microsome and bacteria. Bacterial three-component system, FAD : flavin adenine dinucleotide, FMN : flavin mononucleotide, FdxR : ferredoxin reductase, Fd : ferredoxin, R : substrate

Human P450s are mainly membrane-associated proteins, and they are either in the membrane of mitochondria or in the endoplasmic reticulum of cells. Especially, in humans, P450s are used for body's defenses against xenobiotics by mediating their functional metabolism. On the other hand, bacterial P450s are soluble proteins with high stability, and are generally much easier for heterologous expression. Furthermore, P450 enzymes have high regio- and stereo-selectivity and are becoming increasingly important for efficient production of pharmaceuticals and nutraceuticals. For example, P450sca-2 from *Streptomyces carbophilus* catalyzes hydroxylation of ML-236B at the 6β-position to give pravastatin, a drug biocatalysts for treating hypercholesterolemia (Figure 4A) [**6**]. In addition, vitamin D3 hydroxylase (Vdh) from actinomycete *Pseudonocardia autotrophica* converts vitamin D3 to the dihydroxy-vitamin D3 (Figure 4B) [**7**, **8**].

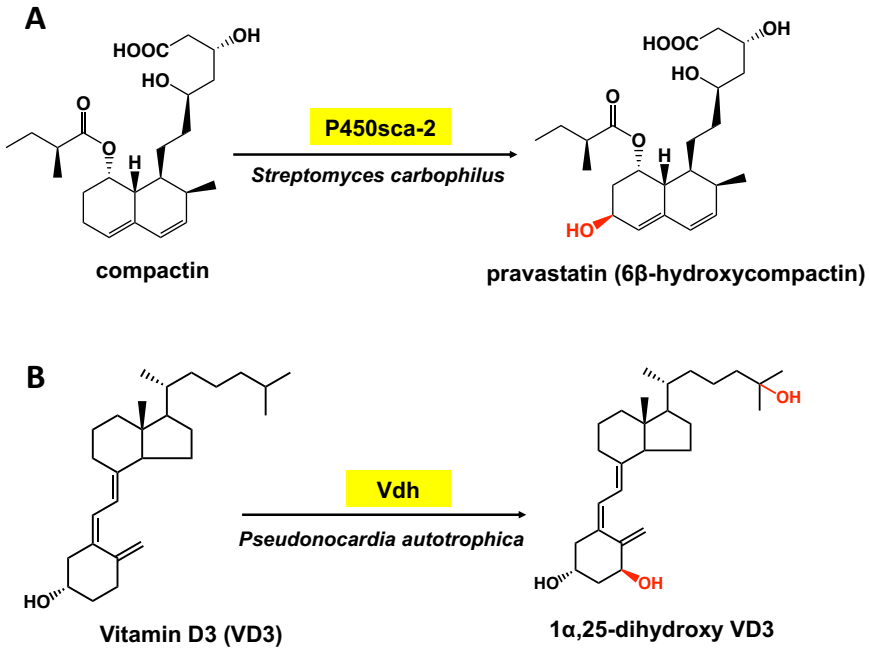

Figure 4. Examples of bioconversion by actinomycete cytochromes P450 (**A**) Compactin is hydroxylated to pravastatin by P450sca-2. (**B**) Vitamin D3 is converted to the active form 1 α,25-dihydroxy VD3 by Vdh.

Thus, *Streptomyces* P450 enzymes are attractive targets for chemists due to their remarkable reactivity. In addition, biotechnology of P450 enzymes will lead to provide versatile biocatalysts.

Streptomyces rochei 7434AN4 produces two polyketide antibiotics, a 17-membered macrocyclic polyketide lankacidin (LC) and a 14-membered macrolide lankamycin (LM) (Figure 5) [**9**].

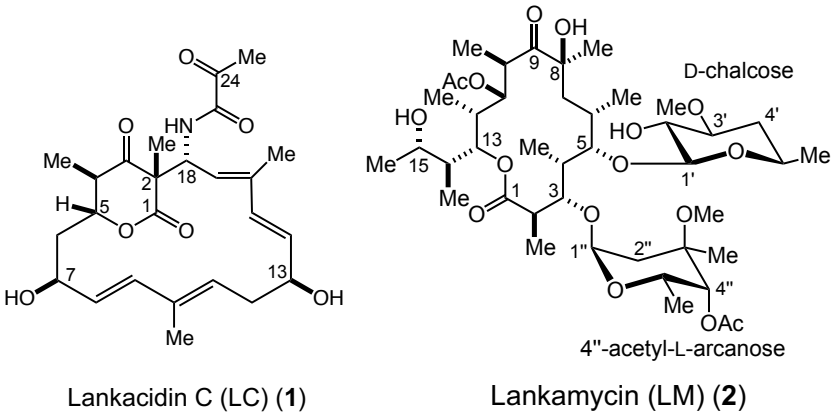

Figure 5. Chemical structures of lankacidin C (1) and lankamycin (2)

Me, methyl; Ac, acetyl

Their biosynthesis gene clusters and their regulatory genes including an SRB (*Streptomyces rochei* butenolide) biosynthesis gene (*srrX*), an SRB receptor gene (*srrA*), and two SARP (*Streptomyces* antibiotic regulatory protein) genes (*srrY* and *srrZ*) are coded on the same plasmid [**10**].

The regulatory system of antibiotics production was consisted by srrX and srrA in *S. rochei* (Figure 6) [**11**]. At the early growth stage, SrrA binds the promoter region of *srrY*, and inhibits its transcription. At the middle growth stage, SRB is biosynthesized by the action of *srrX*. SRB binds to SrrA, which has bound the promoter region of *srrY*, and then dissociates SrrA from the promoter, thus leading to transcription *srrY*, which activates the biosynthesis of lankacidin. SrrY then activates transcription of *srrZ* by binding to the promoter region of *srrZ*, and then activates the biosynthesis of lankamycin [**12**].

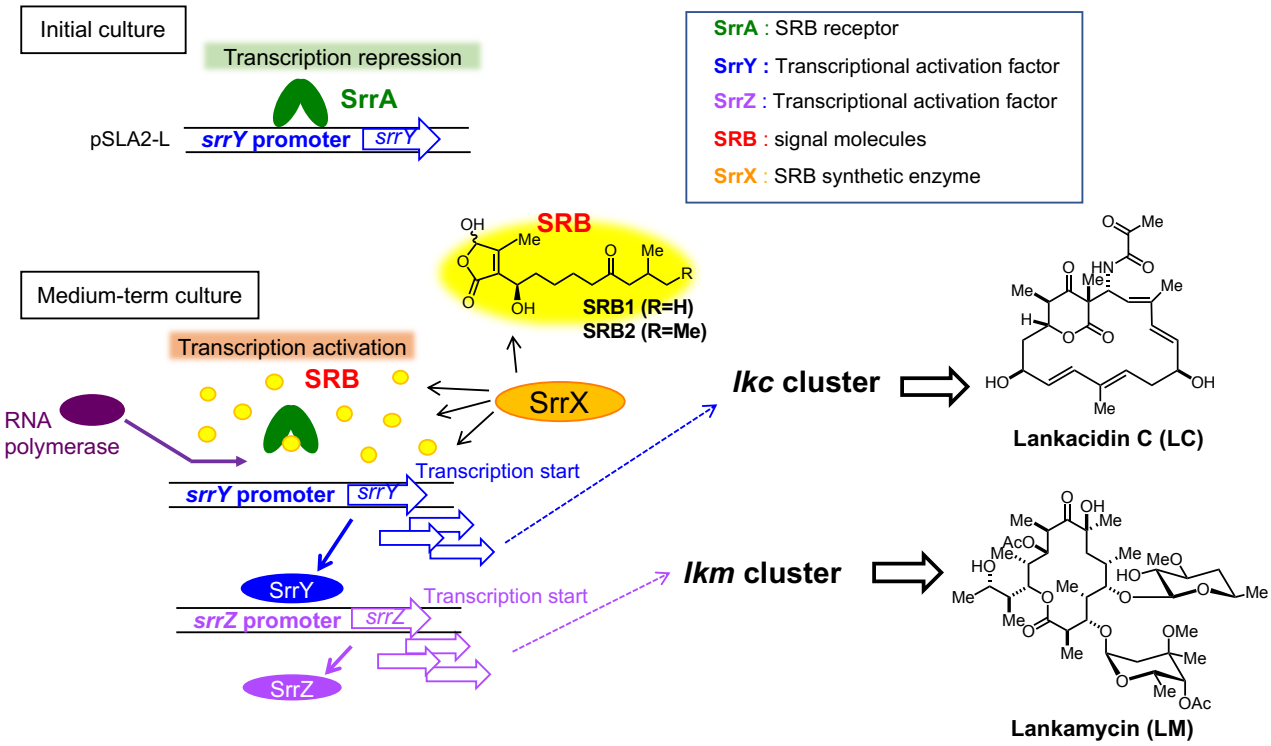

Figure 6. Major secondary metabolic regulatory cascade in *S. rochei*

According to genome sequence analysis, *S. rochei* has 42 P450 genes on a large linear plasmid pSLA2-L (211 kb) and a chromosome (8.36 Mb) (3 in pSLA2-L and 39 in the chromosome) [**13**]. Among the sequenced *Streptomyces* genome, *S. rochei* shows higher P450 population when compared with an average of 34 P450s [**14**]. Especially, pSLA2-L carries 3 P450s in the 210 kb nucleotide, 2 which is related to unusually condensed gene organization for secondary metabolite biosynthesis and their regulation (three-quarters) in pSLA2-L [**10**]. Comprehensive functional analysis of P450s is

required to construct the versatile biocatalysts for creation of highly functional bioactive substances. In this study, I analyzed the following two subjects of P450s on pSLA2-L involved in secondary metabolites production by *S. rochei*, the results of which are described in this doctoral thesis.

1) Analysis of a P450 monooxygenase SrrO, involved in signaling molecule SRB biosynthesis in *Streptomyces rochei*

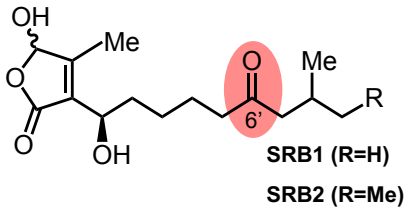

2) Analysis of two cytochrome P450 monooxygenases involved in lankamycin biosynthesis in *Streptomyces rochei*

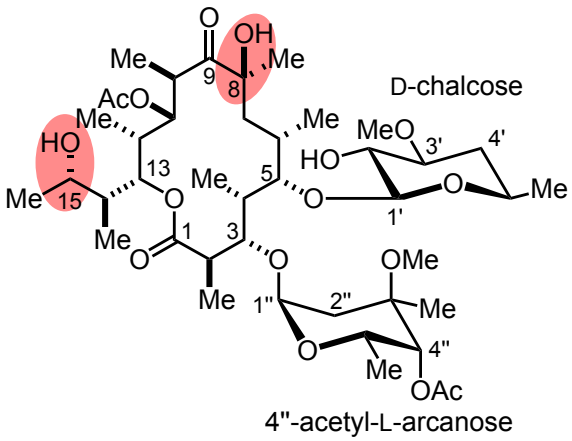

Basic manipulations and materials

Culture medium

Table 2. YM medium

Yeast extract		0.4%
Malt extract		1.0%
D-Glucose		0.4%
Agar	(When necessary)	1.5%
		Adjust to pH 7.3

Table 3. LB medium

Polypepton		1.0%
Yeast extract		0.5%
NaCl		1.0%
Agar	(When necessary)	1.5%
		Adjust to pH 7.0

Table 4. LBBS medium

Yeast extract		0.5%
Polypepton		1.0%
NaCl		1.0%
Sorbitol		18.2%
Betaine hydrochloride		30%
		Adjust to pH 7.0

Table 5. YEME medium [**15**]

Yeast extract		0.3%
Malt extract		0.3%
D-Glucose		1.0%
Polypepton		0.5%
Sucrose		34.0%
		Adjust to pH 7.0
After autoclave add:		
2.5 M $MgCl_2 \cdot 6H_2O$		0.2 mL
For preparing protoplasts, also add: 20% Glycine		2.5 mL

Table 6. R1M medium [**16**]

Glucose	1.00 g
Sucrose	10.3 g
Casamino acid	0.01 g
K_2SO_4	0.025 g
L-Asparagine	0.20 g
Polypepton	0.05 g
Yeast extract	0.08 g
$MgCl_2 \cdot 6H_2O$	0.407 g
Trace element solution	0.2 mL
	Fill up to 79 mL
Agar	2.2%
After autoclave add:	
5.73% TES buffer	10 mL
7.37% $CaCl_2 \cdot 2H_2O$	10 mL
0.5% KH_2PO_4	1 mL

Table7. Trace element solution

$ZnCl_2$	40 mg
$FeCl_3 \cdot 6H_2O$	200 mg
$CuCl_2 \cdot 2H_2O$	10 mg
$MnCl_2 \cdot 4H_2O$	10 mg
$Na_2B_4O_7 \cdot 10H_2O$	10 mg
$(NH_4)_6Mo_7O_{24} \cdot 4H_2O$	10 mg
	Fill up to 1000 mL

Table 8. SNA medium

Nutrient broth	0.8%
Agar	0.7%

YM medium (Table 2) was used for antibiotic production. *Streptomyces* strains for protoplast preparation and protein expression were cultured in YEME liquid medium (Table 5). Protoplasts were regenerated on R1M medium plate (Table 6). For routine cloning, *E. coli* strains were grown in LB medium (Table 3) supplemented with ampicillin (100 μg/mL) when necessary. Genetic manipulations for *Streptomyces* [**15**] and *E. coli* [**17**] were performed according to the described procedures.

Plasmid isolation from *Streptomyces*

The culture broth (5 mL) was harvested, and the resulting pellets were washed with 10.3% sucrose. The cells were resuspended in solution I (200 μL) (Table 9) and treated with lysozyme (1 mg/ mL) at 30 ˚C for 1 h. Protoplasts were disrupted by addition of 400 μl of solution II (Table 10). After addition of 300 μl solution III (Table 11), the mixture was kept on ice for 30 min. After centrifugation at 14,000 rpm for 10 min, the supernatant was mixed with equal volume of isopropanol. The precipitated pellets were suspended with TE buffer (Table 12) and 2 M ammonium acetate (50 μL). The precipitated pellets were washed with 99% ethanol and dissolved in TE buffer (100 μL).

Table 9. Solution I

Tris-HCl	25 mM
EDTA	25 mM
D-Glucose	50 mM
	Adjust to pH8.0

Table 10. Solution II

NaOH	0.2 M
SDS	1.0%

Table 11. Solution III

5 M Potassium acetate	60 mL
Glacial acetic acid	11.5 mL
H_2O	28.5 mL

Table 12. TE buffer

Tris-HCl (pH 8.0)	100 mM
EDTA (pH 8.0)	10 mM

Total DNA preparation for *Streptomyces*

Total DNA was prepared by a neutral method according to the protocol [**18**] with slight modifications. The pellet from 5 mL culture was suspendered in 13 mL of 10.3% sucrose. To the suspension was added 1 mL of 0.5 M EDTA (pH 8.0) and 4 mL of lysozyme (5 mg/mL in Tris-sucrose-EDTA (Table 13), Walco Chemical, Gunma, Japan) was added and incubated at 37 ˚C for 1 h. Two milliliter of Actinase E (5 mg/mL in Tris-

saline-EDTA (Table 14), Kaken Seiyaku, Tokyo, Japan) was added, and the mixture was incubated at 37 ˚C for 1 h. Then the mixture treated with 0.25 mL of 10% SDS was then shaken for an additional 30 min at 37 ˚C. The mixture was then mixed with 0.5 mL of 5 M NaCl, and incubated at 37 ˚C for another 30 min and left at 4 ˚C overnight. The mixture was centrifuged at 12,000 rpm for 20 min, and the supernatant fluid was precipitated with equal volume of 2-propanol. To purify the DNA, the precipitate was dissolved in TE buffer and extracted with phenol-chloroform (1:1, v/v). The aqueous layer was precipitated with 3-times volume of 99% chilled ethanol, and the resulting pellets were dissolved in TE buffer, and stored in −20 ˚C.

Table 13. Tris-sucrose-EDTA

Sucrose	0.3 mM
Tris-base	25 mM
EDTA	30 mM
	Adjust to pH 7.0

Table 14. Tris-saline-EDTA

NaCl	50 mM
Tris-base	30 mM
EDTA	5 mM
	Adjust to pH 8.0

Preparation of protoplasts

Cells were harvested from 100 mL YEME liquid medium (Table 5) by centrifugation. After washing twice with 10.3% sucrose solution, the pellets were treated with lysozyme solution at 30 ˚C for 15 min-1 h. The protoplasts suspension was passed through a cotton filter to exclude the remaining mycelia, and the filtrate was centrifuged. P buffer (Table 15) was added to resuspend the precipitate, and the suspension was dispensed into 50 μL aliquots in chilled, sterile microtubes. The protoplasts aliquots were stored at −80 ˚C.

Table 15. P buffer

Sucrose	103.0 g
K_2SO_4	0.25 g
Trace element solution	2.0 mL
$MgCl_2 \cdot 6H_2O$	4.07 g
	Fill up to 790 mL
After autoclave add:	
5.73% TES buffer	100 mL
7.37% $CaCl_2 \cdot 2H_2O$	100 mL
0.5% KH_2PO_4	10 mL

Transformation of protoplasts

Protoplasts were prepared according to the protocol described by Hopwood *et al.* [**19**]. DNA solution in TE buffer (5 μL) was added to 0.1 mL of a protoplast suspension. Five hundred microliter of T buffer (Table 16), which contains 25% polyethylene glycol

(PEG) 1000, was added to the mixture, and then the suspension was pipetted for several times. This protoplast was spread on RIM medium (Table 6) [**16**]. After 24-36 hours incubation, the plates were overlaid with soft nutrient agar (SNA) (Table 8) containing 50 μg/mL thiostrepton.

Table 16. T buffer

10.3% Sucrose	12.5 mL
2.5% K_2SO_4	0.5 mL
Trace element solution	0.1 mL
5 M $CaCl_2$	1.088 mL
H_2O	37.5 mL
1 M Tris-maleic acid buffer (pH 8.0)	2.72 mL

Plasmid preparation for *Escherichia coli*

Preparation of the plasmid was performed according to the protocol described by Sambrook *et al.* [**20**]. The cell pellet from 1.5 mL of overnight culture was resuspended in solution I (100 μL) (Table 9) and incubated at room temperature for 5 min. The cell suspension was disrupted by addition of solution II (200 μL) (Table 10). The mixture was immediately treated with solution III (150 μL) (Table 11), and then mixed 450 μL of phenol-chloroform (1:1, v/v). Two phases were separated by centrifugation, and the upper aqueous layer was transferred to a new tube. Nucleic acids were precipitated from the supernatant by adding 2.5 volumes of ice-cold 99% ethanol. The mixture was stored in

−80 ˚C for 30 min, and centrifuged. The supernatant was removed, and the resulting pellet was washed with 300 μL of ice-cold 70% ethanol. The dried pellet was dissolved in TE buffer (30 μL) (Table 12) and stored at −20 ˚C.

Southern hybridization analysis

Southern hybridization was performed using DIG labeling kit (Roche Diagnostics, Rotkreuz, Switzerland) according to the manufacture's protocol. A 15 μL of DNA solution was boiled for 10 min and placed on ice immediately. To the denatured DNA, 5 μL of DIG High-prime (Roche Diagnostics, Rotkreuz, Switzerland) was added. The mixture was incubated at 37 ˚C overnight. The labeling reaction was stopped by the addition of 2 μL of 0.5 M EDTA, and then the labeled DNA was treated with 2.5 μL of 4 M LiCl, and 75 μL of 99% ethanol, and placed at –80 ˚C for 30 min. After centrifugation, the pellet was washed with 70% ethanol, and dissolved with 30 μL of distilled water.

After the gel electrophoresis image stained by Ethidium Bromide (EtBr) was taken, the agarose gel was rinsed with 0.25 M HCl for 10 min, and then continued to soak in alkaline transfer buffer (Table 17) for 15 min twice and neutralization buffer (Table 18) for 20 min. The DNA was transferred onto the nitrocellulose membrane by upward capillary transfer method for 8-24 h. The membrane was washed with 2×SSC (Table 19)

briefly, and irradiated by UV light to fix the single-stranded DNA. The membrane was then placed in Hybri-bag Hard (Cosmo Bio, Tokyo, Japan) filled with hybridization buffer (Table 20) and was incubated at 70°C. After one hour, the denatured probe was added to the Hybri-bag, and the membrane was further incubated overnight at 70°C. The incubated membrane was rinsed with 2×SSC-0.1% (w/v) SDS for 5 min at room temperature twice and with 0.1×SSC-0.1% (w/v) SDS at 70 ˚C for 15 min twice.

The membrane was rinsed in buffer I (Table 21) and soaked in buffer II (0.5% (w/v) skim milk in buffer I) for 30 min at room temperature with gentle agitation. After washing with buffer I, the membrane was incubated in buffer I containing anti- digoxygenin-AP Fab fragment (Roche Diagnostics, Rotkreuz, Switzerland) (2 μL in 10 mL) for 1 h. The membrane was washed with buffer I for 15 min twice, and then soaked in buffer III (Table 22). The DIG-labeled DNA was detected using colorimetric detection substrates, NBT/BCIP solution (45 μL NBT solution (Table 23) and 35 μL X-phosphate solution (Table 24) in 10 mL buffer III).

Table 17. Alkaline transfer buffer

NaOH	50 mM
NaCl	30 mM
	Fill up to 1000 mL

Table 18. Neutralization buffer

Tris base	121.1 g
NaCl	87.65 g
	Fill up to 1000 mL
	Adjust to pH 8.0

Table 19. 20×SSC

NaCl	175.32 g
Sodium citrate bi-hydrate	88.23 g
	Fill up to 1000 mL

Table 20. Alkaline transfer buffer

20×SSC	250 mL
Skim milk	5 g
10% SDS	1 mL
10% N-lauroylsarcosine	10 mL
	Fill up to 1000 mL

Table 21. Buffer I

Tris base	121.1 g
NaCl	87.65 g
	Fill up to 1000 mL
	Adjust to pH 7.5

Table 22. Buffer III

Tris base	121.1 g
NaCl	87.65 g
$MgCl_2 \cdot 6H_2O$	10.165 g
	Fill up to 1000 mL
	Adjust to pH 9.5

Table 23. NBT solution

Nitrobluetetrazolium salt	75 mg
70% (v/v) dimethylformamide	1 mL

Table 24. X-phosphate solution

5-Bromo-4-chloro-3-indolylphosphate toluinidium salt	50 mg
100% dimethylformamide	1 mL

Polymerase chain reaction (PCR)

PCR amplification was performed on a 2720 Thermal Cycler (Applied Biosystems) with KOD-Plus- DNA polymerase (Toyobo, Osaka, Japan) according to the standard protocols.

Spectroscopic instruments

NMR spectra were recorded on JEOL ECA-500 and/or ECA-600 spectrometers equipped with a field gradient accessory. Deuterochloroform (99.8 atom% enriched; Kanto Chemical Co., Ltd., Tokyo, Japan) was used as a solvent. Chemical shifts were recorded as a δ value based on a resident solvent signal ($\delta_C = 77.0$), or an internal standard signal of tetramethylsilane ($\delta_H = 0$). High resolution electrospray ionization (HR-ESI) mass spectra were measured by LTQ Orbitrap XL mass spectrometer (Thermo Fisher

Scientific, Massachusetts, USA). High resolution gas chromatography-time of flight (HR-GC-TOF) mass spectra (ionization mode; CI) were acquired on a JMS-T100 GCV 4G (JEOL, Tokyo, Japan). Optical rotations were measured using a DIP-370 polarimeter (JASCO, Tokyo, Japan). IR spectra were recorded on a Shimadzu IRAffinity-1 spectrometer using the ATR (Attenuated Total Reflection) method.

Chapter 1

Analysis of a P450 monooxygenase SrrO, involved in signaling molecule SRB biosynthesis in *Streptomyces rochei*

1.1. Introduction

In *Streptomyces* species, secondary metabolite production and morphological differentiation are generally controlled by diffusible signaling molecules [**21**,**22**]. The signaling molecules that have been hitherto discovered are classified into three groups; γ-butyrolactone-type, furan-type, and butenolide-type [**23**,**24**,**25**,**26**]. For example, γ-butyrolactone-type contains A-factor, an inducer for streptomycin production in *Streptomyces griseus* [**27**,**28**], furan-type does methylenomycin furans that are responsible for methylenomycin production in *Streptomyces coelicolor* [**29**], and butenolide-type contains avenolide, an inducer for avermectin in *Streptomyces avermitilis* [**30**] and SRBs that are responsible for lankacidin/lankamycin production in *Streptomyces rochei* [**31**] (Figure 7).

<table>
<tr><th colspan="4">γ-butyrolactone type</th></tr>
<tr><th>A-factor</th><th>SCB</th><th>IM-2</th><th>VB-A</th></tr>
<tr><td> 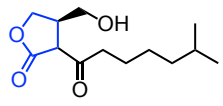 </td><td> 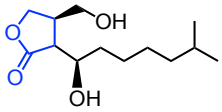 </td><td> 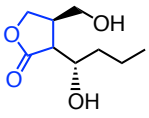 </td><td> 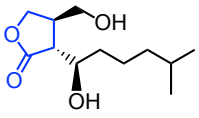 </td></tr>
<tr><td>S. griseus</td><td>S. coelicolor</td><td>S. lavendulae</td><td>S. virginiae</td></tr>
<tr><th>Furan type</th><th colspan="3">Butenolide type</th></tr>
<tr><th>MMF</th><th>Avenolide</th><th>SRB</th><th>SAB</th></tr>
<tr><td> 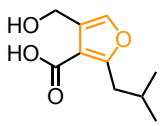 </td><td> 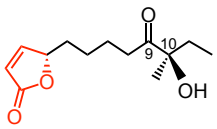 </td><td> 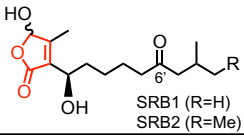 </td><td> 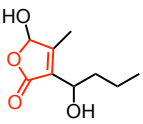 </td></tr>
<tr><td>S. coelicolor A3(2)</td><td>S. avermitilis</td><td>S. rochei</td><td>S. anosochromogenes 7100</td></tr>
</table>

Figure 7. Examples of signaling molecules *hitherto* discovered

In most signaling molecules, their biosynthetic gene clusters have no P450 genes that are possibly responsible for introduction of oxygen-containing functional groups, such as hydroxyl and/or ketone in their structures.

We have elucidated the chemical structures of SRB1(**3**) and SRB2 (**4**), that induce LC (**1**) and LM (**2**) production at 40 nM in *S. rochei*. SRB1 was determined to be 2-(1'-hydroxyl-6'-oxo-8'-methylnonyl)-3-methyl-4-hydroxybut-2-en-1,4-olide ($C_{15}H_{24}O_5$), while SRB2 was 2-(1'-hydroxyl-6'-oxo-8'-methyldecyl)-3-methyl-4-hydroxybut-2-en-1,4-olide ($C_{16}H_{26}O_5$) (Figure 8) [**31**]. Their C-1' stereochemistry was determined to be *R* based on chiral HPLC analysis.

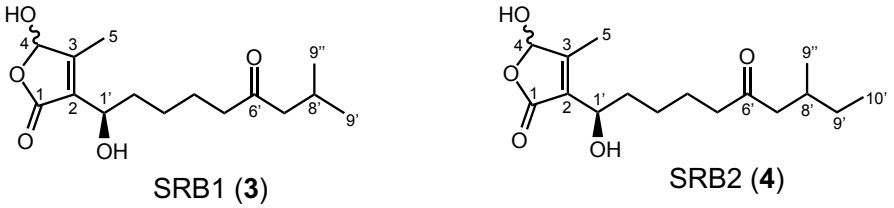

Figure 8. Structures of *Streptomyces rochei* signaling molecules SRBs

It is noteworthy that several possible genes involved in SRB biosynthesis were found around *srrX* (*orf85*) on a large linear plasmid pSLA2-L of *S. rochei*; an NAD-dependent dehydrogenase gene *srrG* (*orf81*), a phosphatase gene *srrP* (*orf83*), a P450 monooxygenase gene *srrO* (*orf84*), and a thioesterase gene *srrH* (*orf86*) (Figure 9) [**10**,**11**].

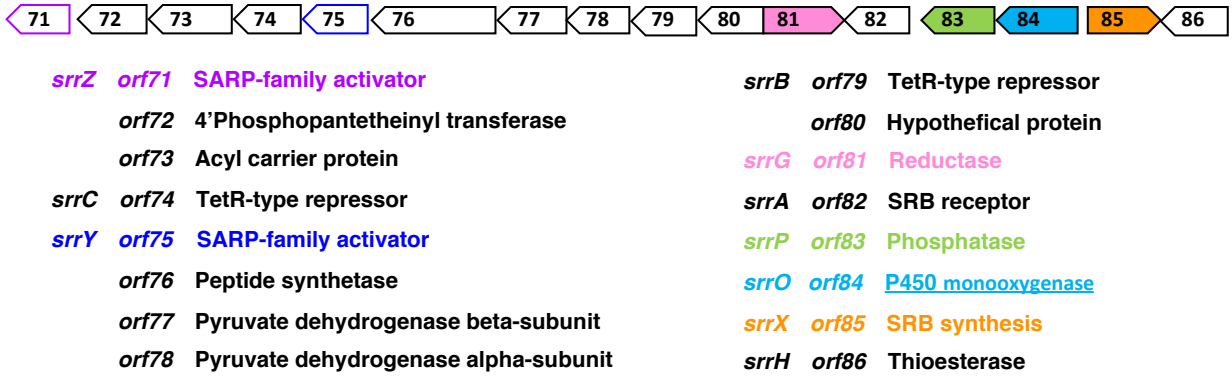

Figure 9. Gene organization of *orf71-86* on pSLA2-L

Based on the structure of SRBs, SrrO may be involved in the oxidation of C-6' position in the biosynthesis pathway of SRBs.

I here analyzed the function of *srrO* by gene inactivation and enzymatic bioconversion experiments, the results of which be described in this chapter.

1.2. Materials and methods

1.2.1. Strains and reagents

All strains and plasmids used in this study were listed in Table 25. Strain 51252 which has only pSLA2-L was used as a parent strain [**9**]. The double mutant of *srrX* and the transcriptional repressor gene *srrB*, KA20, was used as the signaling molecule indicator strain, because this strain, like the *srrB* mutant, produces two antibiotics when SRBs are added [**11**,**31**].

Table 25. Bacteria strains, plasmids, and oligonucleotides used in this chapter

Strains/plasmids/oligonucleotides	Properties/product	Source/ref.*1
Strains		
S. rochei		
7434AN4	Wild type (pSLA2-L,M,S)	[9]
51252	pSLA2-L	[9]
KA20	*ΔsrrXΔsrrB* in strain 51252	[11]
KA54	*ΔsrrO* in strain 51252	This study
S. lividans		
TK64	*pro-2*, *str-6*	[32]
TK64/pNTT01	Strain TK64 with plasmid pNTT01, *tsr*, $(His)_6$-tagged *srrO*	This study
TK64/pHSA81	Strain TK64 with plasmid pHSA81, *tsr*	[33]
E. coli		
XL1-Blue	*recA1 endA1 gyrA96 thi-1 hsdR17 supE44 relA1 lac* [F'*proAB lacI*^{q}*ZΔM15* Tn*10* (*tet*)]	Stratagene
Plasmids		
SuperCos-1	Cosmid vector, *amp*, *kan*	Stratagene
cosmid C7	41.3-kb pSLA2-L DNA (nt 143,101-184,445) cloned into SuperCos-1 at *Bam*HI site	[10]
pRES18	*E. coli-Streptomyces* shuttle vector, *amp*, *tsr*, *lacZ*-α	[20]
Litmus 28i	*E. coli* cloning vector, *amp*, *lacZ*-α	New England Biolabs
pKAR3041	3.8-kb *Eco*RI-*Stu*I fragment containing *srrO* in Litmus 28i	[34]
pKAR3043	1.0-kb *Cla*I fragment of *aac(3)IV* gene carrying apramycin resistance into *Cla*I site of pKAR304	This study
pKAR3044	2.3-kb *Bam*HI fragment carrying *ΔsrrO* in pRES18	This study
pHSA81	Constitutive expression vector in *Streptomyces*, *tsr*	M. Kobayash
pKAR3063H	Constitutive expression vector in *Streptomyces*, *tsr*, N-terminal $(His)_6$-tag	[35]
pNTT01	1.2 kb *Nde*I-*Hin*dIII PCR fragment carrying *srrO* cloned into pKAR3063H	This study
Designed oligonucleotides		
KAR-APR05	5'-GCGAATTCGCATGCATCGATACAGAATGAT-3'	This study
KAR-APR06	5'-TGTAAGCTTATCGATGCATGCACGTGTTGC-3'	This study
NT-srrO-OE-F	5'-ATACATATGCTTCGTCAGGAAGCGCCCTA-3'	This study
NT-srrO-OE-R	5'-TTAAAGCTTCATGCCGCGGCTCCGGGCAC-3'	This study

*1 ; Reference numbers are identical with those indicated in main text.

1.2.2. Construction of the srrO mutant KA54

A 3.8-kb *Stu*I/*Eco*RI-digested DNA fragment (nt 143,844-147,674 of pSLA2-L) containing an *srrO* gene was ligated with 2.8-kb *Stu*I/*Eco*RI-digested DNA fragment of Litmus 28i to give pKAR3041. To a *Cla*I restriction site at the 5'-terminal region of *srrO* was introduced a 1.0-kb *Cla*I fragment of apramycin resistance cassette (*aac(3)IV*). The obtained plasmid pKAR3043 was digested with *Eco*RI and *Stu*I, and the vector of which was replaced with an *Eco*RI-*Sma*I fragment of pRES18, an *E. coli-Streptomyces* shuttle vector [**36**], to afford pKAR3044. This plasmid was transformed into protoplast of strain 51252, and then a KA54 (*srrO* mutant strain) was obtained through homologous recombination according to our protocol [**37**].

1.2.3. Metabolites in an srrO mutant KA54

Metabolites in strain KA54 were analyzed by HPLC and TLC in comparison with those in parent strain 51252. The crude extract was diluted with methanol and applied on a COSMOSIL CHOLESTER column (4.6 x 250 mm, Nacalai Tesque, Kyoto, Japan). The elution was carried out with a mixture of acetonitrile-10 mM sodium phosphate buffer (pH 8.2) (3:7, v/v) at a flow rate of 1.0 mL/min. Eluted substances were detected by a JASCO MD-2010 multiwavelength photodiode array detector at 230 nm. The TLC plates

were developed with a mixture of $CHCl_3$-methanol (15:1, v/v) and baked after spraying with anisaldehyde-H_2SO_4.

1.2.4. Isolation of signaling molecules from the srrO mutant KA54

The preculture solution (20 mL) of Δ*srrO* strain was inoculated into to 2 liter YM medium in 5-liter Erlenmeyer flask, which was grown at 28 ˚C for 36 h. The culture filtrate of total 30 liter culture broth was extracted with equal volume of ethyl acetate (EtOAc) twice. The combined organic phase was dried (Na_2SO_4), filtered, and concentrated under vacuum using a rotary evaporator. The resulting crude extracts were purified by Sephadex LH-20 (GE Healthcare, Chicago, USA) with methanol. To detect fractions containing signaling molecules, each fraction was subjected to bioassay using Δ*srrX*-Δ*srrB* double mutant as a test organism according to our previous report [**31**]. Active fractions were collected and purified by silica gel column chromatography with two different solvent systems of $CHCl_3$-MeOH (50:1, *v*/*v*) and toluene-EtOAc (3:1, *v*/*v*). A mixture of Δ*srrO*-SRB1 and Δ*srrO*-SRB2 which are active components (100 μg from 30-liter culture) was analyzed by electrospray ionization-mass spectrometry (ESI-MS) (Figure 14) and NMR (Figure 15).

The molecular formula of compound 1 (Δ*srrO*-SRB1) was established as $C_{15}H_{26}O_4Na$ by high resolution ESI-MS, since an ion peak $[M+Na]^+$ was observed at *m/z* 293.1727 (calcd for 293.1729).

The molecular formula of compound 2 (Δ*srrO*-SRB2) was established as $C_{16}H_{28}O_4Na$ by high resolution ESI-MS, since an ion peak $[M+Na]^+$ was observed at *m/z* 307.1883 (calcd for 307.1885).

Due to the low quantity of active components (100 mg from 30 liter culture), compounds 1 and 2 were separated by repeated runs of HPLC (25% aqueous acetonitrile containing 0.1% trifluoroacetic acid) at 10.6 min and 17.1 min, respectively. Their C-1' stereochemistry was determined by chiral HPLC using synthetic 6'-deoxo-SRBs (details were shown in sections 1.2.7 and 1.3.3).

1.2.5. Synthesis of 6'-deoxo-SRBs

6-Hydroxyhexyl *p*-toluenesulfonate (**8**)

To a solution of 1,6-hexanediol (**7**) (2.03 g, 17.2 mmol), triethylamine (7.00 mL, 50.5 mmol), and 4,4-dimethylaminopyridine (50 mg, 0.41 mmol) in CH_2Cl_2 (70 mL) was added *p*-toluenesulfonyl chloride (3.28 g, 17.2 mmol) at 0 ˚C, and the mixture was stirred at room temperature for 1 h. After adding of water (50 mL), the mixture was extracted

with EtOAc twice. The combined organic phase was washed with brine, dried (Na_2SO_4), filtered, and concentrated under vacuum using a rotary evaporator. The residue was purified by silica gel with hexane-EtOAc (1:1–1:2, *v*/*v*) to give **8** (2.34 g, 50%) as a colorless oil.

^{1}H-NMR ($CDCl_3$): δ = 1.33 (m, 4H), 1.51 (m, 2H), 1.65 (m, 2H), 2.45 (s, 3H), 3.60 (t, *J* = 6.5 Hz, 2H), 4.02 (t, *J* = 6.3 Hz, 2H), 7.35 (d, *J* = 8.0 Hz, 2H), 7.78 ppm (d, *J* = 8.0 Hz, 2H); ^{13}C-NMR ($CDCl_3$): δ = 21.6, 25.0, 25.1, 28.7, 32.3, 62.5, 127.8, 129.8, 133.0, 144.7; High resolution ESI-MS: observed *m*/*z* 295.0975 $[M+Na]^+$ (calcd for $C_{13}H_{20}O_4SNa$, 295.0975); IR (neat): ν = 3343, 2934, 2860, 2361, 2342, 1354, 1172 cm^{-1}.

6-((Tetrahydro-2*H*-pyran-2-yl)oxy)hexyl *p*-toluenesulfonate (**9**)

A solution of alcohol **8** (2.30 g, 8.45 mmol), 3,4-dihydro-2*H*-pyrane (1.50 mL, 16.4 mmol), and *p*-toluenesulfonic acid monohydrate (45 mg) in CH_2Cl_2 (30 mL) was stirred at room temperature for 8 h. The mixture was quenched by addition of saturated aqueous $NaHCO_3$ (20 mL) in a dropwise manner, and then extracted with EtOAc twice. The combined organic phases were washed with brine, dried (Na_2SO_4), filtered, and concentrated under vacuum using a rotary evaporator. The residue was purified by silica gel with hexane-EtOAc (10:1, *v*/*v*) to give **9** (2.85 g, 95%) as a colorless oil.

^{1}H-NMR ($CDCl_3$): δ = 1.32-1.33 (m, 4H), 1.50-1.84 (m, 10H), 2.45 (s, 3H), 3.32-3.72 (m, 2H), 3.47–3.87 (m, 2H) 4.02 (t, *J* = 6.3 Hz, 2H), 4.54 (t, *J* = 3.3 Hz, 1H), 7.34 (d, *J* = 8.5 Hz, 2H), 7.78 ppm (d, *J* = 8.0 Hz, 2H); ^{13}C-NMR ($CDCl_3$): δ = 19.7, 21.6, 25.2, 25.4, 25.6, 28.7, 29.4, 30.7, 62.4, 67.3, 70.5, 98.9, 127.8, 129.7, 133.1, 144.6; High resolution ESI-MS: observed *m*/*z* 379.1551 $[M+Na]^+$ (calcd for $C_{18}H_{28}O_5SNa$, 379.1550); IR (neat): ν = 2938, 2862, 2361, 2342, 1354, 1175 cm^{-1}.

2-((8-Methylnonyl)oxy)tetrahydro-2*H*-pyran (**10**)

To a suspension of magnesium (1.00 g, 41.1 mmol) and iodine (65 mg) in THF (20 mL) was added 1-bromo-2-methylpropane (4.50 mL, 41.7 mmol) at 0 ˚C, and the mixture was stirred at 0 ˚C for 30 min. A solution of 0.5 M Li_2CuCl_4 in THF (5.00 mL, 2.50 mmol) was added to the mixture at 0 ˚C, and then a solution of tosylate **9** (3.10 g, 8.70 mmol) in THF (10 mL) was added dropwise to the mixture at 0 ˚C, and the mixture was stirred at 0 ˚C for 1 h. The mixture was quenched by addition of saturated aqueous NH_4Cl (20 mL) in a dropwise manner at 0 ˚C, and then extracted with EtOAc twice. The combined organic phases were washed with brine, dried (Na_2SO_4), filtered, and concentrated under vacuum using a rotary evaporator. The residue was purified by silica gel with hexane-EtOAc (25:1, *v*/*v*) to give **10** (2.10 g, 99%) as a colorless oil.

^{1}H-NMR ($CDCl_3$): δ = 0.86 (d, *J* = 7.0 Hz, 6H), 1.13-1.17 (m, 2H), 1.25–1.35 (m, 8H), 1.50–1.60 (m, 7H), 1.71 (m, 1H), 1.83 (m, 1H), 3.36–3.52 (m, 2H), 3.71–3.90 (m, 2H), 4.58 (t, *J* = 3.5 Hz, 1H); ^{13}C-NMR ($CDCl_3$): δ = 14.0, 19.6, 22.6, 25.5, 25.9, 29.2, 29.7, 30.7, 31.6, 33.5, 62.2, 67.6, 98.8; High resolution ESI-MS: observed *m*/*z* 265.2138 $[M + Na]^+$ (calcd for $C_{15}H_{30}O_2Na$, 265.2138); IR (neat): ν = 2924, 2853, 1466, 1366, 1352, 1130, 1117, 1034, 1022 cm^{-1}.

8-Methylnonan-1-ol (**11**)

A mixture of THP ether **10** (2.43 g, 10.0 mmol) and 2M aqueous HCl (5.0 mL) in THF-MeOH (40 mL, 1:1 *v*/*v*) was stirred at room temperature for 4 h. The mixture was concentrated under vacuum using a rotary evaporator. The residue was purified by silica gel with hexane-EtOAc (10:1–2:1, *v*/*v*) to give alcohol **11** (1.47 g, 92%) as a colorless oil.

^{1}H-NMR ($CDCl_3$): δ = 0.86 (d, *J* = 7.0 Hz, 6H), 1.13–1.17 (m, 2H), 1.23–1.38 (m, 8H), 1.49–1.68 (m, 3H) 3.60 (t, *J* = 6.5 Hz, 2H); ^{13}C-NMR ($CDCl_3$): δ = 22.6, 25.7, 27.3, 27.9, 29.5, 29.8, 32.8, 39.0, 63.1; High resolution GC-CI-MS: observed *m*/*z* 157.1589 $[M–H]^+$ (calcd for $C_{10}H_{21}O$, 157.1592); IR (neat): ν = 3329, 2955, 2928, 2859, 1458, 1057 cm^{-1}.

8-Methylnonanal (**12**)

A solution of alcohol **11** (1.02 g, 6.44 mmol), pyridinium chlorochromate (2.48 g, 11.5 mmol), and sodium acetate (228 mg, 2.78 mmol) in CH_2Cl_2 (50 mL) was stirred at room temperature for 2 h. The mixture was diluted with ether (70 mL), and filtered through a pad of Celite. The filtrate and washings were concentrated under vacuum using a rotary evaporator. The residue was purified by silica gel with hexane-EtOAc (15:1, *v*/*v*) to give aldehyde **12** (869 mg, 86%) as a colorless oil.

^{1}H-NMR ($CDCl_3$): δ = 0.86 (d, *J* = 7.0 Hz, 6H), 1.16 (m, 2H), 1.26–1.33 (m, 6H), 1.51 (m, 1H), 1.63 (m, 2H), 2.42 (dt, *J* = 1.5 and 7.3 Hz, 2H), 9.76 (t, *J* = 2.0 Hz, 1H); ^{13}C-NMR ($CDCl_3$): δ = 22.1, 22.6, 27.1, 27.9, 29.2, 29.6, 38.9, 43.9, 203.0; High resolution GC-CI-MS: observed *m*/*z* 157.1589 $[M+H]^+$ (calcd for $C_{10}H_{21}O$, 157.1592); IR (neat): ν = 2951, 2924, 2855, 1726, 1709, 1466 cm^{-1}.

(1'*R*)-2-(1'-Hydroxyl-8'-methylnonyl)-3-methyl-4-(L-menthyloxy)but-2-en-1,4-olide (**14a**) and (1'*S*)-2-(1'-Hydroxyl-8'-methylnonyl)-3-methyl-4-(L-menthyloxy)but-2-en-1,4-olide (**14b**).

A solution of *n*-butyl lithium (2.10 mL, 1.64 M in hexane, 3.44 mmol) was added in a dropwise manner to a solution of diisopropylamine (470 μL, 3.34 mmol) in THF (7 mL) at −78 ˚C, and the mixture was stirred. After 30 min, hexamethylphosphoric triamide

(HMPA) (2.00 mL) was added to the mixture at −78 ˚C. A solution of 3-methyl-4-(L-menthyloxy)but-2-en-1,4-olide (**13**) (745 mg, 2.95 mmol) [**31**,**38**,**39**] in THF (7 mL) was added to the mixture at −78 ˚C over 15 min, and the mixture was further stirred at −78 ˚C temperature for 1 h. Then, a solution of aldehyde **12** (685 mg, 4.38 mmol) in THF (7 mL) was added dropwise at −78 ˚C over 10 min, and the mixture was further stirred at −78 ˚C for 1.5 h. Saturated aqueous NH_4Cl (20 mL) was added to the mixture, and the mixture was extracted with CH_2Cl_2 twice. The combined organic phases were washed with brine, dried (Na_2SO_4), filtered, and concentrated under vacuum using a rotary evaporator. The residue was purified by silica gel chromatography with hexane-EtOAc (10:1–7:1, *v*/*v*) to obtain a 2:1 mixture of **14a** and **14b** (452 mg, 38%) as a colorless oil, which were further separated by repeated runs of flash chromatography with hexane-EtOAc (10:1, *v*/*v*). Their absolute configuration at C-1' was established by the modified Mosher method [**40**].

Compound **14a**: $[\alpha]_D^{20} = -83.1$ (*c* = 0.32, $CHCl_3$); ^{1}H-NMR ($CDCl_3$): δ = 0.86 (d, J = 6.4 Hz, 6H), 1.15 (m, 2H), 1.26–1.33 (m, 6H), 1.41–1.55 (m, 2H), 1.65 (m, 2H), 1.84 (m, 1H), 1.98 (s, 3H), 2.88 (br, 1H), 4.46 (br, *J* = 7.5 Hz, 1H), 5.70 (s, 1H), menthyl resonances: 0.81 (d, *J* = 6.8 Hz, 3H), 0.86 (m, 1H), 0.88 (d, *J* = 7.1 Hz, 3H), 0.96 (d, *J* = 6.4 Hz, 3H), 1.02 (m, 2H), 1.22–1.27 (m, 1H), 1.28–1.42 (m, 1H), 1.64–1.70 (m, 2H), 2.08–2.14 (m, 2H), 3.62 (dt, *J* = 4.3 and 11 Hz, 1H); ^{13}C-NMR ($CDCl_3$): δ = 11.5, 22.6,

25.5, 27.2, 27.9, 29.3, 29.7, 36.7, 38.9, 67.0, 100.8, 130.6, 155.3, 171.4, menthyl resonances: 15.9, 20.8, 22.2, 23.2, 25.3, 31.4, 34.2, 40.5, 47.7, 79.5; High resolution ESI-MS: observed *m*/*z* 409.3320 $[M+H]^+$ (calcd for $C_{25}H_{45}O_4$, 409.3312); IR (neat): ν = 2951, 2922, 2868, 2854, 1751, 1456, 1384, 1367, 1331, 1126, 1093, 945 cm^{-1}.

Compound **14b**: $[\alpha]_D^{28}$ = −62.5 (*c* = 0.460, $CHCl_3$); ^{1}H-NMR ($CDCl_3$): δ = 0.86 (d, *J* = 6.7 Hz, 6H), 1.15 (m, 2H), 1.24–1.33 (m, 6H), 1.40–1.55 (m, 2H), 1.66 (m, 2H), 1.83 (m, 1H), 1.99 (s, 3H), 2.77 (br, 1H), 4.47 (br, *J* = 6.4 Hz, 1H), 5.71 (s, 1H), menthyl resonances: 0.81 (d, *J* = 6.8 Hz, 3H), 0.86 (m, 1H), 0.88 (d, *J* = 7.1 Hz, 3H), 0.96 (d, *J* = 6.4 Hz, 3H), 1.02 (m, 2H), 1.22–1.27 (m, 1H), 1.28–1.42 (m, 1H), 1.64–1.70 (m, 2H), 2.08–2.14 (m, 2H), 3.62 (dt, *J* = 4.3 and 11 Hz, 1H); ^{13}C-NMR ($CDCl_3$): δ = 11.5, 22.6, 25.5, 27.2, 27.9, 29.3, 29.7, 36.7, 38.9, 67.0, 100.8, 130.6, 155.3, 171.4, menthyl resonances: 15.9, 20.8, 22.2, 23.2, 25.3, 31.4, 34.2, 40.5, 47.7, 79.5; High resolution ESI-MS: observed *m*/*z* 409.3315 $[M+H]^+$ (calcd for $C_{25}H_{45}O_4$, 409.3312); IR (neat): ν = 2951, 2922, 2868, 2855, 1751, 1456, 1385, 1368, 1330, 1094, 945 cm^{-1}.

6′-deoxo-SRB1a (**5a**)

To a solution of menthyl ester **14a** (34 mg, 83.2 μmol) in CH_2Cl_2 (4.0 mL) was added 10% BBr_3 solution in CH_2Cl_2 (400 μL, 420 μmol) at −78 ˚C, and the mixture was stirred at −78 ˚C for 3 h. Saturated aqueous $NaHCO_3$ (3 mL) was carefully added, and the

mixture was extracted with EtOAc twice. The combined organic phases were washed with brine, dried (Na_2SO_4), filtered, and concentrated under vacuum using a rotary evaporator. The residue was purified by silica gel chromatography with hexane-EtOAc (2:1, *v*/*v*) to obtain 6′-deoxo-SRB1a (**5a**) (17 mg, 79%) as a colorless oil.

Mixture of C-4 epimers: $[\alpha]_D^{18}$ = +126.4 (*c* = 0.11, $CHCl_3$); ^{1}H-NMR ($CDCl_3$): δ = 0.86 (d, *J* = 6.7 Hz, H-9’ and H-9’’, 6H), 1.15 (m, H-7’, 2H), 1.26 (m, H-3’a, H-4’, and H-6′, 5H), 1.29 (m, H-5’, 2H), 1.39 (m, H-3’b, 1H), 1.51 (m, H-8’, 1H), 1.65 (m, H-2’a, 1H), 1.81 (m, H-2’b, 1H), 2.07 (s, H-5, 3H), 4.47 (m, H-1’, 1H), 5.85 (brs, H-4, 1H); ^{13}C-NMR ($CDCl_3$): δ = 11.4/11.6 (C-5), 22.6 (C-9’ and C-9’’), 25.5 (C-3’), 27.3 (C-6′), 27.9 (C-8’), 29.3 (C-5’), 29.7/29.8 (C-4’), 36.0/36.2 (C-2’), 39.0 (C-7’), 66.7 (C-1’), 98.8 (C-4), 130.1/130.5 (C-2), 157.9 (C-3), 171.7/172.0 (C-1); High resolution ESI-MS: observed *m*/*z* 293.1718 $[M+Na]^+$ (calcd for $C_{15}H_{26}O_4Na$, 293.1723); IR (neat): *v* = 3399, 2957, 2924, 2855, 2361, 2342, 1749, 1734 cm^{-1}.

6′-deoxo-SRB1b (**5b**)

The compound **14b** (20 mg, 49 μmol) was treated in the same manner as described for the preparation of **5a** to obtain 6′-deoxo-SRB1b (**5b**) (8.1 mg, 62%) as a colorless oil.

Mixture of C-4 epimers: $[\alpha]_D^{25}$ = +1.32 (*c* = 0.180, $CHCl_3$); ^{1}H-NMR ($CDCl_3$): δ = 0.86 (d, *J* = 6.7 Hz, H-9’ and H-9’’, 6H), 1.15 (m, H-7’, 2H), 1.26 (m, H-3’a, H-4’, and

H-6′, 5H), 1.29 (m, H-5’, 2H), 1.39 (m, H-3’b, 1H), 1.51 (m, H-8’, 1H), 1.65 (m, H-2’a, 1H), 1.81 (m, H-2’b, 1H), 2.07 (s, H-5, 3H), 4.47 (m, H-1’, 1H), 5.85 (brs, H-4, 1H); ^{13}C-NMR ($CDCl_3$): δ = 11.4/11.6 (C-5), 22.6 (C-9’ and C-9’’), 25.5 (C-3’), 27.3 (C-6′), 27.9 (C-8’), 29.3 (C-5’), 29.8 (C-4’), 36.0/36.4 (C-2’), 39.0 (C-7’), 66.8 (C-1’), 98.7/98.8 (C-4), 130.1/130.6 (C-2), 157.4 (C-3), 171.6/171.7 (C-1); High resolution ESI-MS: observed *m*/*z* 293.1720 $[M+Na]^+$ (calcd for $C_{15}H_{26}O_4Na$, 293.1723); IR (neat): *v* = 3361, 2951, 2924, 2855, 1743, 1466 cm^{-1}.

2-(((S)-8-Methyldecyl)oxy)tetrahydro-2*H*-pyran (**15**)

A suspension of (*S*)-(+)-1-chloro-2-methylbutane (5.00 mL, 41.7 mmol), magnesium (1.01 g, 41.7 mmol), and iodine (50 mg) in THF (20 mL) was refluxed for 45 min. A solution of 0.5 M Li_2CuCl_4 solution in THF (5.00 mL, 2.50 mmol) was added to the mixture at 0 ˚C. And then a solution of tosylate **9** (2.31 g, 6.48 mmol) in THF (9 mL) was added dropwise to the mixture at 0 ˚C, and the mixture was stirred at 0 ˚C for 1 h. Saturated aqueous NH_4Cl (20 mL) was added in a dropwise manner at 0 ˚C, and the mixture was extracted with EtOAc twice. The combined organic phases were washed with brine, dried (Na_2SO_4), filtered, and concentrated under vacuum using a rotary evaporator. The residue was purified by silica gel with hexane-EtOAc (25:1, *v*/*v*) to obtain THP-ether **15** (1.65 g, 99%) as a colorless oil.

Diastereomer mixture: ^{1}H-NMR ($CDCl_3$): δ = 0.83 (d, *J* = 6.4 Hz, 3H), 0.85 (t, *J* = 6.7 Hz, 3H), 1.12 (m, 2H), 1.24–1.36 (m, 12H), 1.53–1.61 (m, 5H), 1.72 (m, 1H), 1.83 (m, 1H), 3.36–3.52 (m, 2H), 3.71–3.90 (m, 2H), 4.58 (t, *J* = 3.5 Hz, 1H), 5.70 (s, 1H); ^{13}C-NMR ($CDCl_3$): δ = 11.4, 19.2, 19.7, 25.5, 26.2, 27.0, 29.5, 29.5, 29.8, 29.9, 30.8, 34.4, 36.6, 62.3, 67.7, 98.8; High resolution ESI-MS: observed *m*/*z* 279.2295 $[M+Na]^+$ (calcd for $C_{16}H_{32}O_2Na$, 279.2295); IR (neat): *v* = 2955, 2924, 2852, 1458, 1377, 1034, 1022 cm^{-1}.

(*S*)-8-Methyldecan-1-ol (**16**)

The THP-ether **15** (1.65 g, 6.43 mmol) was treated in the same manner as described for the preparation of **11** to obtain alcohol **16** (1.10 g, 99%) as a colorless oil.

$[\alpha]_D^{26}$ = +3.50 (*c* = 1.00, $CHCl_3$); ^{1}H-NMR ($CDCl_3$): δ = 0.84 (d, *J* = 6.1 Hz, 3H), 0.85 (t, *J* = 7.3 Hz, 3H), 1.07–1.16 (m, 2H), 1.26-1.36 (m, 11H), 1.56 (m, 2H), 3.62 (t, J=6.7, 2H); ^{13}C-NMR ($CDCl_3$): δ = 11.3, 19.1, 25.7, 27.0, 29.4, 29.9, 32.7, 34.3, 36.6, 62.9; High resolution GC-CI-MS: observed *m*/*z* 171.1744 $[M+Na]^+$ (calcd for $C_{11}H_{23}O$, 171.1749); IR (neat): *v* = 3318, 2959, 2924, 2853, 1458, 1377, 1055 cm^{-1}.

(*S*)-8-Methyldecanal (**17**)

The compound **16** (810 mg, 4.70 mmol) was treated in the same manner as described for the preparation of **12** to obtain **17** (746 mg, 93%) as a colorless oil.

$[\alpha]_D^{27}$ = +0.75 (*c* = 1.00, $CHCl_3$); ^{1}H-NMR ($CDCl_3$): δ = 0.84 (d, *J* = 6.5 Hz, 3H), 0.85 (t, *J* = 7.0 Hz, 3H), 1.07–1.16 (m, 2H), 1.24–1.30 (m, 9H), 1.62 (m, 2H), 2.42 (dt, *J* = 2.4 and 7.3, 2H), 9.77 (t, *J* = 2.4 Hz, 1H); ^{13}C-NMR ($CDCl_3$): δ = 11.4, 19.2, 22.1, 26.9, 29.2, 29.5, 29.7, 34.4, 36.5, 43.9, 203.0; High resolution GC-CI-MS: observed *m*/*z* 171.1751 $[M+H]^+$ (calcd for $C_{10}H_{23}O$, 171.1749); IR (neat): *v* = 2957, 2924, 2855, 1707, 1458, 1412, 1287 cm^{-1}.

(1'*R*,8*S*)-2-(1'-Hydroxyl-8'-methyldecyl)-3-methyl-4-(L-menthyloxy)but-2-en-1,4-olide (**18a**) and (1'*S*,8*S*)-2-(1'-Hydroxyl-8'-methyldecyl)-3-methyl-4-(L-menthyloxy)but-2-en-1,4-olide (**18b**).

Compound **17** (696 mg, 4.09 mmol) and L-menthyloxy-butenolide (962 mg, 3.81 mmol) were treated in the same manner as described for the preparation of **14** to obtain a 2:1 mixture of **18a** and **18b** (806 mg, 50%) as a colorless oil, which was also further separated by flash chromatography.

Compound **18a**: $[\alpha]_D^{23}$ = −70.7 (*c* = 1.71, $CHCl_3$); ^{1}H-NMR ($CDCl_3$): δ = 0.84 (d, *J* = 6.4 Hz, 3H), 0.85 (d, *J* = 7.0 Hz, 3H), 1.24–1.34 (m, 10H), 1.63–1.66 (m, 2H), 1.84 (m, 1H), 1.98 (s, 3H), 2.83 (br, 1H), 4.45 (br, *J* = 7.5 Hz, 1H), 5.70 (s, 1H), menthyl resonances: 0.81 (d, *J* = 6.8 Hz, 3H), 0.86 (m, 1H), 0.88 (d, *J* = 7.1 Hz, 3H), 0.96 (d, *J* = 6.4 Hz, 3H), 1.02 (m, 2H), 1.22–1.27 (m, 1H), 1.28–1.42 (m, 1H), 1.64–1.70 (m, 2H),

2.08–2.14 (m, 2H), 3.62 (dt, J = 4.3 and 11 Hz, 1H); ^{13}C-NMR ($CDCl_3$): δ = 11.4, 11.5, 19.2, 25.5, 27.0, 29.4, 29.5, 29.9, 34.3, 36.6, 36.7, 67.0, 100.9, 130.6, 155.3, 171.4, menthyl resonances: 15.9, 20.8, 22.2, 23.2, 25.4, 31.5, 34.2, 40.5, 47.7, 79.5; High resolution ESI-MS: observed m/z 445.3289 $[M+Na]^+$ (calcd for $C_{26}H_{46}O_4Na$, 445.3288); IR (neat): ν = 2953, 2922, 2868, 2854, 1751, 1456, 1331, 1096, 943 cm^{-1}.

Compound **18b**: $[\alpha]_D^{22}$ = −95.4 (c = 1.00, $CHCl_3$). ^{1}H-NMR ($CDCl_3$): ^{1}H-NMR ($CDCl_3$): δ = 0.84 (d, J = 6.4, 3H), 0.85 (d, J = 7.0, 3H), 1.24-1.34 (m, 10H), 1.63 (m, 2H), 1.83 (m, 1H), 1.98 (s, 3H), 2.77 (br, 1H), 4.47 (br, 1H), 5.71 (s, 1H), menthyl resonances: 0.81 (d, J = 6.8 Hz, 3H), 0.86 (m, 1H), 0.88 (d, J = 7.1 Hz, 3H), 0.96 (d, J = 6.4 Hz, 3H), 1.02 (m, 2H), 1.22-1.27 (m, 1H), 1.28-1.42 (m, 1H), 1.64-1.70 (m, 2H), 2.08-2.14 (m, 2H), 3.62 (dt, J = 4.3 and 11 Hz, 1H); ^{13}C-NMR ($CDCl_3$): δ = 11.4, 11.5, 19.2, 25.6, 27.0, 29.4, 29.5, 29.9, 34.3, 36.5, 66.9, 100.7, 130.7, 155.3, 171.4, menthyl resonances: 15.7, 20.9, 22.2, 23.1, 25.2, 31.4, 34.2, 40.4, 47.7, 79.5; High resolution ESI-MS: observed m/z 445.3287 $[M+Na]^+$ (calcd for $C_{26}H_{46}O_4Na$, 445.3288); IR (neat): ν = 2953, 2922, 2868, 2855, 1751, 1456, 1369, 1331, 1096, 943 cm^{-1}.

6′-deoxo-SRB2a (**6a**)

The compound **18a** (19 mg, 45 μmol) was treated in the same manner as described for the preparation of **5a** to obtain 6′-deoxo-SRB2a (**6a**) (10 mg, 80%) as a colorless oil.

Mixture of C-4 epimers: $[\alpha]_D^{20}$ = +78.3 (*c* = 0.180, $CHCl_3$); ^{1}H-NMR ($CDCl_3$): δ = 0.83 (d, *J* = 6.4 Hz, H-9’’, 3H), 0.86 (t, *J* = 6.7 Hz, H-10’, 3H), 1.07 (m, H-7’a, 1H), 1.12 (m, H-9’a, 1H), 1.28 (m, H-3’a, H-4’, H-5’, H-6′, H-7’b, H-8’, and H-9’b, 10H), 1.40 (m, H-3’b, 1H), 1.66 (m, H-2’a, 1H), 1.81 (br, H-2’b, 1H), 2.07 (s, H-5, 3H), 4.46 (m, H-1’, 1H), 5.85 (brs, H-4, 1H); ^{13}C-NMR ($CDCl_3$): δ = 11.4 (C-10’), 11.4/11.5 (C-5), 19.2 (C-9’’), 25.5 (C-3’), 27.0 (C-6′), 29.4 (C-5’), 29.5 (C-9’), 29.9 (C-4’), 34.4 (C-8’), 36.2 (C-2’), 36.6 (C-7’), 66.8 (C-1’), 98.6/98.7 (C-4), 130.2 (C-2), 157.2 (C-3), 171.5 (C-1); High resolution ESI-MS: observed *m/z*307.1881 $[M+Na]^+$ (calcd for $C_{16}H_{28}O_4Na$, 307.1880); IR (neat): *v* = 3385, 2955, 2924, 2855, 1736 cm^{-1}.

6′-deoxo-SRB2b (**6b**)

The compound **18b** (15 mg, 36 μmol) was treated in the same manner as described for the preparation of **5a** to obtain 6′-deoxo-SRB2b (**6b**) (7.3 mg, 72%) as a colorless oil.

Mixture of C-4 epimers: $[\alpha]_D^{20}$ = –5.09 (*c* = 0.530, $CHCl_3$); ^{1}H-NMR ($CDCl_3$): δ = 0.83 (d, *J* = 6.4 Hz, H-9’’, 3H), 0.86 (t, *J* = 6.7 Hz, H-10’, 3H), 1.07 (m, H-7’a, 1H), 1.12 (m, H-9’a, 1H), 1.28 (m, H-3’a, H-4’, H-5’, H-6′, H-7’b, H-8’, and H-9’b, 10H), 1.40 (m, H-3’b, 1H), 1.66 (m, H-2’a, 1H), 1.81 (br, H-2’b, 1H), 2.07 (s, H-5, 3H), 4.46 (m, H-1’, 1H), 5.85 (brs, H-4, 1H); ^{13}C-NMR ($CDCl_3$): δ = 11.4 (C-10’), 11.4/11.5 (C-5), 19.2 (C-9’’), 25.5 (C-3’), 27.0 (C-6′), 29.3 (C-5’), 29.5 (C-9’), 29.8 (C-4’), 34.3 (C-8’), 36.1/36.4

(C-2'), 36.6 (C-7'), 66.8 (C-1'), 98.5/98.7 (C-4), 130.2/130.7 (C-2), 157.1 (C-3), 171.5 (C-1); High resolution ESI-MS: observed *m*/*z* 307.1880 $[M+Na]^+$ (calcd for $C_{16}H_{28}O_4Na$, 307.1880); IR (neat): ν = 3385, 2955, 2924, 2854, 1736, 1458 cm^{-1}.

1.2.6. Chiral HPLC analysis

Natural Δ*srrO*-SRB1 and Δ*srrO*-SRB2 were analyzed by chiral HPLC with a Chiral MB-S column (4.6 I.D. × 250 mm, microporous silica gel coated with optically active N-substituted polymaleimides; Tokyo Kasei, Co. Ltd., Tokyo, Japan). The mobile phase was composed of two solvents; solvent A is 20% aqueous acetonitrile with 0.1% trifluoroacetic acid and solvent B is 10% aqueous acetonitrile with 0.1% trifluoroacetic acid. The samples were eluted at a flow rate of 1.0 mL/min with detection at 210 nm. The linear-gradient elution program was set as follows: 100% A (0−10 min), 0−100% A (10−25 min), 0−100% A (25−35 min) and 100% A (35−60 min). The injection volume of each sample was 10 μL. 6'-deoxo-SRB1 (**5**) and 6'-deoxo-SRB2 (**6**) from Δ*srrO* were eluted at 21.1 and 53.3 min, respectively. Synthetic **5a**, **5b**, **6a**, and **6b** were eluted at 21.1, 20.2, 53.3, and 50.0 min, respectively.

1.2.7. Gel shift assay

Preparation of a DNA probe containing the promoter region of *srrY* (*srrY*p) and an SrrA protein (SRB receptor), a target gene of SrrA, was described previously [**12**,**33**]. The binding reaction mixture contained the binding buffer (20 mM Tris-HCl [pH 8.0], 100 mM NaCl, 1 mM dithiothreitol, 0.1 mg of bovine serum albumin and 5% glycerol), 0.35 nM labeled DNA, and 2 μM SrrA protein. To analyze the ligand affinity of 6'-deoxo-SRB on the binding of SrrA, several concentrations of synthetic 6'-deoxo-SRBs and SRBs were added to the reaction mixture.

1.2.8. Preparation of the Streptomyces lividans recombinant for SrrO protein

A 1.2-kb PCR fragment containing *srrO* (nt 145,325-144,081 complement of pSLA2-L) was amplified using the template cosmid C7 [**10**] and two primers (NT-srrO-OE-F and NT-srrO-OE-R) (Table 25). The amplified product was digested with *Nde*I and *Hind*III and cloned into pKAR3063H [**35**], a $(His)_6$-tag containing derivative of a constitutive expression vector pHSA81 (Profs. Michihiko Kobayashi and Yoshiteru Hashimoto, personal communication), to give pNTT01 (Figure 21). The *Streptomyces lividans* TK64 recombinant harboring pNTT01 was grown at 28 ˚C for 72 h in YEME liquid medium (34% sucrose) with 10 μg/mL of thiostrepton.

1.2.9. Bioconversion of 6'-deoxo-SRB1 in the SrrO recombinant

Two-day-growth culture (100 mL) of *S. lividans* TK64/pNTT01 (+SrrO) was added 2 μmol of the substrate (6'-deoxo-SRB), and the fed cultures were further incubated for 0–5 h periods. The culture supernatant was extracted with EtOAc twice, and the combined organic phase was dried (Na_2SO_4), filtered, and concentrated under vacuum using a rotary evaporator. The resulting crude extracts were analyzed by ESI-MS and TLC. As a negative control, the cell culture of *S. lividans* TK64/pHSA81 (control) [**41**] was used.

1.3. Results

1.3.1. Construction and metabolite analysis of an srrO mutant KA54

The P450 monooxygenase gene *srrO* was inactivated to investigate the function of *srrO* in SRB biosynthesis. An apramycin resistance gene cassette was introduced into a 5'-terminal region of *srrO*, and double crossover mutant Δ*srrO* (named as KA54) was obtained through homologous recombination. Gene replacement was verified by Southern hybridization experiment. A 4.4-kb *Bsp*EI-*Xho*I fragment in parent strain was changed into two fragments with 2.3-kb and 3.1-kb in Δ*srrO* (Figure 10).

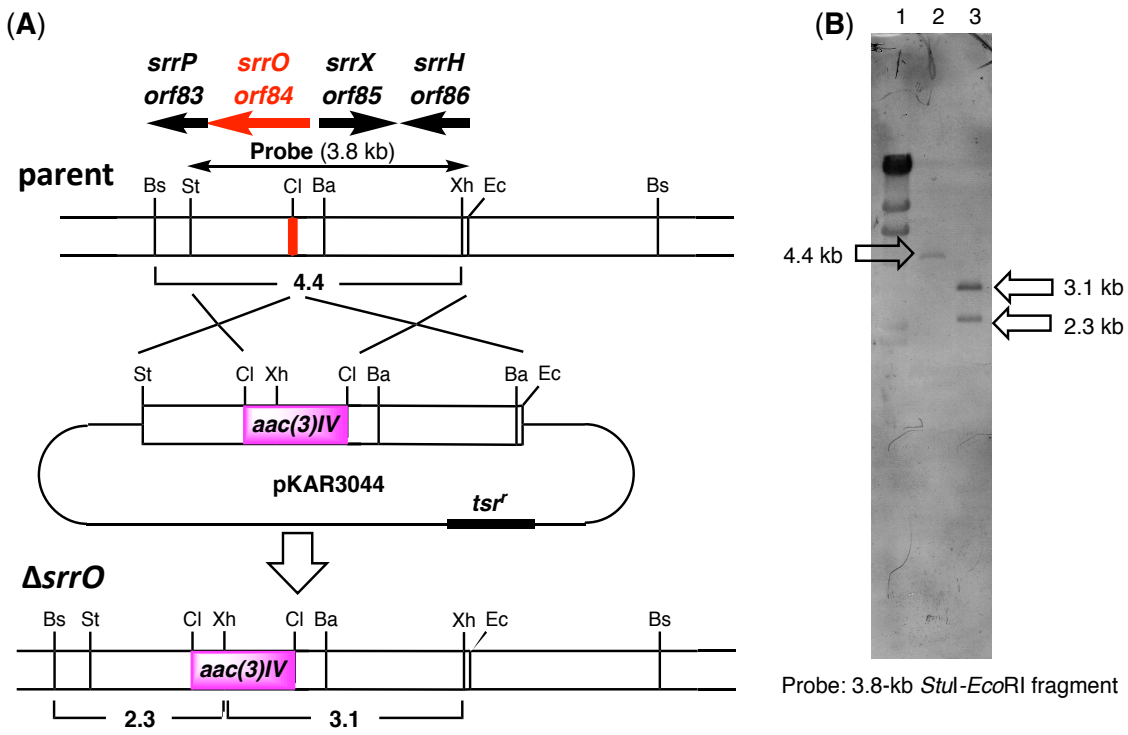

Figure 10. **Gene Disruption of *srrO* (*orf84*)**. (**A**) Construction of the *srrO* mutant strain. St, *Stu*I; Ec, *Eco*RI; Bs, *Bsp*EI; Cl, *Cla*I; Xh, *Xho*I. *aac(3)IV*, apramycin resistance gene cassette; *tsr*, thiostrepton resistance gene cassette. (**B**) Southern hybridization analysis. Lane 1, λ/*Hind*III; lane 2, parent/*Bsp*EI-*Xho*I; lane 3, Δ*srrO*/*Bsp*EI-*Xho*I.

A metabolite profile of Δ*srrO* strain was analyzed in comparison with that of parent strain. As shown in Figure 11, Δ*srrO* produced lankacidin and lankamycin in a comparative level to parent, suggesting that the disruption of the *srrO* showed no effect on the production of lankacidin and lankamycin. This finding let me to consider the following two possibilities; (1) SrrO is not involved in SRB biosynthesis, and (2) the signaling molecule(s) in the Δ*srrO* strain has(have) an ability to induce lankacidin and lankamycin production.

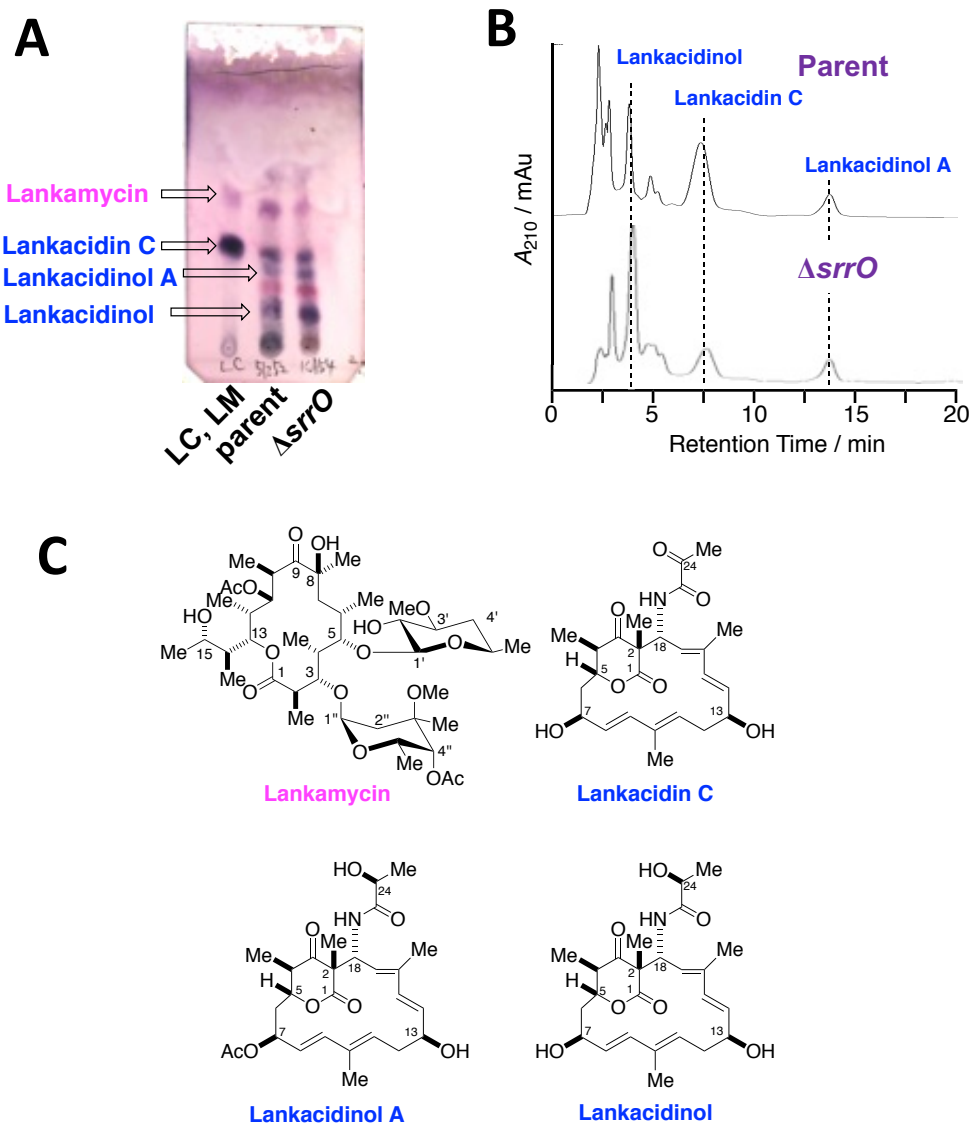

Figure 11. Metabolite analysis of Δ*srrO* strain. (**A**) TLC analysis of metabolites in Δ*srrO* and parent. LC, LM; standard sample of lankacidin C and lankamycin. (**B**) HPLC analysis of metabolites in Δ*srrO* and parent. Chromatogram was monitored by UV absorbance at 230 nm. (**C**) Chemical structures of lankacidin C, lankacidin derivatives and lankamycin. Me, methyl; Ac, acetyl.

1.3.2. Structural elucidation of signaling molecules in KA54

To investigate or evaluate these possibilities mentioned above, I carried out the isolation of signaling molecules in Δ*srrO* (termed as component 1). The Δ*srrO* culture was stopped for a period of 36 hours before the signal molecules were used to induce the production of lankacidin and lankamycin. I extracted metabolites from a 30-L culture with ethyl acetate (EtOAc), and purified the resulting crude extract by the following chromatography with a help of bioassay. The double mutant of *srrX* and the transcriptional repressor gene *srrB*, was used as the signaling molecule indicator strain, because this strain, like the *srrB* mutant, produces two antibiotics in the presence of signal molecules (Figure 12) [**11**, **31**].

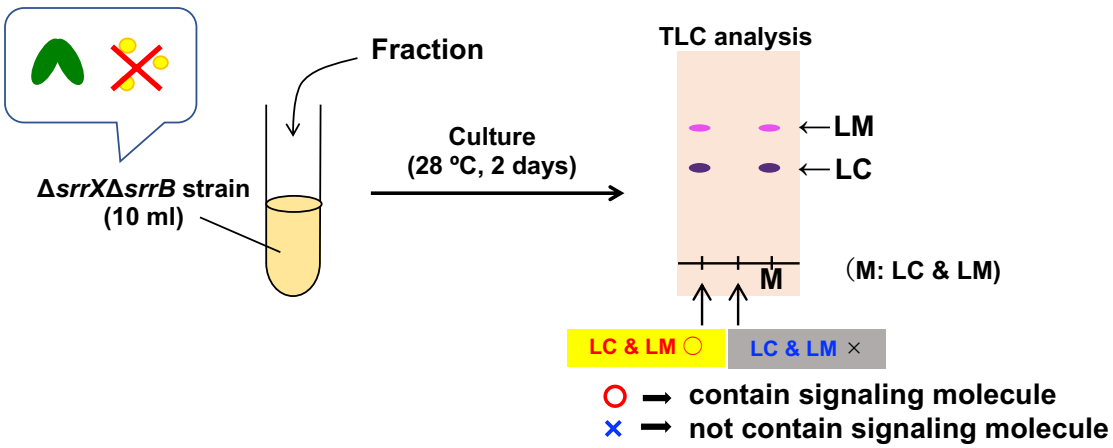

Figure 12. Signaling molecule detection assay

Active fractions were collected and purified by silica gel column chromatography with two different solvent systems of $CHCl_3$-MeOH (50:1, v/v) and toluene-EtOAc (3:1, v/v) (Figure 13).

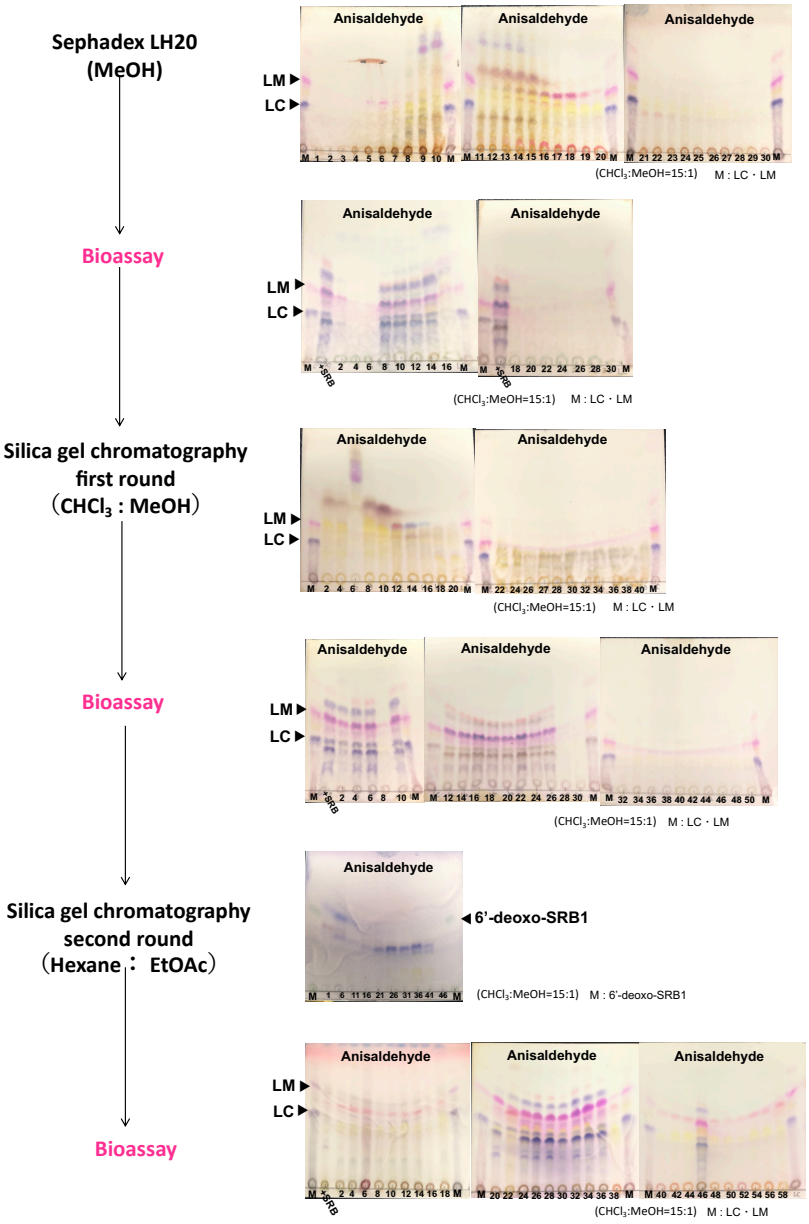

Figure 13. TLC of chromatography fractions and bioassay. (**A**) TLC analysis of Shephadex LH20 fractions and bioassay. (**B**) TLC analysis of silica gel chromatography fractions and bioassay at first round. (**C**) TLC analysis of silica gel chromatography fractions and bioassay at second round.

Then, active components 1 and 2 were separated by repeated runs of HPLC (25% aqueous acetonitrile containing 0.1% trifluoroacetic acid).

The active components were further analyzed by electrospray ionization-mass spectrometry (ESI-MS) analysis. Its spectrum indicated that the presence of two active components in the ratio 1:1 (Figure 14).

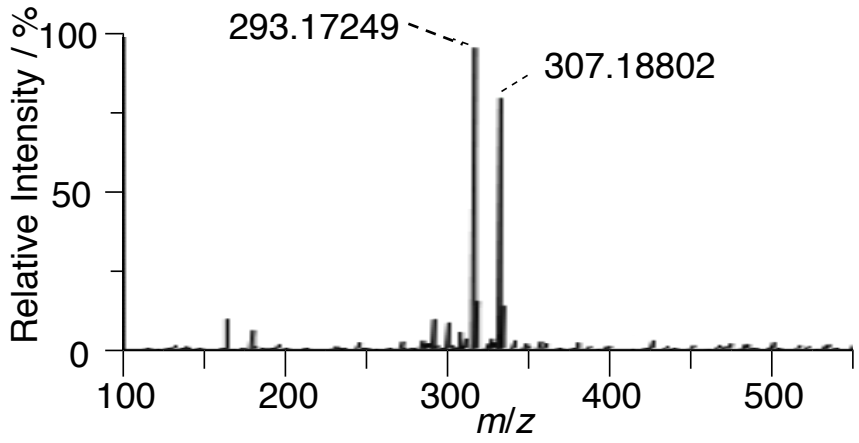

Figure 14. ESI-MS spectrum of active components (1 and 2)

The molecular formulae for active component 1 and active component 2 were established to be $C_{15}H_{26}O_4$ and $C_{16}H_{28}O_4$, respectively. These values were one oxygen smaller and two hydrogen larger when compared with those for SRB1 and SRB2, respectively. Owing to the low amounts of active compounds, I further analyzed their structural assignments as a mixture (component with $C_{15}H_{26}O_4$ was termed as Δ*srrO*-SRB1, while $C_{16}H_{28}O_4$ as Δ*srrO*-SRB2).

Next, the NMR spectra of Δ*srrO*-SRBs were measured and compared with those of SRB1 and SRB2 in parent. ESI-MS analysis suggested that one oxygen atom was replaced with two hydrogens in Δ*srrO*-SRBs. When ^{1}H NMR of Δ*srrO*-SRBs was compared with that of natural SRBs, three signals including a highly deshielded singlet methine proton at δ_H5.87, a deshielded methine proton at δ_H 4.48, and a singlet methyl proton at δ_H 2.07 were conserved (Figure 15). These signals supported the presence of a 2-(1'-hydroxyl-alkyl)-3-methyl-4-hydroxybut-2-en-1,4-olide skeleton (red-color dashed blanket in Figure 15). This butenolide skeleton was further verified by a 2D NMR technique including HMQC and HMBC spectra, which showed a good agreement with our previous report for natural SRBs [**31**]. Concerning the alkyl side chain branched at C-2, methylene proton signals at δ_H 2.26 (doublet), 2.18 (double-doublet), and 2.37–2.40 (multiplet) for C-5' and C-7' in natural SRBs could not be detected in Δ*srrO*-SRBs (Figure 15). Moreover, carbonyl carbon at δ_C 213.1 in natural SRBs could not be detected in HMBC and ^{13}C NMR spectra of Δ*srrO*-SRBs, suggesting the replacement of C-6′ ketone with methylene in Δ*srrO*-SRBs.

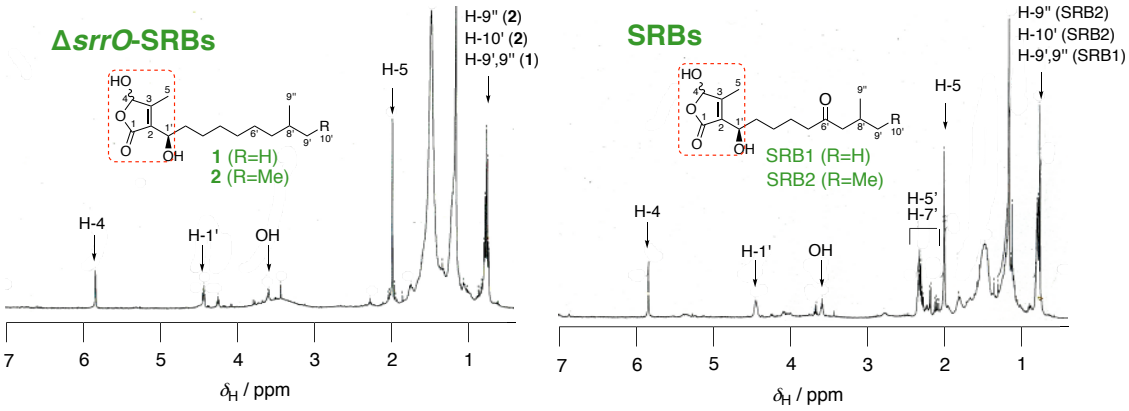

Figure 15. **^{1}H NMR spectrum of Δ*srrO*-SRBs (1 and 2) and SRBs**

Thus, Δ*srrO*-SRB1 and Δ*srrO*-SRB2 were identified as 2-(1'-hydroxyl-8'-methylnonyl)-3-methyl-4-hydroxybut-2-en-1,4-olide (6′-deoxo-SRB1; component 1) and 2-(1'-hydroxyl-8'-methyldecyl)-3-methyl-4-hydroxybut-2-en-1,4-olide (6′-deoxo-SRB2; component 2), respectively (Figure 16).

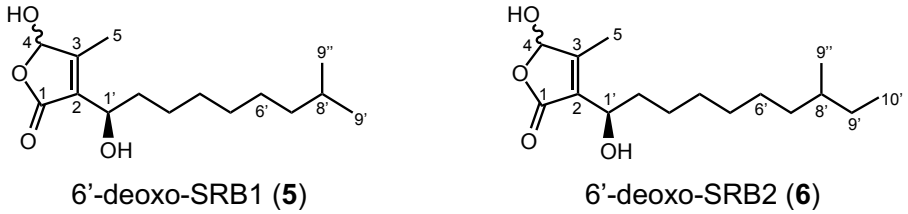

Figure 16. **Structures of 6'-deoxo-SRB (5) and 6'-deoxo-SRB2 (6) isolated from Δ*srrO* of *S. rochei***

1.3.3. Synthesis of 6'-deoxo-SRBs

In order to verify the proposed structures of components 1 and 2, the (1'*R*)-isomers (**5a** and **6a**) and the (1'*S*)-isomers (**5b** and **6b**) were synthesized (Scheme 1).

The commercially available 1,6-hexanediol (**7**) was treated with 1 equivalent of *p*-toluenesulfonyl chloride to give monotosylate **8**, which was then converted to tetrahydropyranyl ether **9** in 95% yield. Compound **9** was subjected to the cross coupling with Grignard reagent isobutylmagnesium bromide in the presence of Li_2CuCl_4 [**42**,**43**], to generate a C_{10} unit (compound **10)** in 99% yield. Hydrolyzing of compound **10** with aqueous HCl formed isodecanol **11** in 91% yield. Alcohol **11** was oxidized with pyridinium chlorochromate (PCC) to give aldehyde **12** in 86% yield, which was subsequently coupled with enantiomerically pure 3-methyl-4-(L-menthyloxy)but-2-en-1,4-olide (**13**) [**31**,**38**,**39**] in the presence of lithium diisopropylamide (LDA) to give a diastereomeric mixture of **14a** and **14b** in the ratio 2:1 in 38% yield. They were separated by repeated runs of flash silica gel chromatography to obtain compounds **14a** and **14b** with over 95% diastereomeric excess based on the peak intensities of hemiacetal H-4 proton signals (δ_H 5.69 for **14a** and δ_H 5.71 for **14b**). In addition, the C-1' configuration was determined using the modified Mosher ester method [**37**]. These isomers **14a** and **14b** were separately deprotected with boron tribromide to form (1'*R*)-6′-deoxo-SRB1 (**5a**) and (1'*S*)-6′-deoxo-SRB1 (**5b**) in 79% and 62% yields, respectively.

6'-deoxo-SRB2a (**6a**) and 6'-deoxo-SRB2b (**6b**) were synthesized in a similar method for the preparation, except for **5a** and **5b**, except for a Grignard reagent, (*S*)-(2-methylbutyl) magnesium chloride, to form a C_{11} unit **15** (Scheme 1B).

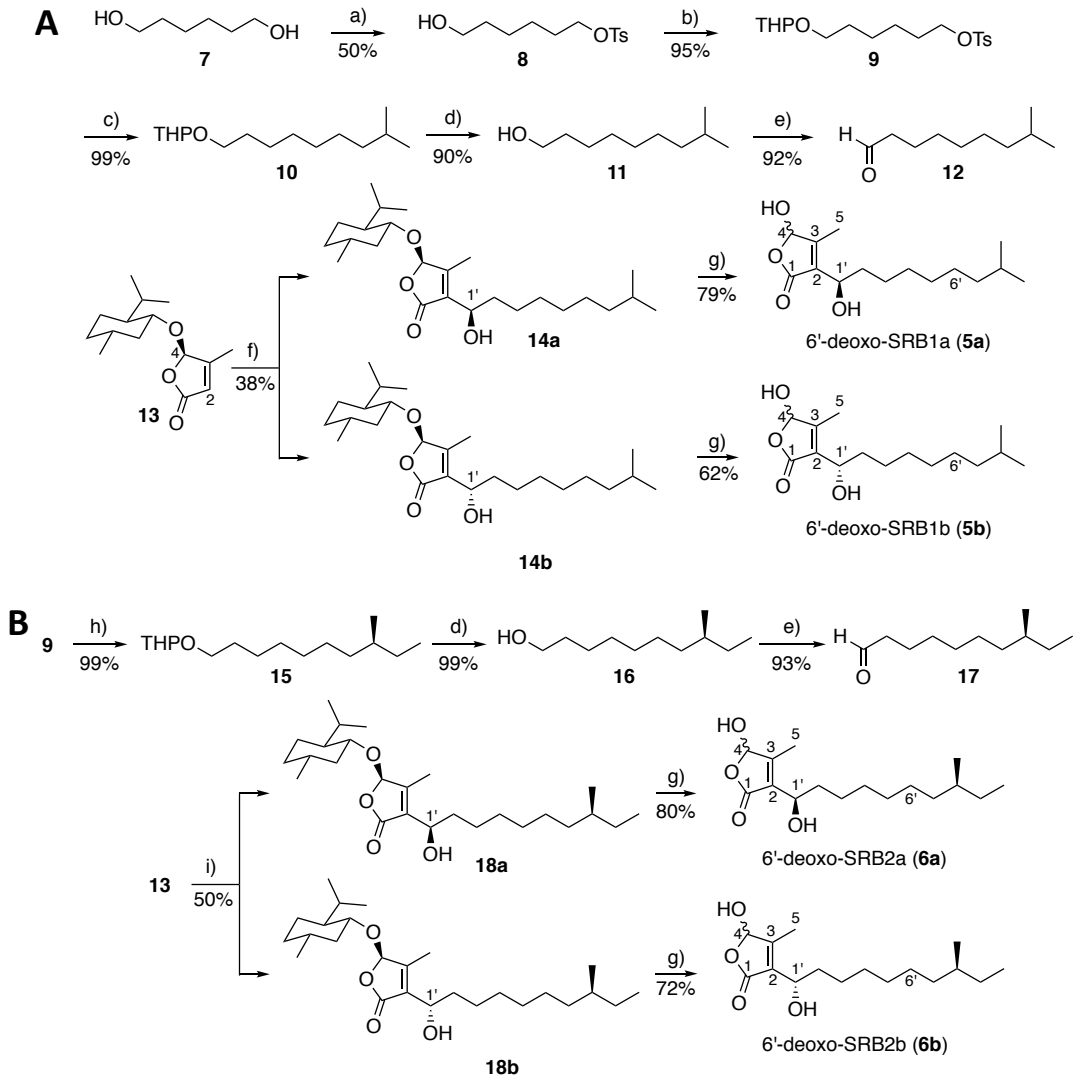

Scheme 1. Synthesis of SRB intermediates (A) 6′-deoxo-SRB1 and (B) 6′-deoxo-SRB2. a) *p*-toluenesulfonyl chloride, Et_3N, 4,4-dimethylamino-pyridine, CH_2Cl_2; b) 3,4-dihydro-2*H*-pyran, *p*-toluenesulfonic acid, CH_2Cl_2; c) isobutylmagnesium bromide, Li_2CuCl_4, THF; d) 2M HCl, THF-MeOH (1:1, *v*/*v*); e) pyridinium chlorochromate, CH_2Cl_2; f) LDA, THF-HMPA, and then **12**; g) BBr_3, CH_2Cl_2; h) (*S*)-(2-methylbutyl)magnesium chloride, Li_2CuCl_4, THF; i) LDA, THF-HMPA, and then **17**.

To confirm the C-1' stereochemistry in compounds 1 and 2 in Δ*srrO* strain, chiral HPLC analysis was performed (Figure 17). Comparative HPLC analysis with chiral column showed that the retention times of compounds 1 and 2 (21.1 and 53.3 min, respectively) were identical to those of the synthetic (1'*R*)-isomers **5a** and **6a**, whereas the synthetic (1'*S*)-isomers **5b** and **6b** eluted slightly earlier at 20.2 and 50.0 min. Thus, the C-1' stereochemistry in 6′-deoxo-SRBs in Δ*srrO* was the same as with SRBs in parent.

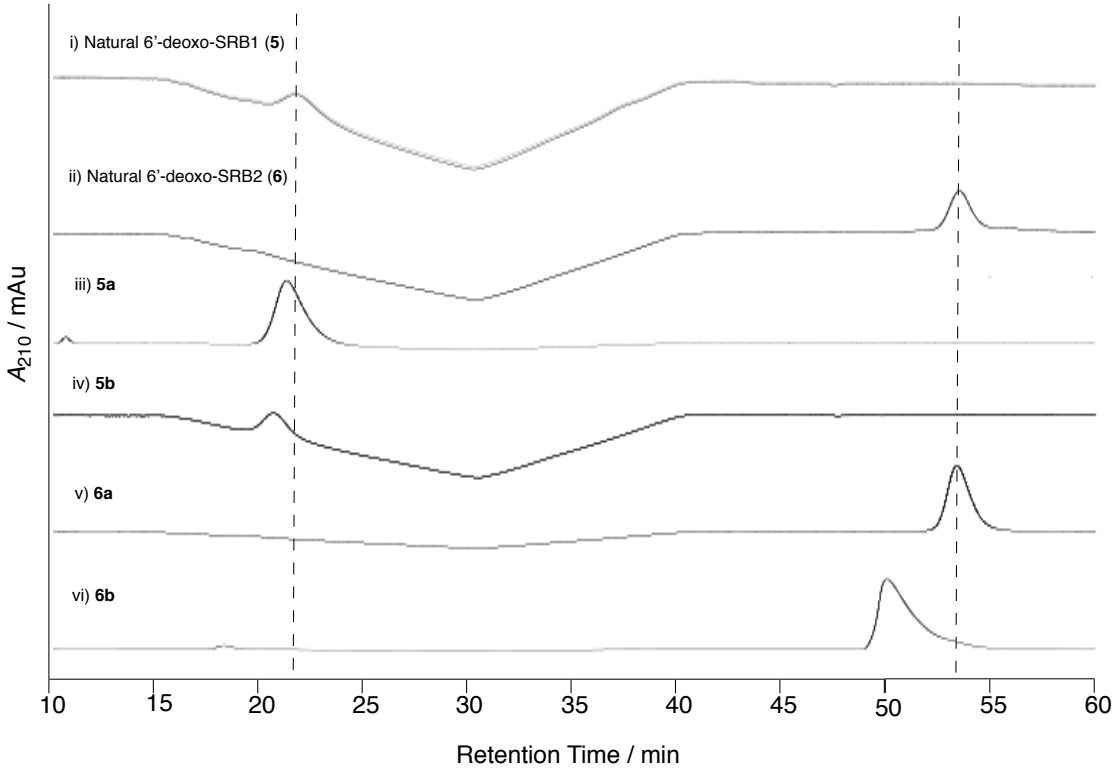

Figure 17. Determination of the C-1' configuration of natural 6′-deoxo-SRBs (1 and 2) isolated from Δ*srrO* strain. Chiral HPLC analysis of i) natural 6′-deoxo-SRB1 (**5**), ii) natural 6′-deoxo-SRB2 (**6**), iii) synthetic **5a**, iv) **5b**, v) **6a**, and vi) **6b**. Elution profiles were monitored by UV absorbance at 210 nm.

1.3.4. Ligand Affinity of 6'-deoxo-SRBs

A bioassay method using the *srrX* mutant was not suitable to compare an antibiotic-inducing activity of SRBs and 6'-deoxo-SRBs. Because 6'-deoxo-SRBs could be converted to SRBs in some extent by SrrO protein expressed in the *srrX* mutant. Antibiotic production is induced by dissociation of signaling molecule-SrrA protein complex from a main target gene *srrY*, an SARP-type activator for lankacidin and lankamycin production in *S. rochei* [**12**] (Figure 6). Therefore, I evaluated the antibiotic-inducing activity of 6′-deoxo-SRBs by minimum concentration to dissociate SrrA protein from a *srrY* gene (Figure 18).

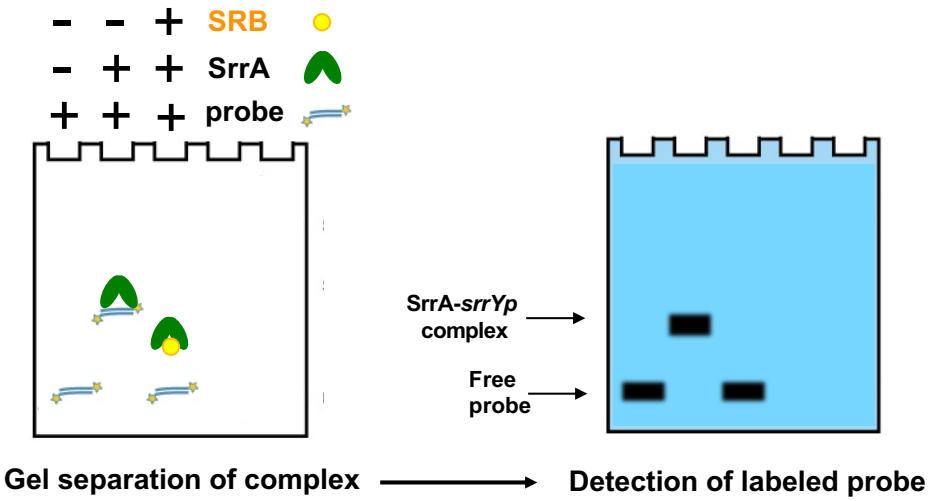

Figure 18. Schematic diagram of gel shift assay

Gel shift assay was performed using a recombinant SrrA protein and a ^{32}P-labeled DNA probe which contained *srrY*-promoter (*srrY*$_p$) region in the presence of either 6′-deoxo-SRB1 or SRB1 (Figure 19A). As shown in Figure 19B, minimum concentration to dissociate SrrA and DNA probe of 6'-deoxo-SRB1 was 100-fold higher than that of SRB1. This finding suggested that C-6' keto group is important for improvement of antibiotic-inducing activity in *S. rochei*.

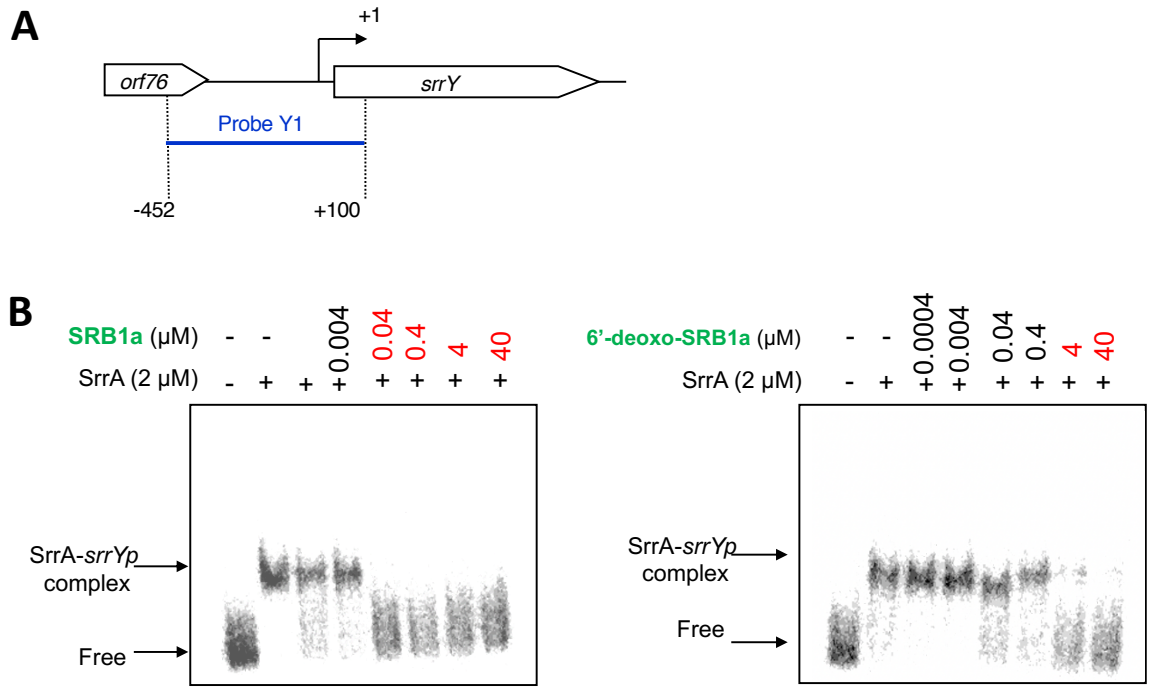

Figure 19. Gel shift assay of SrrA-binding in the upstream region of *srrY*. (**A**) Location of probe Y1 is containing the *srrY*-promoter region (*srrY*$_p$). The description of probe preparation was described previously paper [**12**]. (**B**) Assay of the SRB1 and 6′-deoxo-SRB1 on the binding of SrrA. Each reaction mixture contained 0.35 nM probe Y1 and 2 μM recombinant SrrA protein. To the reaction mixture, various concentrations of either synthetic SRB1 ((1'*R*)-isomer; Figure 1) [**31**] or synthetic 6′-deoxo-SRB1 ((1'*R*)-isomer; Figure 4) was added.

1.3.5. Enzymatic Bioconversion of 6'-deoxo-SRBs by SrrO Protein

The SrrO expression system was constructed to examine the enzymatic conversion of 6'-deoxo-SRBs in *Streptomyces*. The *srrO* gene was cloned into pKAR3063H [**35**], a $(His)_6$-tag derivative of streptomycete constitutive expression vector pHSA81 (Profs. Michihiko Kobayashi and Yoshiteru Hashimoto, personal communication), to afford pNTT01 (Figure 20A). To obtain the recombinant strain, this plasmid was transformed into the heterologous host, *Streptomyces lividans* TK64. I confirmed protein expression of $(His)_6$-SrrO with 45-kDa in size by SDS-PAGE (Figure 20B).

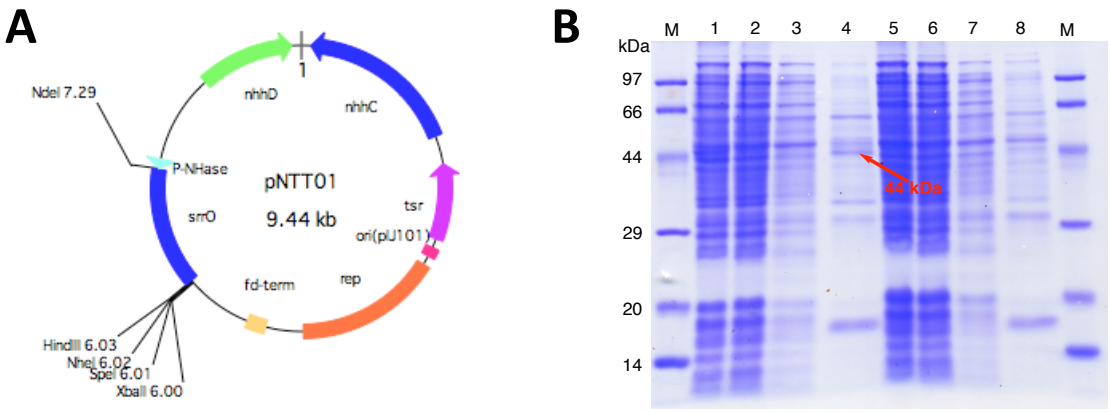

Figure 20. Overexpression of the SrrO protein. (**A**) The vector map of the SrrO overexpression plasmid pNTT01, a vector part of which was pHSA81 derivative (Profs. M. Kobayashi and Y. Hashimoto, personal communication). (**B**) SDS-PAGE of the recombinant SrrO protein expressed in *S. lividans* TK64. Lane M, molecular weight marker; lane 1, flow through of the *S. lividans* TK64/pNTT01 recombinant (+ SrrO); lane 2, cell-free supernatant of the *S. lividans* TK64/pNTT01 recombinant; lane 3, wash fraction of the *S. lividans* TK64/pNTT01 recombinant; lane 4, elution fraction of the *S. lividans* TK64/pNTT01 recombinant; lane 5, cell-free supernatant of the *S. lividans* TK64/pHSA81 recombinant (control); lane 6, flow-through fraction of the *S. lividans* TK64/pHSA81 recombinant; lane 7, wash fraction of the *S. lividans* TK64/pHSA81 recombinant; lane 8, elution fraction of the *S. lividans* TK64/pHSA81 recombinant. Purification of $(His)_6$-tagged protein was performed according to the manufacture's protocol.

Most *Streptomyces* P450 enzymes associate with electron-recycling redox partners, ferredoxin/ferredoxin reductase. As shown in Introduction Section, they flexibly accept heterologous redox partners in other *Streptomyces* [**5**]. Therefore, I performed enzymatic bioconversion of 6'-deoxo-SRB1 (**5**) using the recombinant SrrO protein with a help of heterologous *S. lividans* redox partners. In ESI-MS analysis of the recombinant *S. lividans*

TK64/pNTT01 (Figure 21A(i)), two molecular ion peaks at m/z 307 and 309 were detected. In TLC analysis of the recombinant *S. lividans* TK64/pNTT01 (Figure 21A(ii)), compound 1 (Rf = 0.8 in hexane-EtOAc = 1:2) was converted to two compounds (lane 2); spot A showed a same Rf value with synthetic SRB1 (Rf = 0.5 in hexane-EtOAc = 1:2), while another spot B did lower Rf value (Rf = 0.2 in hexane-EtOAc = 1:2).

As shown in Figure 21B, time-dependent oxidation reaction of compound 1 (6'-deoxo-SRB1) was observed in ESI-MS spectra. Molecular ion peak at 293 ($[M+Na]^+$ = $C_{15}H_{26}O_4Na$) for compound 1 diminished in a time-dependent manner (Figure 21B Panels i-vii), while that at 309 ($[M+Na]^+$ = $C_{15}H_{26}O_5Na$) appeared as a major peak at the 1 h period (Figure 21B Panel ii). After 2 h periods, molecular ion peak at 307 ($[M+Na]^+$ = $C_{15}H_{24}O_5Na$) corresponding to SRB1 became a major peak (Figure 21B Panel iii). Based on the C-6' oxidation degree in SRB biosynthesis, the compound whose molecular ion peak at 309 was estimated to be an intermediate 6'-deoxo-6'-hydroxy-SRB1 (Figure 21C), which possibly corresponded to spot B with lower Rf value on TLC (Figure 21A(ii)). Thus, it was suggested that SrrO converts 6'-deoxo-SRB1 into SRB1 via 6'-deoxo-6'-hydroxy-SRB1 in SRB biosynthesis.

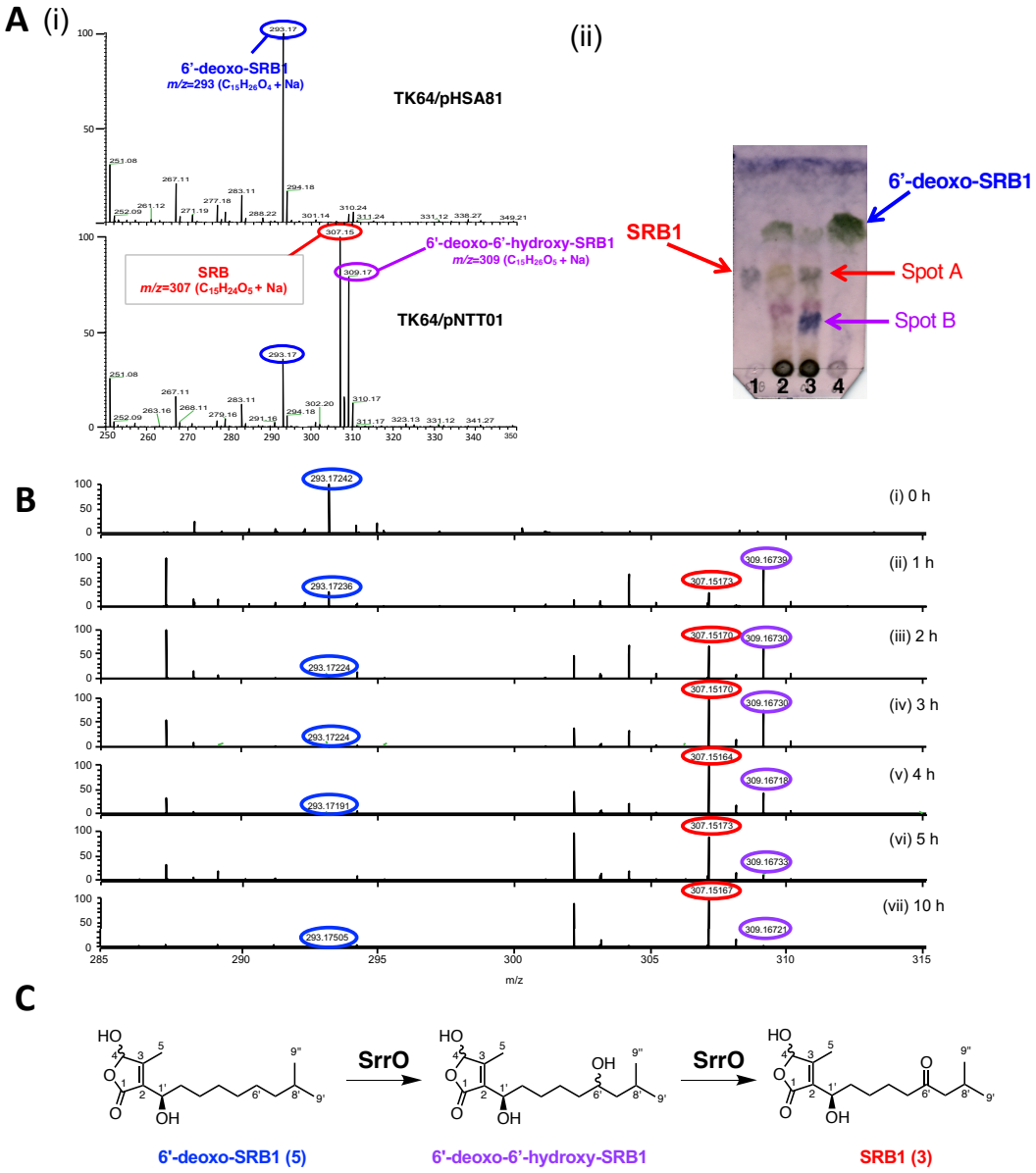

Figure 21. Enzymatic conversion of 6′-deoxo-SRB1 (5) by SrrO in the *Streptomyces lividans* TK64/pNTT01 recombinant. (**A**) (i) ESI-MS spectra of reaction mixture in *S. lividans* TK64/pNTT01 (+SrrO) (upper panel) and *S. lividans* TK64/pHSA81 (control) (down panel). (ii) TLC analysis of reaction mixture. Lane 1, the chemical synthetic SRB1, lane 2, reaction mixture in *S. lividans* TK64/pHSA81; lane 3, reaction mixture in *S. lividans* TK64/pNTT01; lane 4, the chemical synthetic 6′-deoxo-SRB1. Developing solvent of TLC was hexane-EtOAc = 1:2 (v/v), and baked after staining with anisaldehyde. (**B**) ESI-MS spectra of time-course enzymatic conversion of 6′-deoxo-SRB1. Samples were collected at 0, 1, 2, 3, 4, 5, and 10 h periods. (**C**) Scheme for two-stage oxidation of 6′-deoxo-SRB1 by SrrO.

To judge the substrate preference on the C-1' configuration, I performed enzymatic conversion on a mixture of (1'*R*)-6'-deoxo-SRB1 (**5a**) and (1'*S*)-6'-deoxo-SRB1 (**5b**) (Figure 22). In chiral HPLC analysis, a slightly rapid decrease of peak intensity (around 1.3-fold) for **5b** (45.8 min) was detected when compared with that for **5a** (46.6 min). This result suggested that SrrO slightly prefers unnatural (1'*S*)-isomer **5b** to a natural (1'*R*)-isomer **5a**.

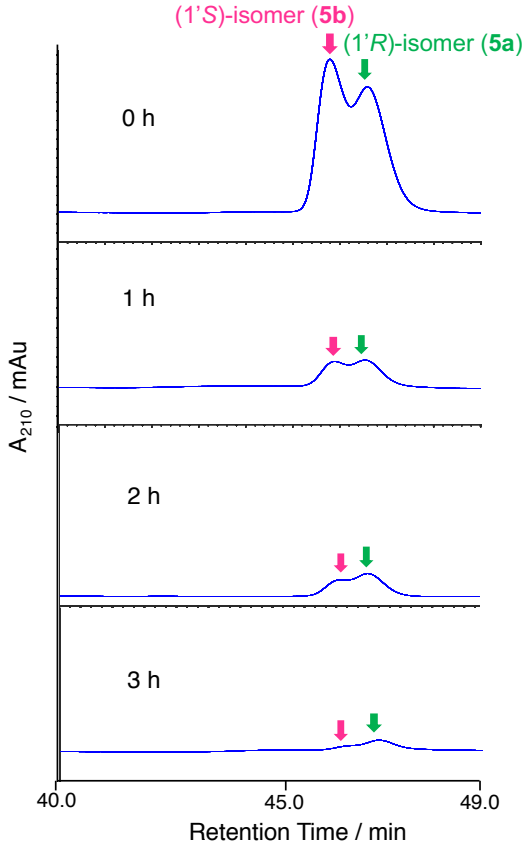

Figure 22. Substrate recognition of the C-1' stereochemistry by SrrO. Conversion efficiency of a mixture of (1'*R*)-isomer 6'-deoxo-SRB1a and (1'*S*)-isomer 6'-deoxo-SRB1b was analyzed by chiral HPLC. Chromatogram was monitored by UV absorbance at 210 nm.

1.4. Discussion

In this chapter, the function of the P450 monooxygenase gene *srrO* in SRB biosynthesis was analyzed through gene disruption, gel-shift assay, and *in vivo* enzymatic conversion. The *srrO* distruptant (Δ*srrO*) produced lankacidin and lankamycin in a comparative yield with the parent, and accumulated novel signaling molecules, 6′-deoxo-SRB1 and 6′-deoxo-SRB2. In chiral HPLC analysis, the C-1’ stereochemistry of 6’-deoxo-SRB1 and 6’-deoxo-SRB2 was *R*. Based on a ligand activity of signaling molecules for dissociation of their receptor SrrA, 6’-deoxo-SRB1 exhibits the 100-fold less binding activity compared with SRB1.

Nevertheless, 6′-deoxo-SRBs could also bind to the specific SRB receptor SrrA, and induce lankacidin and lankamycin production in *S. rochei*. At this time, I have no answer why oxidation of C-6′ methylene to ketone by SrrO took place at the final step in SRB biosynthesis. One of the plausible reasons is an increase of hydrophilic property to improve antibiotic-inducing activity. To my best knowledge, this is a first report to obtain biosynthetic intermediates of signaling molecules in *Streptomyces* species.

SrrO protein catalyzes two-stage oxidation of 6′-deoxo-SRBs via 6′-deoxo-6′-hydroxy-SRBs to form SRBs. The *srrO* recombinant converted 6′-deoxo-SRB1 to SRB1 in a time-dependent manner, whereas the recombinant harboring empty vector pHSA81

(control) was unable to oxidize 6'-deoxo-SRB1 (Figure 21). In addition, the intermediate of oxidation reaction, 6′-deoxo-6′-hydroxy-SRB1 could not be converted to SRB1 in the control recombinant *S. lividans* TK64/pHSA81 (data not shown). Hence, two-stage oxidation is enzymatically catalyzed by SrrO in SRB biosynthesis. SrrO could oxidize the C-6′ methylene group on not only natural (1'*R*)-isomers (6'-deoxo-SRB1a) but unnatural (1'*S*)-isomers (6'-deoxo-SRB1b) (Figure 22). This finding indicated that C-1' stereochemistry of SRBs is strictly controlled at an earlier biosynthetic step, possibly by NAD-dependent dehydrogenase SrrG.

From a genomic analysis of *S. rochei*, several possible genes for SRB biosynthesis and antibiotic regulation were found around SRB biosynthesis gene *srrX* (*orf85*) on pSLA2-L; the NAD-dependent dehydrogenase gene *srrG* (*orf81*), the phosphatase gene *srrP* (*orf83*), the P450 monooxygenase gene *srrO* (*orf84*), and the thioesterase gene *srrH* (*orf86*), together with the repressor genes *srrA* (*orf82*) and *srrB* (*orf79*). The expected biosynthetic pathway of SRBs were shown in Figure 23, based on the homology to biosynthetic pathways for other signaling molecules, A-factor in *S. griseus* [**28**], and virginia butanolides in *S. virginiae* [**44**], and antifungal butenolide gladiofungin (=gladiostatin) in *Burkholderia gladioli* HKI0739/BCC0238 and BCC1622 [**45**,**46**]. Medium-chain β-keto acid (C_{12} or C_{13}) was derived from the fatty acid biosynthesis

pathway, in which four units of malonyl CoA are condensed with either an isobutyryl CoA unit for SRB1 or a 2-methylbutyryl CoA unit for SRB2. These β-keto acid CoA esters are condensed with a C_3 unit (a hydrate form of glyceraldehyde 3-phosphate) by SrrX, then followed by spontaneous dephosphorylation, dehydroxylation, and intramolecular aldol condensation to generate the butenolide skeleton. The C-1' ketone group in butenolide intermediate will be regio- and stereospecifically reduced to a hydroxyl group by dehydrogenase SrrG to synthesize 6′-deoxo-SRBs. Finally, the two-stage oxidation by SrrO is taken place to form SRBs.

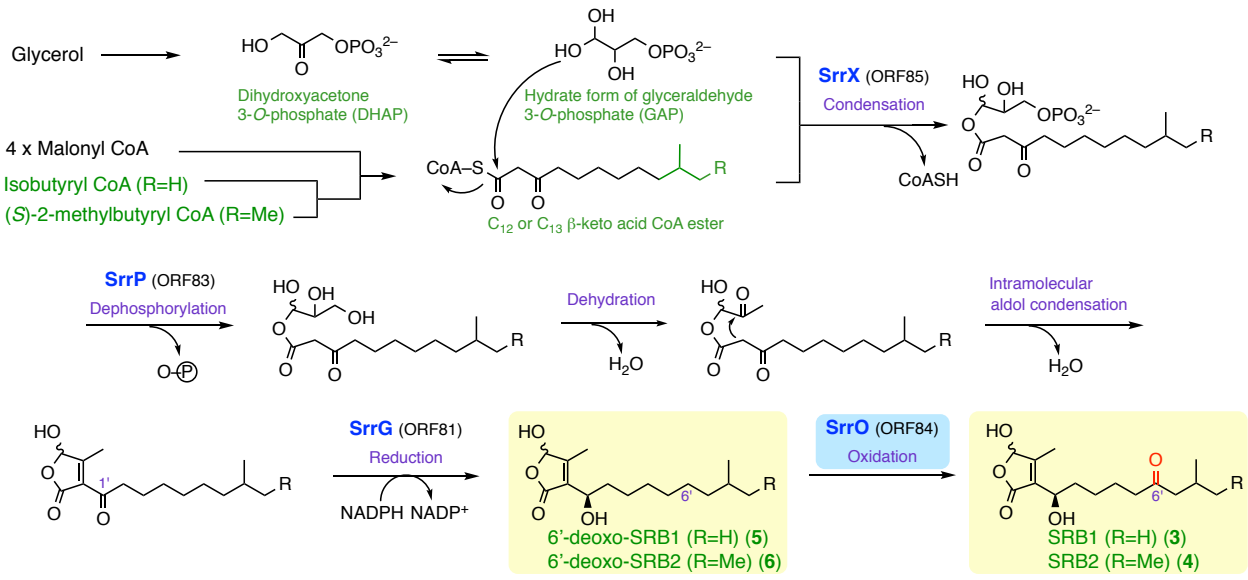

Figure 23. The expected biosynthetic pathway of SRBs in *S. rochei*

Me; methyl.

Chapter 2

Analysis of two cytochrome P450 monooxygenases involved in lankamycin biosynthesis in *Streptomyces rochei*

2.1. Introduction

Macrolide antibiotics are an important class of secondary metabolites that are clinically used for the treatment of bacterial infectious diseases [**47**]. Macrolides are generally assembled by modular polyketide synthases (PKSs) and consist of large-membered macrolactone skeletons. In many cases, macrolides harbor several deoxysugar moieties, which are attached by specific glycosyltransferases [**48**]. Furthermore, macrolides contain hydroxyl groups in their skeletons, many of which are introduced by cytochrome P450 enzymes [**4**].

Lankamycin (**2**; Figure 5) is a 14-membered macrolide antibiotic with moderate antibacterial activity against Gram-positive bacteria [**49**]. *Streptomyces rochei* 7434AN4 produces lankamycin (**2**) together with lankacidin (Figure 5), a 17-membered carbocyclic polyketide with significant antimicrobial [**50**] and microtubule-stabilizing activities [**51,52**]. Crystallographic analysis revealed that both antibiotics inhibit peptide synthesis synergistically by targeting the neighboring sites in the large bacterial ribosomal subunit [**53**,**54**]. Mochizuki *et al*. revealed that the lankamycin biosynthetic gene (*lkm*) cluster is located on the largest linear plasmid pSLA2-L (210 614 bp) [**10**]. Two cytochrome P450 monooxygenase genes, *lkmF* (*orf26*) and *lkmK* (*orf37*), and two glycosyltransferase genes,

lkmI (*orf31*) and *lkmL* (*orf40*), are coded as post-PKS modification enzymes in the *lkm* cluster on pSLA2-L (Figure 24).

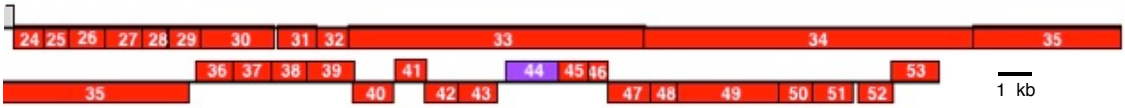

LkmD	ORF24	NDP-hexose 4,6-dehydratase
LkmE	ORF25	thioesterase
LkmF	ORF26	P450-like hydroxylase
LkmBIII	ORF27	NDP-4-keto-2,6-dideoxyhexose 3-C-methyltransferase
LkmG	ORF28	NDP-hexose 3-O-methyltransferase
LkmBII	ORF29	NDP-4-keto-2,6-dideoxyhexose 2,3-enoyl reductase
LkmH	ORF30	b-glycosidase
LkmI	ORF31	glycosyltransferase
LkmCII	ORF32	NDP-4-keto-6-deoxyhexose 3,4-isomerase
LkmAIII	ORF33	type-I PKS (module 5 and 6) (KS5, AT5, KR5, ACP5,KS6, AT6, KR6, ACP6, TE)
LkmAII	ORF34	type-I PKS (module 3 and 4) (KS3, AT3, KR3*, ACP3,KS4, AT4, KR4, DH4, ER4, ACP4)
LkmAI	ORF35	type-I PKS (Loading domain, module 1 and 2) (AT0, ACP0, KS1, AT1, KR1, ACP1, KS2, AT2, KR2, ACP2)
LkmJ	ORF36	O-acyltransferase
LkmK	ORF37	P450-like hydroxylase
LkmCIV	ORF38	NDP-6-deoxyhexose 3,4-dehydratase
LkmCV	ORF39	NDP-4,6-dideoxyhexose 3,4-enoyl reductase
LkmL	ORF40	glycosyltransferase
LkmBIV	ORF41	NDP-3-methyl-4-keto-2,6-dideoxyhexose 4-ketoreductase
LkmCVI	ORF42	NDP-3-keto-6-deoxyhexose 3-ketoreductase
LkmM	ORF43	glycosyltransferase
LkmN	ORF44	ABC transporter
LkmO	ORF45	NDP-hexose 3-O-methyltransferase
LkmEVII	ORF46	NDP-4-keto-6-deoxyhexose 3,5-epimerase
LkmP	ORF47	adenosylhomocysteinase
LkmQ	ORF48	5,10-methylenetetrahydrofolate reductase
LkmR	ORF49	5-methyltetrahydrofolate-homocysteine S-methyltransferase
LkmS	ORF50	glucose kinase
LkmT	ORF51	S-adenosylmethionine synthase
LkmU	ORF52	NDP-glucose synthase
LkmBVI	ORF53	NDP-4-keto-6-deoxyhexose 2,3-dehydratase

Figure 24. Gene organization of *lkm* cluster on pSLA2-L

To determine the post-PKS biosynthesis pathway of lankamycin, these genes were inactivated, and their metabolites were analyzed [**34**,**55**]. The *lkmF*-disrupted strain accumulated 8-deoxylankamycin (**19**), while the *lkmK*-disrupted strain did 15-deoxylankamycin (**20**) and 8,15-dideoxylankamycin (**21**). This finding indicates that LkmF is a C-8 monooxygenase and LkmK is a C-15 monooxygenase in lankamycin biosynthesis. Production of **21** in the *lkmK*-disrupted strain indicated that C-15

hydroxylation by LkmK occurred first and then C-8 hydroxylation by LkmF occurred. On the other hand, the *lkmI* disruption led to accumulate 3-*O*-L-arcanosyllankanolide (**22**), while the *lkmL*-disrupted strain produced 8-deoxylankanolide (**23**). The structures of these metabolites revealed that LkmI transfers D-chalcose to the C-5 hydroxyl and LkmL does L-arcanose to the C-3 hydroxyl during lankamycin biosynthesis in *S. rochei*. Production of two aglycons in *lkmL* mutant suggested that LkmI could transfer D-chalcose to the C-5 hydroxyl only in the presence of L-arcanose moiety at C-3. Based on these results, we proposed a post-PKS biosynthetic pathway of lankamycin including two hydroxylation and two glycosylation steps (Figure 26) [**55**,**56**]. Aglycone 8,15-dideoxylankanolide (**24**) is first hydroxylated at C-15 by LkmK to produce 8-deoxylankanolide (**23**), which is then attached with L-arcanose at the C-3 hydroxyl by LkmL to form 3-*O*-L-arcanosyl-8-deoxylankanolide (**25**). This monoglycoside **25** is further hydroxylated at C-8 by LkmF to give 3-*O*-L-arcanosyl lankanolide (**22**), attached with D-chalcose at the C-5 hydroxyl by LkmI, and finally acetylated at C-4″ and C-11 hydroxyls to afford lankamycin (**2**).

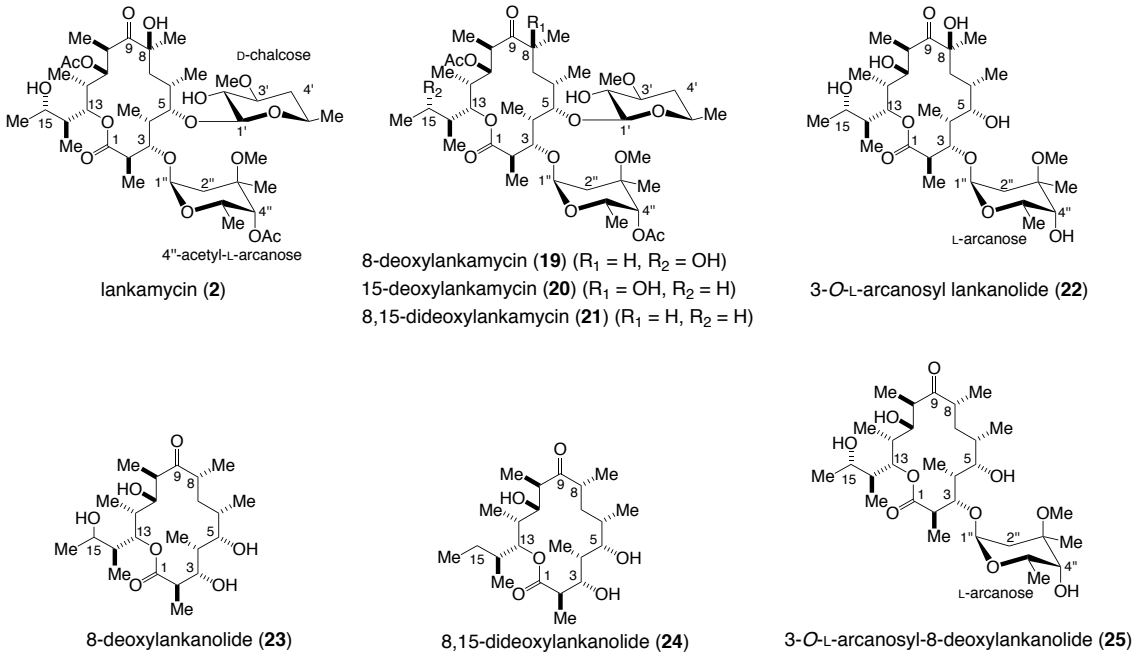

Figure 25. Structures of lankamycin and its derivatives. lankamycin (**2**), 8-deoxylankamycin (**19**), 15-deoxylankamycin (**20**), 8,15-dideoxylankamycin (**21**), 3-*O*-L-arcanosyllankanolide (**22**), 8-deoxylankanolide (**23**), 8,15-dideoxylankanolide (**24**), and 3-*O*-L-arcanosyl-8-deoxylankanolide (**25**). Ac, acetyl; Me, methyl.

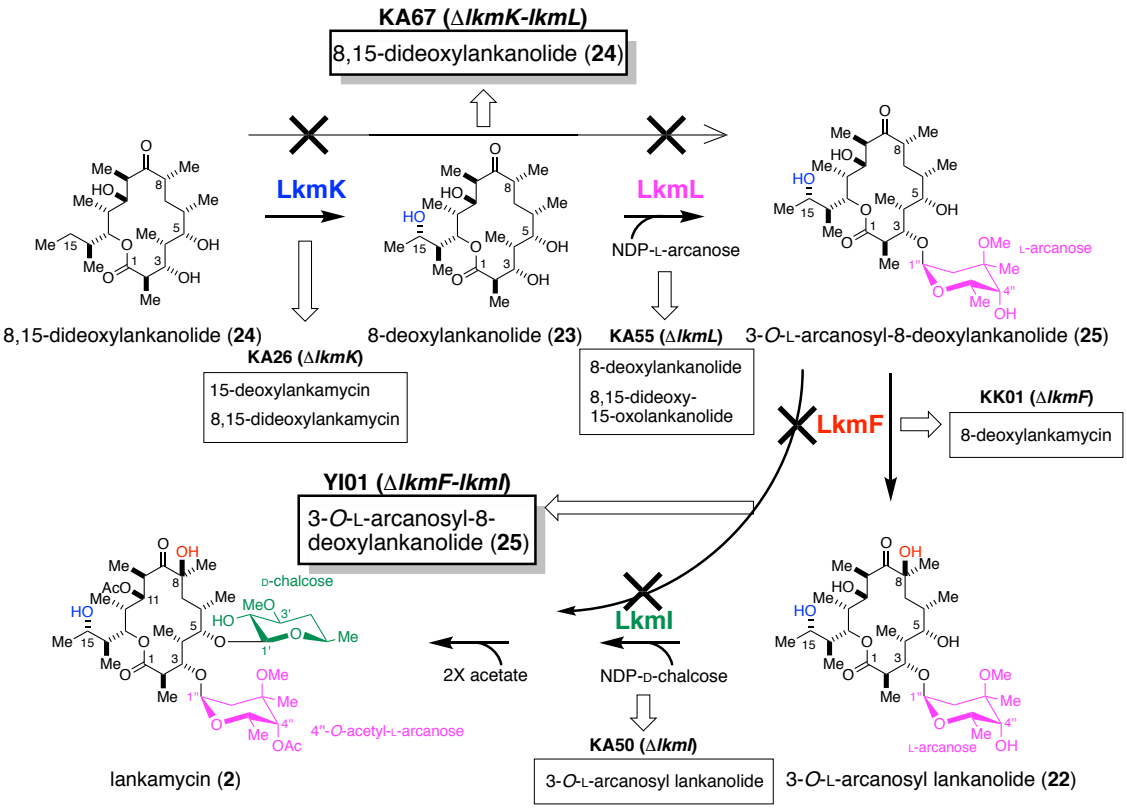

Figure 26. Possible post-PKS biosynthetic pathway of lankamycin. Compounds in the boxes are metabolites produced by each disrupted-strain indicated above. Strains KA26 and KA28 (Δ*lkmK*) accumulated both 15-deoxylankamycin (**20**) and 8,15-dideoxylankamycin (**21**), while strain KK01 (Δ*lkmF*) did 8-deoxylankamycin (**19**). Strain KA55 (Δ*lkmL*) accumulated 8-deoxylankanolide (**23**), while strain KA50 (Δ*lkmI*) did 3-*O*-L-arcanosyllankanolide (**22**).

Antimicrobial activity of the three deoxylankamycins (compound **19**-**21**) produced by *lkmK*-disrupted strain and *lkmF*-disrupted strain were tested against *Micrococcus luteus* (Figure 27) [**34**]. Compared with lankamycin (compound **2**, 100%), they showed decreased antimicrobial activity in the reverse order of the number of hydroxyl groups; (compound **19**, 50% activity; compound **20**, 18% activity; compound **21**, 2.5% activity).

This result suggests the importance of hydroxyl groups in lankamycin skeleton for their antimicrobial activity.

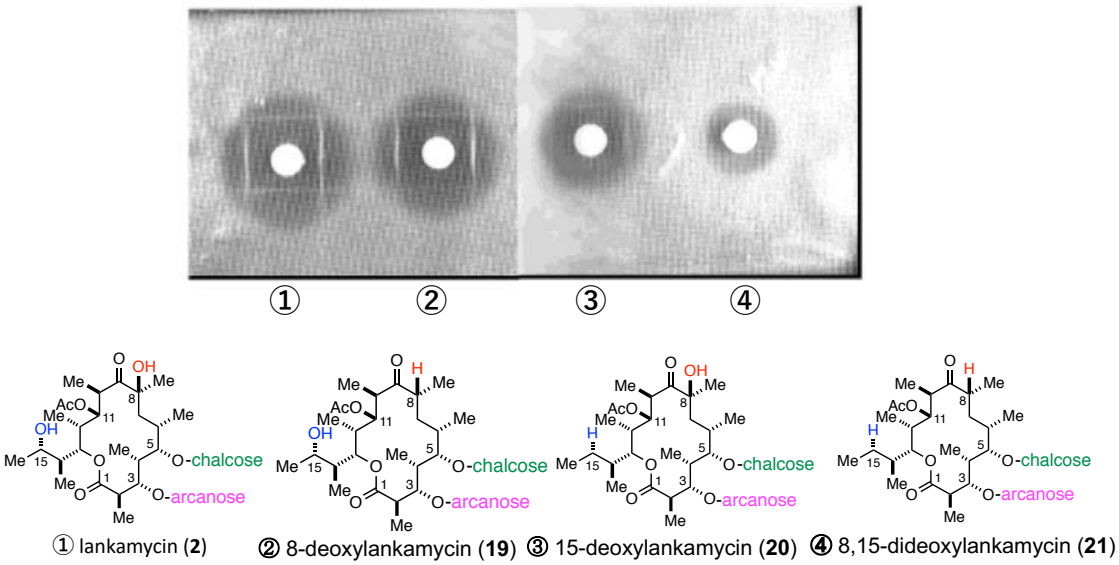

Figure 27. Antimicrobial activities of lankamycin and deoxylankamycins. ① lankamycin (**2**); ② 8-deoxylankamycin (**19**); ③ 15-deoxylankamycin (**20**); ④ 8,15-dideoxylankamycin (**21**). Me, methyl; Ac, acetyl.

In this chapter, I constructed two double mutants of P450 genes in combination with glycosyltransferase genes. In addition, the function of two P450 enzymes, LkmF and LkmK, was also extensively investigated to determine the gross biosynthetic pathway to evaluate their substrate specificity.

2.2. Materials and methods

2.2.1. Strains and reagents

All strains and plasmids used in this chapter were listed in Table 26. Strain KA28, an *lkmK* mutant of strain KA07 (*srrB* mutation) [**11**], was constructed in a similar manipulation for the construction of strain KA26, an *lkmK* mutant of strain 51252. Strain KA28 was used as a parent strain for the *lkmK–lkmL* double mutant. Strain KA50 [**55**], an *lkmI* mutant of strain 51252, was used as a parent for the *lkmF–lkmI* double mutant.

Table 26. Bacterial strains, plasmids, and oligonucleotides used in chapter 2

Strains/plasmids/oligonucleotides	Properties/product	Source/ref. [*1]
Strains		
Streptomyces rochei		
7434AN4	Producer of **1, 2**; Wild type (pSLA2-L,M,S)	[9]
51252	Producer of **1, 2**; pSLA2-L	[9]
KA07	Producer of **1, 2**; Δ*srrB* in strain 51252	[11]
KK01	Producer of **19**; *lkmK*::*kan* in strain 51252	[34]
KA26	Producer of **20** and **21**; *lkmK*::*kan* in strain 51252	[34]
KA28	Producer of **20** and **21**; *lkmK*::*kan* in strain KA07	This study
KA50	Producer of **22**; *lkmI*::*kan* in strain 51252	[55]
KA55	Producer of **23**; *lkmL*::*kan* in strain KA07	[55]
KA67	Producer of **24**; *lkmL*::*kan* in strain KA28	This study
YI01	Producer of **25**; Δ*lkmF* in strain KA50	This study
Streptomyces lividans		
TK64	*pro-2*, *str-6*	[15]
TK64/pYK01	Strain TK64 with plasmid pYY03, *tsr*, $(His)_6$-tagged *lkmF*	This study
TK64/pHSA81	Strain TK64 with plasmid pHSA81, *tsr*	[33]
Escherichia coli		
XL1-Blue	*recA1 endA1 gyrA96 thi-1 hsdR17 supE44 relA1 lac* [F'*proAB lacI*^{q}*ZΔM15* Tn*10* (*tet*)]	Stratagene
BL21(DE3)	F$^-$ *ompT hsdS*$_B$ (r_B^- m_B^-) *gal dcm* (DE3)	Novagen
Plasmids		
SuperCos-1	Cosmid vector, *amp*, *kan*	Stratagene
cosmid 14F1	35.3-kb pSLA2-L DNA (nt 73,334-108,629) cloned into SuperCos-1 at *Bam*HI site	[10]
cosmid B10	45.4-kb pSLA2-L DNA (nt 3,341-48,756) cloned into SuperCos-1 at *Bam*HI site	[10]
pRES18	*E. coli-Streptomyces* shuttle vector, *amp*, *tsr*, *lacZ*-α	[36]
pKAR2015	5.6-kb *Pst*I-*Bam*HI fragment carrying *lkmL*::*kan* in pRES18	[55]
pKK2601	3.0-kb *Bam*HI fragment containing *lkmF* in pUC19	[34]
pKAR2016	0.7-kb *Nru*I-*Aor*51HI fragment eliminated from pKK2601	This study
pKAR2017	2.3-kb *Bam*HI fragment carrying Δ*lkmF* in pRES18	This study
pCYP-camAB	pET11a derivative, *camA*, *camB*, *amp*, *lacI*	[57]
pCYP101-AB1	1.2 kb *Nde*I-*Spe*I PCR fragment carrying *lkmK* (primers; lkmK-f and lkmK-r) cloned into pCYP-camAB	This study
pHSA81	Constitutive expression vector in *Streptomyces*, *tsr*	M. Kobayashi
pYK01	1.2 kb *Nde*I-*Bam*HI PCR fragment carrying *lkmF* cloned into pHSA81	This study
Designed oligonucleotides		
lkmK-f	5'-GACATATGAACCAGCCGCAACTG-3'	This study
lkmK-r	5'-ATACTAGTCACCCCCAGGAGACGGGCAG-3'	This study
YK-LkmF-f1	5'-GTAAGCTTCATATGACGACTGACGC-3'	This study
YK-LkmF-r2	5'-TCTGGATCCTCATCGCCCCAGCCTCCACG-3'	This study

*1 ; Reference numbers are identical with those indicated in main text.

2.2.2. Construction of plasmid for an lkmK–lkmL double mutant KA67

A targeting plasmid pKAR2015 (*lkmL*::*kan*^{R}) was constructed previously [**55**]. This plasmid was introduced into protoplast of the *lkmK* mutant KA28.

2.2.3. Construction of plasmid for an lkmF–lkmI double mutant YI01

A 0.7-kb *Nru*I-*Aor*51HI fragment containing the *lkmF* gene was eliminated from plasmid pKK2601 [**34**] to afford pKAR2016. The vector part of pKAR2016 was replaced by pRES18, an *E. coli–Streptomyces* shuttle vector [**36**], to give a targeting plasmid pKAR2017 (*lkmF*). This plasmid was then introduced into protoplast of the *lkmI* mutant KA50.

2.2.4. Construction procedure for mutants KA67 and YI01

Gene disrupted strains were obtained through homologous recombination as described previously [**37**]. Gene replacement was confirmed by Southern hybridization experiment using DIG DNA Labeling and Detection Kit (Roche Diagnostics, Rotkreuz, Switzerland) according to the manufacturer's protocol. The double-knockout mutants of *lkmK–lkmL* and *lkmF–lkmI* were named as KA67 and YI01, respectively.

2.2.5. Analysis of metabolites

Metabolites were analyzed by thin layer chromatography (TLC) and electrospray ionization-mass spectrometry (ESI-MS). TLC was developed with a mixture of $CHCl_3$-methanol (15:1, v/v) and baked after spraying with anisaldehyde-H_2SO_4. ESI-MS spectra were recorded on an LTQ Orbitrap XL mass spectrometer (Thermo Fisher Scientific, Waltham, MA, USA).

2.2.6. Isolation of metabolites

Strains were cultured in YM liquid medium at 28 °C for 3 days, and the supernatant was extracted twice with the same volume of EtOAc. The combined organic phase was dried with Na_2SO_4, filtered, and concentrated to dryness. The resulting crude extract was subjected to Sephadex LH-20 (GE Healthcare, Chicago, USA) gel filtration chromatography with methanol. The fractions containing lankamycin derivatives were collected and purified by silica gel chromatography with two different solvent systems of $CHCl_3$-methanol = 100:1-30:1 (v/v) and toluene-EtOAc = 1:3 (v/v). The ^{1}H and ^{13}C NMR assignments for 8,15-dideoxylankanolide (**24**) and 3-*O*-L-arcanosyl-8-deoxylankanolide (**25**) are shown in Table 27. Average yield of **24** from strain KA67 and **25** from strain YI01 were 3.3 and 0.5 mg/L, respectively.

2.2.7. Preparation of the E. coli recombinant for LkmK protein

A 1.2-kb PCR fragment containing *lkmK* (nt 87 725-88 939 of pSLA2-L) was amplified using the template cosmid B10 [**10**] and two primers, lkmK-f and lkmK-r (Table 26). The PCR fragment was digested with *Nde*I and *Spe*I and cloned into pCYPcamAB [**57**], an inducible expression vector carrying putidaredoxin reductase (*camA*)/putidaredoxin (*camB*) genes, to give pCYP101-AB1.

2.2.8. Preparation of the S. lividans recombinant for LkmF protein

A 1.2-kb PCR fragment containing *lkmF* (nt 44 847-46 067 of pSLA2-L) was amplified using the template cosmid B10 [**10**] and two primers, YK-LkmF-f1 and YK-LkmF-r2 (Table 26). The PCR fragment was digested with *Nde*I and *Bam*HI and cloned into pHSA81 (Prof. Kobayashi and Hashimoto, pers. comm.), a constitutive expression vector for Actinomycetes, to afford pYK01. The *S. lividans* TK64 recombinant harboring pYK01 was grown at 28 ˚C for 72 h in YEME liquid medium (34% sucrose) with 10 μg/mL of thiostrepton.

2.2.9. Bioconversion of 15-deoxy compounds in the LkmK recombinant (E. coli)

Escherichia coli BL21(DE3)/pCYP101-AB1 (+LkmK) was cultured in M9 mix medium (6.78 g/L Na_2HPO_4 , 3 g/L KH_2PO_4 , 0.5 g/L NaCl, 1 g/L NH_4Cl, 1% casamino acid, 0.4% D-glucose, 0.1 mM $CaCl_2$, 1 mM $MgCl_2$, 0.1 mM $FeSO_4$, 20 mg/L thymine, 80 mg/L 5-aminolevulinic acid) supplemented with ampicillin (100 μg/mL) at 37 °C. When the cell density (optical density at 600 nm [OD_{600}]) reached 0.8, isopropyl *β*-D-thiogalactopyranoside (0.1 mM as final concentration) was added to the culture medium to induce gene expression. The mixture was further incubated at 22 ˚C overnight.

Cells were collected by centrifugation, and the resultant was suspended with 25 ml of CV-2 mM DTT buffer (50 mM NaH_2PO_4, 1 mM EDTA, 10% glycerol, and 1 mM D-glucose were autoclaved, and then 2 mM DTT was added). The suspension was added 2 μmol of the substrate. After incubation at 28 ˚C for 24 h, the mixture was extracted with equal volume of EtOAc twice. The combined organic phase was concentrated under vacuum using a rotary evaporator and then analyzed by TLC and ESI-MS. The cell culture of *E. coli* BL21(DE3)/pCYPcamAB (control) was also used for negative control. Substrate specificity was investigated by varying the substrate (**20**, **21**, **24**).

2.2.10. Bioconversion of 8-deoxy compounds in the LkmF recombinant (S. lividans)

To a two-day-growth culture (100 ml) of *S. lividans* TK64/pYK01 (+LkmF) was added 2 μmol of the substrate, and the fed cultures were further incubated for 24 h. The culture supernatant was extracted with EtOAc twice, and the combined organic phase was dried (Na_2SO_4), filtered, and concentrated under vacuum using a rotary evaporator. The crude extracts were analyzed by TLC and ESI-MS. The cell culture of *S. lividans* TK64/pHSA81 (control) was also used for negative control. Substrate specificity was investigated by varying the substrate (**19**, **21**, **23-25**).

2.3. Results

2.3.1. Isolation of possible biosynthetic intermediates for lankamycin from the lkmK-lkmL and lkmF–lkmI double-knockout mutants

To obtain an aglycon substrate 8,15-dideoxylankanolide (**24**) for LkmK protein, I constructed the *lkmK–lkmL* double mutant. The targeting plasmid pKAR2015 harboring *lkmL*::*kan*^{R} was introduced into protoplast of the *lkmK* mutant KA28, and then homologous recombination was carried out. To confirm the disruption of *lkmL* in the *lkmK* mutant, Southern hybridization was carried out. A 5.6-kb *Bam*HI–*Bgl*II fragment

in the *lkmK* mutant KA28 was changed to two fragments at 4.4 and 2.4 kb in the *lkmK–lkmL* double mutant KA67 (Figure 28A).

To obtain a possible substrate 3-*O*-L-arcanosyl-8-deoxylankanolide (**25**) for LkmF protein, the *lkmF-lkmI* double mutant was constructed. The targeting plasmid pKAR2016 was constructed by deletion of 0.7-kb *Nru*I-*Aor*51HI fragment from *lkmF* and was introduced into protoplast of the *lkmI* mutant KA50. Gene disruption in possible *lkmF–lkmI* double mutant YI01 was confirmed by Southern hybridization (Figure 28B).

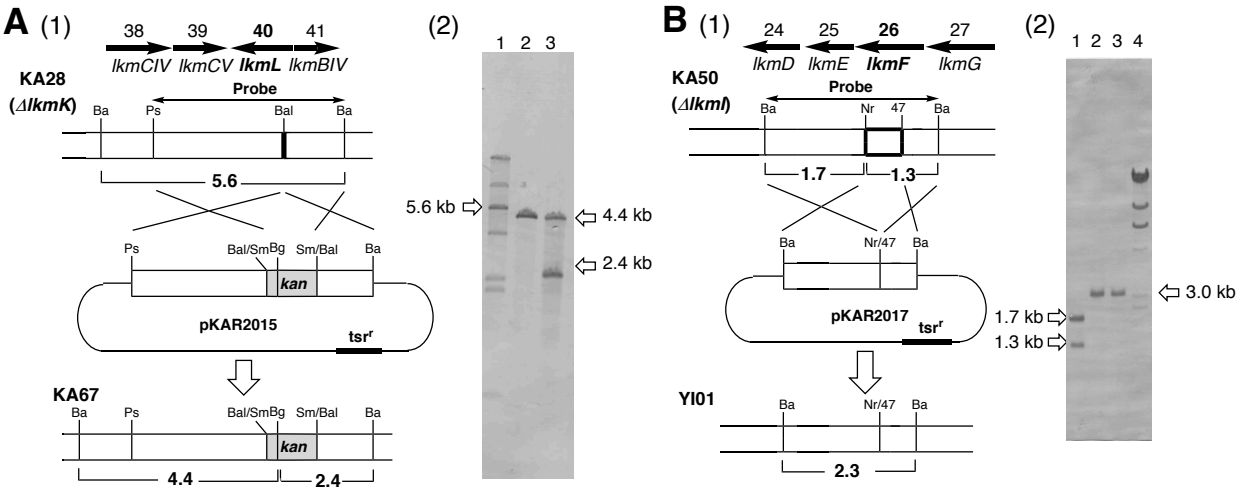

Figure 28. Construction of the KA67 and YI01. (**A**) (1) Construction of the *lkmK–lkmL* double mutant KA67. Ps, *Pst*I; Ba, *Bam*HI; Bal, *Bal*I; Sm, *Sma*I. (2) Southern blot analysis of total DNA. Lane 1, λ/*Hin*dIII; lane 2, strain KA28 (*lkmK*)/*Bam*HI–*Bgl*II; lane 3, strain KA67 (*lkmK lkmL*)/*Bam*HI–*Bgl*II. (**B**) (1) Construction of the *lkmF–lkmI* double mutant YI01. Ba, *Bam*HI; Nr, *Nru*I; 47, *Eco*47III. (2) Southern blot analysis of total DNA. Lane 1, strain KA50 (*lkmI*)/*Bam*HI; lanes 2 and 3, strain YI01 (*lkmF lkmI*)/*Bam*HI; lane 4, λ/*Hin*dIII.

Metabolite profile of *lkmK-lkmL* double mutant KA67 was compared with that of its parent strain KA28 by TLC. As shown in Figure 29A, mutant KA67 accumulated new compound **24** at R_f = 0.60 ($CHCl_3$-MeOH = 15:1). The molecular formula of **24** was determined by high-resolution ESI-MS analysis to be $C_{23}H_{42}O_6$. The ^{1}H- and ^{13}C-NMR assignments of **24** are shown in Table 27. When compared with 8-deoxylankanolide (**23**) [**55**], a deshielded methine carbon C-15 (δ_C 66.3) was changed to a methylene carbon (δ_C 24.8). Other signals showed a good agreement with those of **23**, suggesting that compound **24** is 8,15-dideoxylankanolide.

Table 27. ^{1}H- and ^{13}C-NMR data of lankamycin and lankanolide derivatives

	lankamycin (**2**)		8,15-dideoxylankanolide (**24**)		3-O-L-arcanosyl-8-deoxylankanolide (**25**)		8-deoxylankanolide (**23**)		3-O-L-arcanosyl-lankanolide (**22**)	
No.	d_C[a]	d_H[b]	d_C[a]	d_H[b]	d_C[a]	d_H[b]	d_C[a]	d_H[b]	d_C[a]	d_H[b]
1	176.7 (s)	–	178.2 (s)	–	176.7 (s)	–	178.2 (s)	–	175.9 (s)	–
2	44.8 (d)	2.80 (br)	44.0 (d)	2.81 (m)	44.6 (d)	2.82 (m)	43.3 (d)	2.79 (m)	44.6 (d)	2.77 (m)
3	77.8 (d)	3.95 (d, 4.9)[e]	79.5 (d)	3.92 (d, 10.4)[e]	77.3(d)	3.68 (m)[e]	79.3 (d)	3.90 (d, 10.4)[e]	78.4 (d)	3.86 (d, 10.0)[e]
4	44.1 (d)	1.83 (m)	37.5 (d)	1.86 (m)[d]	41.4 (d)	1.55 (m)	37.6 (d)	1.82 (m)	42.0 (d)	1.43 (m)
5	84.5 (d)	3.51 (m)	76.5 (d)	4.01 (d, 3.0)	85.0 (d)	3.65 (br)	76.4 (d)	3.97 (br)[d]	79.7 (d)	3.50 (br)
6	33.9 (d)	2.21 (br)	35.5 (d)	2.03 (m)	37.5 (d)	1.40 (br)	35.5 (d)	1.96 (m)	37.6 (d)	2.54 (br)
7	39.4 (t)	1.93[d]	37.7 (t)	1.25,1.66	34.0 (t)	1.35,1.66[d]	37.5 (t)	1.25,1.65[d]	38.2 (t)	1.80,1.87[d]
8	80.2 (s)	–	39.2 (d)	2.63 (m)	45.3 (d)	2.66 (m)	39.6 (d)	2.61 (m)	80.4 (s)	–
9	214.4 (s)	–	213.4 (s)	–	218.7 (s)	–	213.9 (s)	–	220.0 (s)	–
10	38.2 (d)	3.15 (q, 6.7)[f]	43.5 (d)	2.77 (m)	39.3 (d)	2.94 (m)	44.0 (d)	2.80[d]	39.1 (d)	3.02 (q, 7.0)[f]
11	71.0 (d)	4.87 (d, 8.9)[f]	70.8 (d)	3.67 (m)	70.8 (d)	3.39 (d, 9.8)[f]	71.1 (d)	3.70 (d, 9.2)[f]	70.1 (d)	3.40 (d, 9.8)[f]
12	39.4 (d)	1.93[d]	37.4 (d)	1.91[d]	39.4 (d)	1.88[d]	37.5 (d)	2.07[d]	38.7 (d)	1.88[d]
13	73.0 (d)	4.83 (d, 6.4)[g]	79.1 (d)	4.88 (dd, 10.4, 1.5)	75.0 (d)	5.31 (d, 8.6)[g]	76.8 (d)	5.17 (d, 10.0)[g]	74.9 (d)	5.38 (d, 8.9)[g]
14	42.7 (d)	1.82 (m)	35.0 (d)	1.86 (m)[d]	41.5 (d)	1.95 (m)	40.1 (d)	2.12 (m)	41.5 (d)	1.96 (m)
15	69.1 (d)	3.71 (m)	24.8 (t)	1.48 (m)	68.7 (d)	3.82 (m)	66.3 (d)	3.98 (br)[d]	68.8 (d)	3.80 (m)
1'	102.5 (d)	4.33 (d, 7.7)	–	–	–	–	–	–	–	–
2'	75.3 (d)	3.34 (dd, 7.7, 8.9)	–	–	–	–	–	–	–	–
3'	80.2 (d)	3.25 (m)	–	–	–	–	–	–	–	–
4'	37.1 (t)	1.25,2.07 (m)	–	–	–	–	–	–	–	–
5'	67.3 (d)	3.51 (m)	–	–	–	–	–	–	–	–
6'	21.0 (q)[c]	1.22 (d, 6.1)	–	–	–	–	–	–	–	–
1"	96.6 (d)	5.05 (d, 4.6)	–	–	98.7 (d)	4.96 (d, 5.0)	–	–	98.8 (d)	4.94 (d, 4.6)
2"	30.6 (t)	1.67,2.09 (m)	–	–	30.5 (t)	1.66,2.01 (m)	–	–	30.6 (t)	1.66,1.98 (m)
3"	72.6 (s)	–	–	–	73.9 (s)	–	–	–	73.9 (s)	–
4"	73.9 (d)	4.67 (s)[h]	–	–	73.3 (d)	3.13 (d, 8.3)[h]	–	–	73.2 (d)	3.12 (s)[h]
5"	62.6 (d)	4.47 (q, 6.6)[h]	–	–	63.8 (d)	4.51 (q, 6.8)[h]	–	–	63.7 (d)	4.51 (q, 6.8)[h]
6"	16.8 (q)	1.08[d]	–	–	16.7 (q)	1.23[d]	–	–	16.7 (q)	1.22[d]
3'-OCH_3	56.9 (q)	3.44 (s)	–	–	–	–	–	–	–	–
3"-OCH_3	49.3 (q)	3.30 (s)	–	–	49.3 (q)	3.26 (s)	–	–	49.4 (q)	3.26 (s)
3"-CH_3	20.9 (q)[c]	1.21[d]	–	–	21.3 (q)	1.22[d]	–	–	21.2 (q)	1.22[d]
2-CH_3	20.7 (q)	1.17 (d, 7.4)	14.7 (q)	1.30 (d, 6.7)	15.2 (q)	1.23[d]	14.7 (q)	1.30 (d, 6.7)	15.6 (q)	1.22[d]
4-CH_3	20.9 (q)[c]	1.06[d]	6.9 (q)	1.07 (d, 7.0)	8.7 (q)	1.06 (d, 6.7)	6.9 (q)	1.07 (d, 6.7)	8.9 (q)	1.05 (d, 7.0)
6-CH_3	14.4 (q)	1.16 (d, 6.8)	16.5 (q)	1.05[d]	17.9 (q)	1.07 (d, 7.0)[d]	16.6 (q)	1.04[d]	20.6 (q)	1.22[d]
8-CH_3	27.0 (q)	1.34 (s)	13.2 (q)	1.06[d]	16.3 (q)	1.17 (d, 6.7)	13.4 (q)	1.05[d]	26.8 (q)	1.45 (s)
10-CH_3	10.1 (q)[c]	1.10[d]	6.3 (q)	1.03 (d, 7.4)	8.5 (q)	1.01 (d, 6.7)	6.5 (q)	1.01 (d, 6.7)	10.0 (q)	1.10 (d, 6.8)
12-CH_3	9.8 (q)	1.02[d]	9.1 (q)	0.87 (d, 6.8)	9.5 (q)	0.92 (d, 7.0)	9.4 (q)	0.89 (d, 6.7)	9.4 (q)	0.91 (d, 7.0)
14-CH_3	11.2 (q)	0.83 (d, 7.0)	15.7 (q)	0.91 (d, 6.8)	10.7 (q)	0.88 (d, 6.7)	9.5 (q)	0.94[d]	10.6 (q)	0.87 (d, 7.0)
15-CH_3	19.7 (q)	1.15 (d, 6.4)	10.4 (q)	0.91[d]	18.7 (q)	1.16 (d, 6.0)	21.1 (q)	1.21 (d, 6.4)	18.6 (q)	1.19 (d, 9.4)
11-$CO\underline{CH_3}$	20.9 (q)[c]	2.08 (s)	–	–	–	–	–	–	–	–
11-$\underline{C}OCH_3$	170.1 (s)	–	–	–	–	–	–	–	–	–
4"-$CO\underline{CH_3}$	21.0 (q)[c]	2.13 (s)	–	–	–	–	–	–	–	–
4"-$\underline{C}OCH_3$	170.7 (s)	–	–	–	–	–	–	–	–	–

[a]: Multiplicity is shown in parenthesis. [b]: Multiplicity and J value in Hz are shown in parenthesis. [c]: Assignments are exchangeable. [d]: Obscured by overlapping. [e]: Vicinal proton coupling constant $J_{3,4}$ is ~0 Hz. [f]: Vicinal proton coupling constant $J_{10,11}$ is ~0 Hz. [g]: Vicinal proton coupling constant $J_{12,13}$ is ~0 Hz. [h]: Vicinal proton coupling constant $J_{4",5"}$ is ~0 Hz.

On the other hand, the *lkmF–lkmI* double mutant YI01 accumulated new compound **25** at R_f = 0.30 ($CHCl_3$-MeOH = 15:1) when compared with that of the parent *lkmI* mutant KA50 by TLC (Figure 29B). The molecular formula of compound **25** was determined to be $C_{31}H_{56}O_{10}$, which was one oxygen atom smaller than 3-*O*-L-arcanosyllankanolide (**22**) by ESI-MS. In ^{13}C-NMR and DEPT (Distortionless Enhancement by Polarization Transfer) spectra of compound **25**, a quaternary carbon C-8 (δ_C 80.4) was changed to a methine carbon (δ_C 45.3). In addition, a singlet methyl proton at C-8 (δ_H 1.45) was changed to a doublet methyl (δ_H 1.17). Other signals were almost consistent with those of **22**, suggesting that compound **25** is 3-*O*-L-arcanosyl-8-deoxylankanolide.

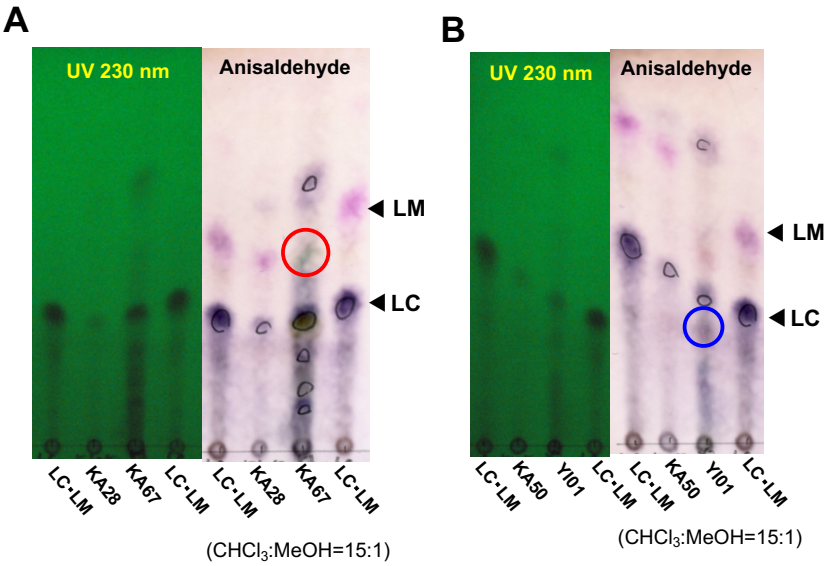

Figure 29. TLC of KA67 and YI01 metabolites. (**A**) Metabolite profile of *lkmK-lkmL* double mutant KA67 and its parent strain KA28. Red circle; compound **24** (**B**) Metabolite profile of *lkmF-lkmI* double mutant YI01 and its parent strain KA50. Blue circle; compound **25**

2.3.2. Enzymatic bioconversion of deoxy substrates by LkmK and LkmF

In order to examine the substrate specificity of a C-15 hydroxylase LkmK, I constructed an *lkmK* expression system in *E. coli* using co-expression vector pCYPcamAB that harbors putidaredoxin/putidaredoxin reductase genes [**57**]. Protein expression of *lkmK* was confirmed in the cell-free extract of *E. coli* BL21(DE3)/pCYP101-AB1 by SDS-PAGE (Figure 30B).

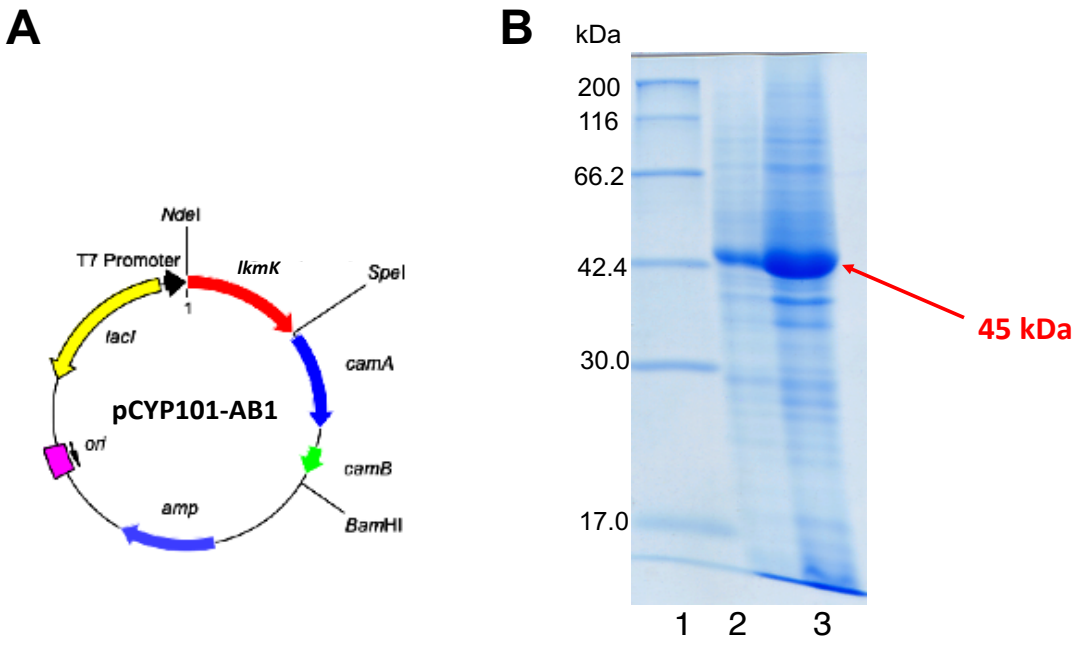

Figure 30. Overexpression of the LkmK protein. (**A**) Physical map of the LkmK overexpression plasmid pCYP101-AB1, a vector part of which was pCYPcamAB [**57**]. (**B**) SDS-PAGE of the recombinant LkmK protein expressed in *E. coli* BL21(DE3). Lane 1, molecular size marker; lane 2, cell-free supernatant of the *E. coli* BL21(DE3)/pCYPcamAB recombinant (control); lane 3, cell-free supernatant of the *E. coli* BL21(DE3)/pCYP101-AB1 recombinant (+ LkmK)

Three 15-deoxy lankamycin derivatives (compounds **20**, **21**, **24**) were added to the *E. coli* BL21(DE3)/pCYP101-AB1 and their assay mixtures were analyzed by ESI-MS. Treatment of 15-deoxylankamycin (**20**) in the LkmK expression recombinant gave an obvious molecular ion peak at *m*/*z* 855 $[M+Na]^+$, which was one oxygen atom larger than that of the substrate (**20**) and was identical to that of **2** (Figure 31). In TLC analysis, a lower R_f value spot appeared at R_f = 0.70 ($CHCl_3$-MeOH = 15:1), which was consistent with lankamycin (**2**) (data not shown). 8,15-dideoxylankamycin (**21**) and 8,15-dideoxylankanolide (**24**) were also treated with LkmK, and also converted to molecular ion peaks at *m*/*z* 839 $[M+Na]^+$ and *m*/*z* 453 $[M+Na]^+$, respectively. Their molecular formulae corresponded to 8-deoxylankamycin (**19**) and 8-deoxylankanolide (**23**), respectively. These results indicated that the LkmK protein catalyzes a C-15 hydroxylation regardless of the presence of two deoxysugar moieties.

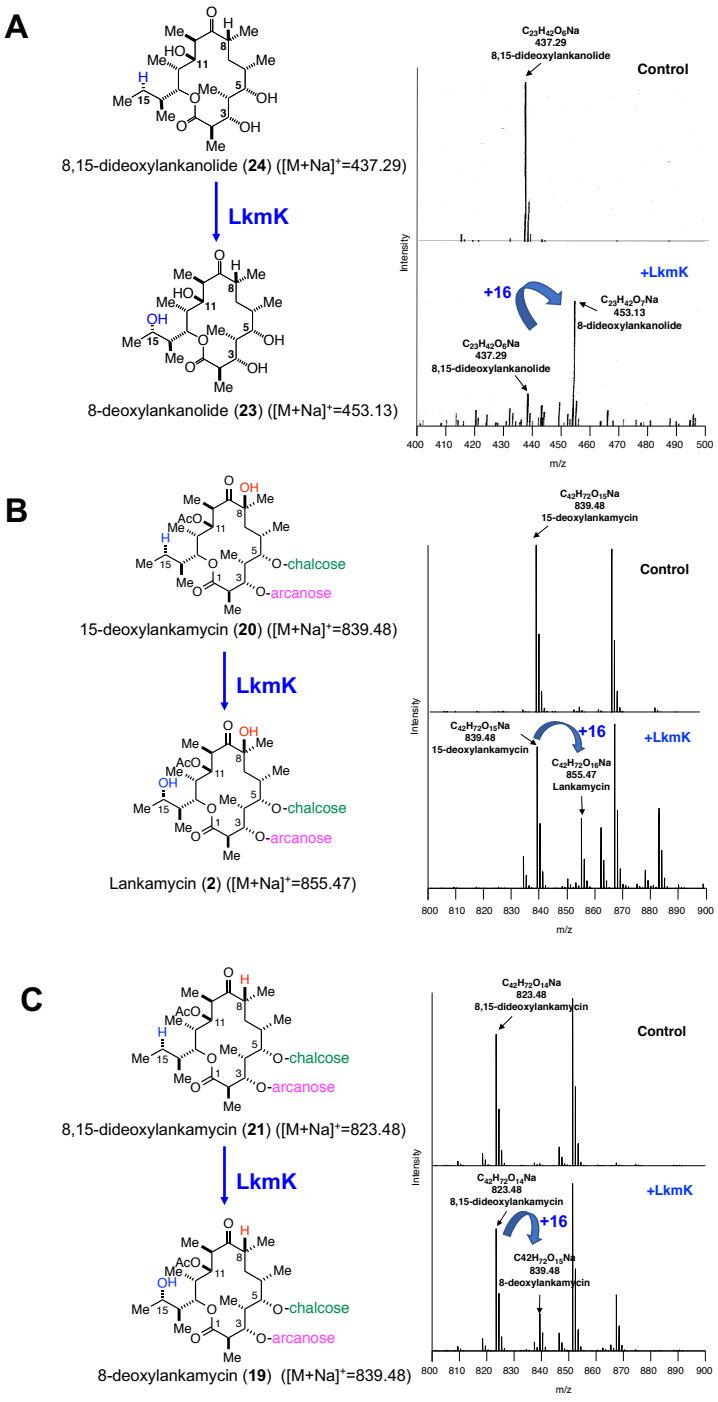

Figure 31. Substrate specificity of LkmK protein. ESI-MS spectra obtained by *in vivo* enzymatic conversion of compounds **24**, **20**, **21** in *E. coli* BL21(DE3)/pCYP101-AB1. (**A**) Conversion of compound **24** (8,15-dideoxylankanolide). (**B**) Conversion of compound **20** (15-deoxylankamycin). (**C**) Conversion of compound **21** (8,15-dideoxylankamycin).

To examine the enzymatic conversion of a possible substrate 3-*O*-L-arcanosyl-8-deoxylankanolide (**25**), an LkmF expression system in *E. coli* was constructed in a similar manipulation with that of LkmK; however, no enzymatic conversion reaction was observed (data not shown). As an alternative approach, *Streptomyces* expression system was constructed as a similar manipulation with SrrO-expression system, which was already described in Chapter 1. The *lkmF* gene was cloned into pHSA81, a streptomycete constitutive expression vector (Prof. Kobayashi and Hashimoto, pers. comm.), to obtain pYK01. Protein expression of *lkmF* was confirmed in the cell-free supernatant of the *S. lividans* TK64 recombinant harboring pYK01 by SDS-PAGE (Figure 32). I performed enzymatic bioconversion of various 8-deoxy lankamycin derivatives (**19**, **21**, **23**-**25**) with the help of heterologous *S. lividans* redox partners (as described in General Introduction) according to a preceding paper [**58**].

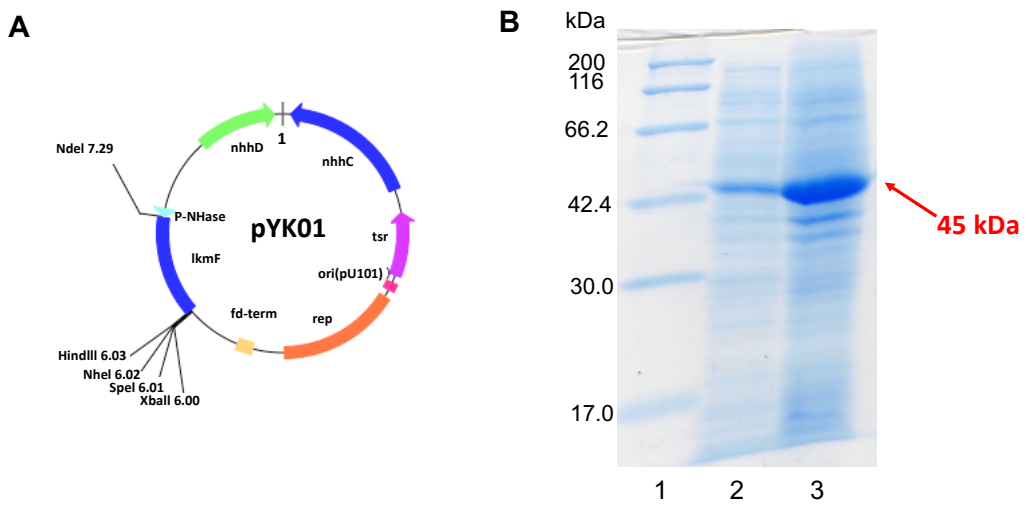

Figure 32. Overexpression of the LkmF protein. (**A**) Physical map of the LkmF overexpression plasmid pYK01, a vector part of which was pHSA81 (Profs. Y. Hashimoto and M. Kobayashi, personal communication). (**B**) SDS-PAGE of the recombinant LkmF protein expressed in *S. lividans* TK64. Lane 1, molecular size marker; lane 2, cell-free supernatant of the *S. lividans* TK64/pHSA81 recombinant (control); lane 3, cell-free supernatant of the *S. lividans* TK64/pYK01 recombinant (+ LkmF).

These 8-deoxy compounds were treated with pYK01 and their assay mixtures were analyzed by ESI-MS (Figure 33). In bioconversion of **25** in the *lkmF* recombinant, a molecular ion peak appeared at *m/z* 669 $[M+Na]^+$, which was one oxygen atom larger than that of the substrate **25** and was identical to that of **22** (Figure 33E). Thus, compound **25** was converted into **22** in the LkmF recombinant. Other 8-deoxy lankamycin derivatives, 8-deoxylankamycin (**19**) from strain KK01 [**34**], 8,15-deoxylankamycin (**21**) from strain KA26 [**34**], 8-deoxylankanolide (**23**) from strain KA55 [**55**], and 8,15-

deoxylankanolide (**24**) from strain KA67, could not be oxidized (Figure 33A-D), suggesting the strict substrate specificity for LkmF.

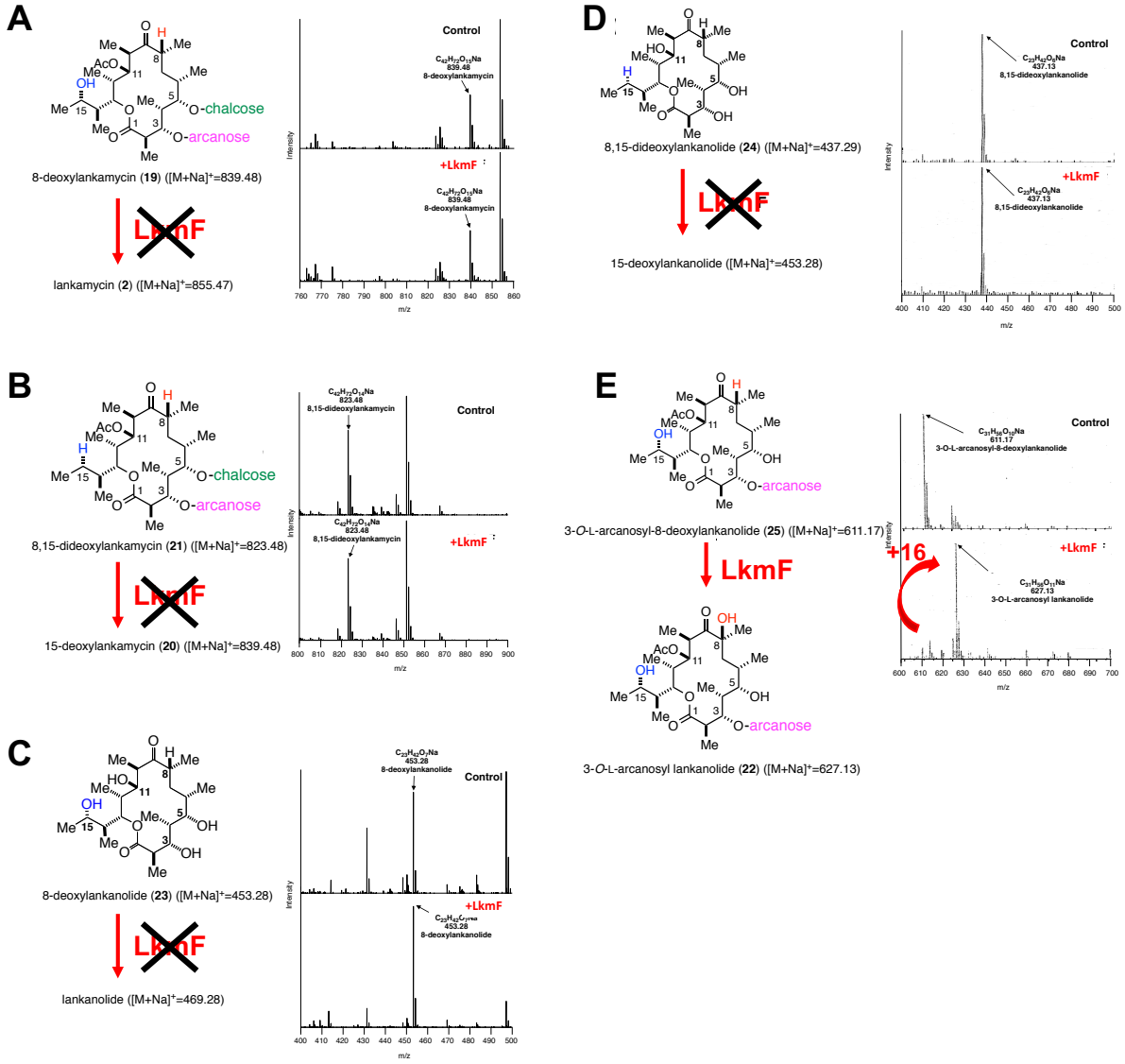

Figure 33. Substrate specificity of LkmF protein. ESI-MS spectra obtained by *in vivo* enzymatic conversion of compounds **19**, **20**, **23**-**25** in *S. lividans* TK64/pYK01. (**A**) Conversion of compound **19** (8-deoxylankamycin). (**B**) Conversion of compound **20** (8,15-dideoxylankamycin). (**C**) Conversion of compound **23** (8-deoxylankanolide). (**D**) Conversion of compound **24** (8,15-dideoxylankanolide). (**E**) Conversion of compound **25** (3-*O*-L-arcanosyl-8-deoxylankanolide).

2.4. Discussion

In this chapter, I analyzed the role of two P450 monooxygenases, LkmK and LkmF in lankamycin biosynthesis through gene disruption and *in vivo* enzymatic conversion.

LkmK catalyzes C-15 hydroxylation at a first step of post-PKS pathway for lankamycin biosynthesis. Aglycon 8,15-dideoxylankanolide (**24**) was converted into 8-deoxylankanolide (**23**) in the LkmK recombinant. In addition, other 15-deoxy compounds, 15-deoxylankamycin (**20**), and 8,15-deoxylankamycin (**21**) were also oxidized to the corresponding 15-hydroxy compounds, lankamycin (**2**), and 8-deoxylankamycin (**19**), respectively (Figure 31). As to the bioconversion efficiency, the gross aglycon substrate 8,15-dideoxylankanolide (**24**) for LkmK was almost converted to 8-deoxylankanolide (**23**) by LkmK (Figure 31). On the contrary, the conversion efficiencies of both 15-deoxylankamycin (**20**) and 8,15-dideoxylankamycin (**21**) were low. These results suggest that 8,15-dideoxylankanolide is preferred as a substrate over, 15-deoxylankamycin (**20**), and 8,15-dideoxylankamycin (**21**). The *lkmE* (type-II thioesterase gene) mutant accumulated two 15-norlankamycin derivatives, LM-NS01A and LM-NS01B (Figure 34), both of which harbored a 1-carboxyethyl group at C-13 side chain instead of 3-hydroxy-2-methyl butyrate group [**59**]. Their biosynthetic origin of a starter unit may be isobutyryl CoA, a derivative of valine, instead of 2-methylbutyryl CoA. Deuterium labeling

experiment revealed that a pro-*S* methyl group of isobutyrate moiety at C-13 in 8,15-dideoxy-15-norlankanolide was stereospecifically oxidized by LkmK to a carboxylate moiety during the biosynthesis of LM-NS01A and LM-NS01B (Figure 34) [**59**].

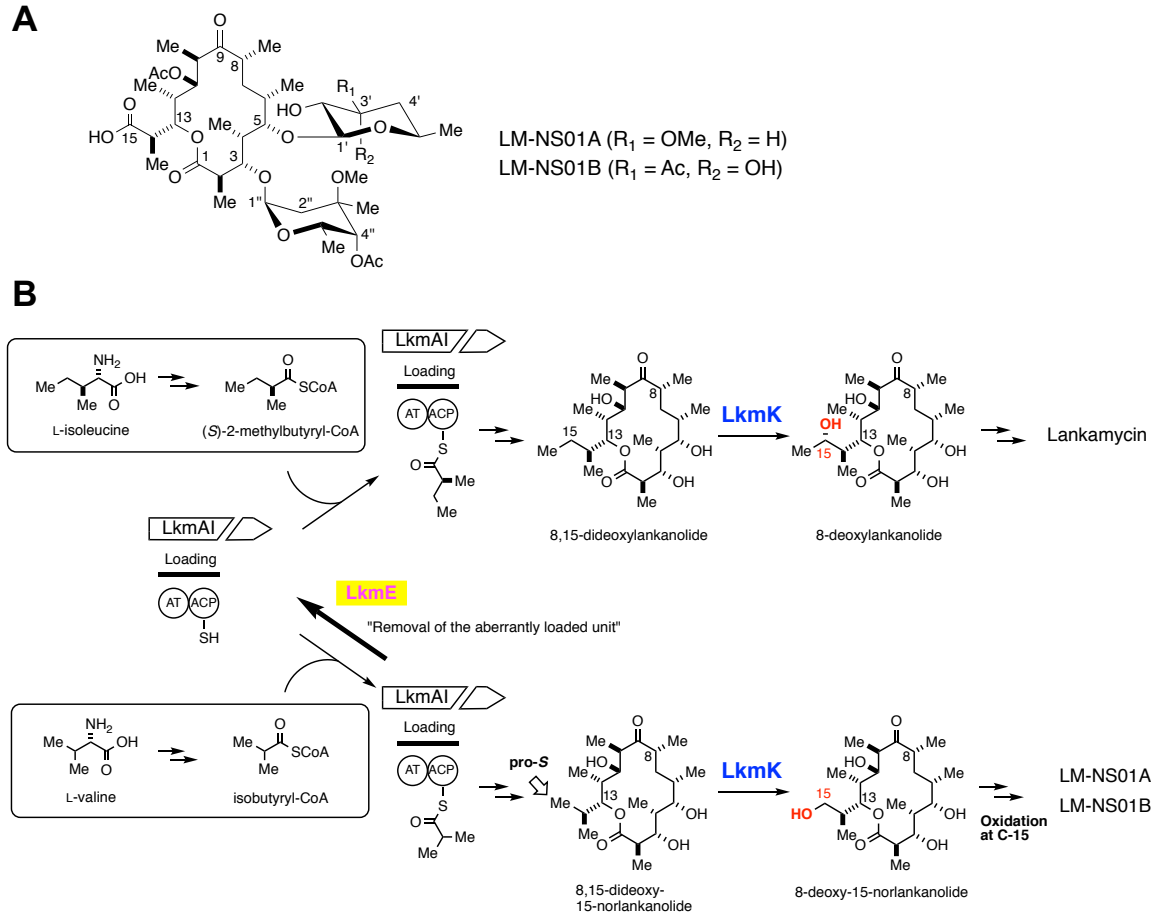

Figure 34. (**A**) Structure of 15-nor-lankamycin derivatives, LM-NS01A and LM-NS01B, isolated from *lkmE* mutant. (*lkmE*; type-II thioesterase gene) (**B**) Possible biosynthetic pathway of lankamycin (upper panel), and LM-NS01A and LM-NS01B (lower panel).

Thus, *in vivo* bioconversion and gene inactivation experiments strongly indicated that LkmK recognizes a broader substrate independent to two deoxysugar moieties and the side chain at C-13 in the lankamycin skeleton.

In the case of erythromycin A biosynthesis, the post-PKS pathway was confirmed as follows: EryF [**60**] catalyzes the C6-hydroxylation of 6-deoxyerythronolide B, the initial reaction in multistep pathway, and the resulting erythronolide B receives two deoxysugar units at C-3 and C-5 hydroxyls by glycosyltransferases EryBV and EryCIII, respectively, to give diglycoside erythromycin D, which is then hydroxylated at C-12 position by EryK [**61**,**60**] to synthesize erythromycin A (Figure 35). The *eryF* mutant accumulated the biologically active diglycoside 6-deoxyerythromycin A, suggesting that hydroxylation to the C-6 moiety by EryF proceeds independently of two glycosylation steps by EryBV and EryCIII and the C-12 hydroxylation step by EryK [**62**]. This finding was similar to the case of the *lkmK* mutant in lankamycin biosynthesis.

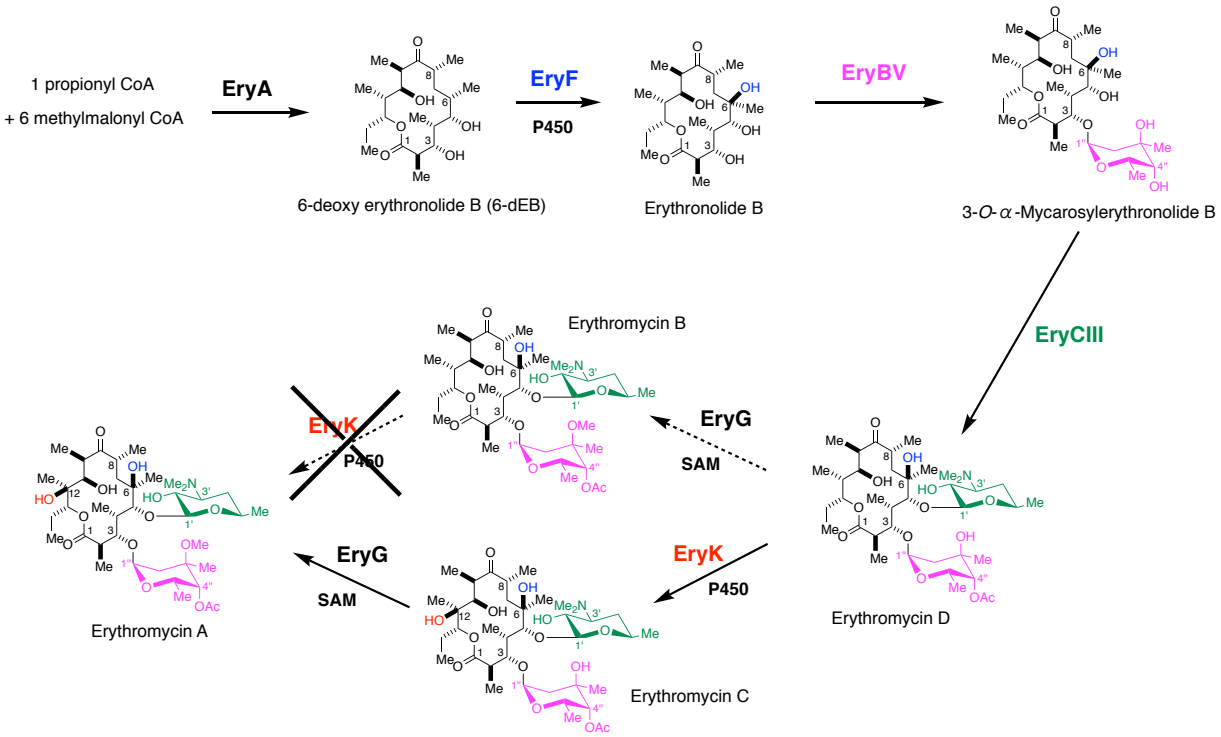

Figure 35. Possible post-PKS biosynthetic pathway of Erythromycin A [59]

LkmF catalyzes C-8 hydroxylation in lankamycin biosynthesis. Although LkmK can recognize broader substrates, LkmF only accepts 3-*O*-L-arcanosyl-8-deoxylankanolide (**25**) as a substrate and converts it to 3-*O*-L-arcanosyllankanolide (**22**), which then receives the transfer of D-chalcose at C-5 and two steps of acetylation at C-11 and C-4″ to synthesize lankamycin (**2**). Both the *lkmL* and *lkmE* mutants accumulated 8-deoxy compounds [**55**,**59**]. This result indicated that LkmF has a strict substrate recognition in lankamycin biosynthesis. As shown in Figure 34, two 15-nor lankamycin derivatives, LM-NS01A and LM-NS01B, are 8-deoxy compounds. Thus, not only the C-3 L-arcanosyl

moiety but also the C-13 side chain might be important for the recognition of LkmF in lankamycin biosynthesis. Diglycoside 8-deoxylankamycin (**19**) could not be recognized by LkmF, indicating the strict biosynthetic order from LkmL through LkmF to LkmI to synthesize lankamycin in *S. rochei*.

LkmK and LkmF showed the considerable sequence similarity (51% identity and 85% similarity); however, cross-reactivity on C-8/C-15 positions could not be detected in both gene inactivation and *in vivo* bioconversion experiments. Thus, these two P450 monooxygenases are regiospecific enzymes in lankamycin biosynthesis.

General conclusions

The cytochrome P450 enzymes have a potential to catalyze a variety of metabolic and biosynthetic chemical reactions. These enzymes are of particular interest to the toxicology, drug metabolism, and pharmacology fields [**62**,**63**]. Cytochromes P450s are not usually abundant in bacteria, but the *Streptomyces* species harbored a significant number of P450s.

Streptomyces rochei 7434AN4, which produces lankacidin and lankamycin, has 42 P450 genes. In this study, I revealed the functions of three P450 genes responsible for antibiotic-inducible signaling molecules SRBs and a 14-membered macrolide lankamycin biosynthesis. In the General Conclusion Section, I will focus to their future perspectives for drug-discovery.

Regarding to SRBs, signaling molecules play an important role to induce secondary metabolite production in several *Streptomyces*. In the extensive genome sequencing, many *Streptomyces* strains have more than 30 secondary metabolites biosynthetic gene clusters. However, many biosynthetic gene clusters (80-90%) are weakly expressed or not at all in normal culture conditions, resulting in a potential bottleneck for natural product discovery. In *S. rochei*, 40 biosynthesis gene clusters (35 in the chromosome and

5 in pSLA2-L) are found. Nevertheless, only 6 compounds are detected at the moment (Figure 36) [**10**,**13**].

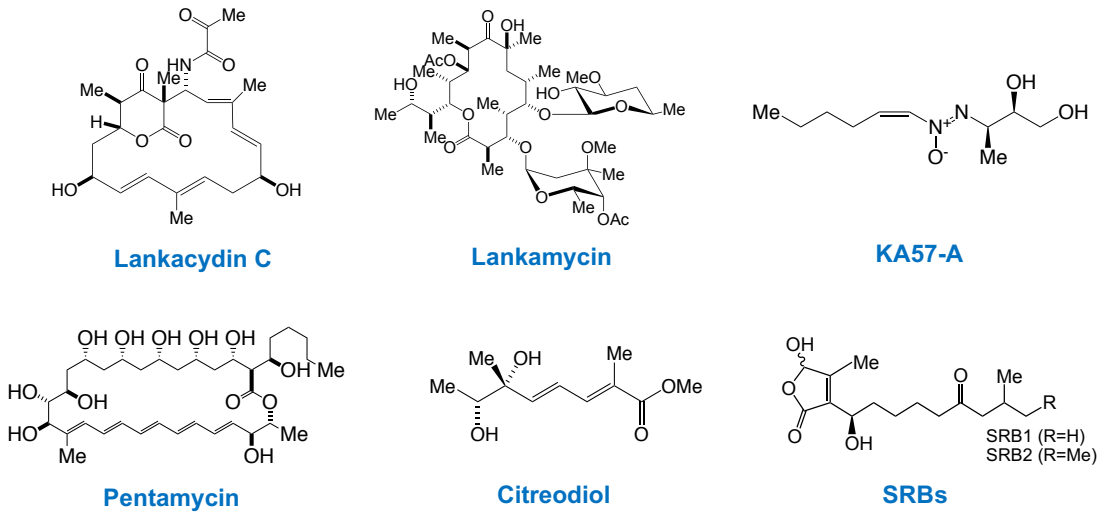

Figure 36. Secondary metabolites of *S. rochei* hitherto discovered

Although I do not yet have the answer why many of them are silent or poorly expressed, a lack of specific signaling molecules is one of a plausible possibility [**65**,**66**]. The previous findings based on screening of signaling-molecule producers suggested that at least 60% of *Streptomyces* species may use γ-butyrolactone type [**27**], 24% of them use avenolide [**67**]. Although the presence of novel-type signaling molecule, together with signaling-molecule deficient strains could not be eliminated, remaining (around 16%) will be either butenolide type or furan type (Figure 37).

Streptomyces strains generally have extra receptor genes than signal molecule synthesis genes, suggesting that the receptor homologs may have a potential to recognize heterologous signaling molecules (For example, *S. rochei* has 2 signal molecule synthesis homologs and 7 receptor homologs). Thus, signaling molecules have a potential to contribute as "genetic engineering-free" genome mining tools, to act as communication signals between actinomycetes, between different bacteria, and/or between interkingdom.

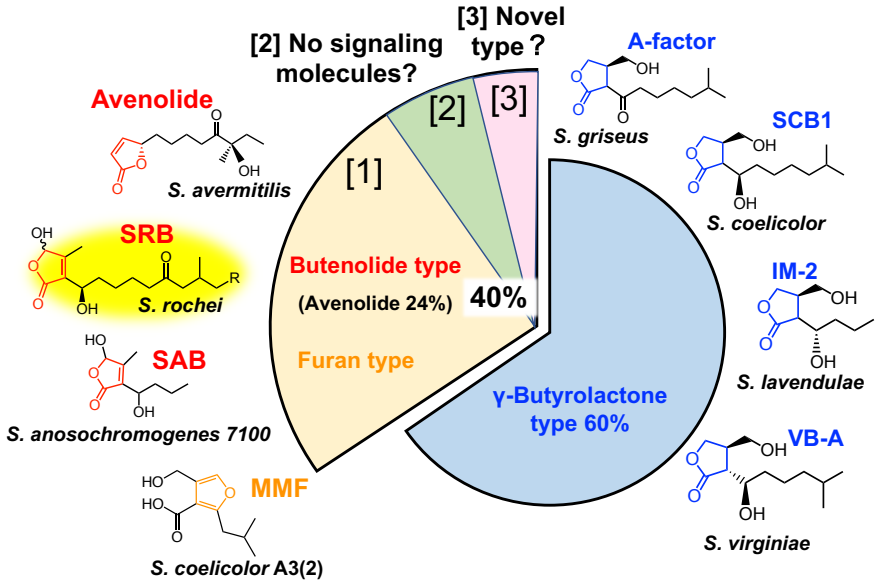

Figure 37. Diversity distribution of signaling molecule [27] [67]

Regarding to lankamycin, P450 enzymes LkmF and LkmK catalyze C-8/C-15 hydroxylation in lankamycin skeleton, and enhance are responsible for improvement of antimicrobial activity. The macrolide skeleton of lankamycin is quite similar to that of

erythromycin A. The major differences are the positions of hydroxylation (C-8 and C-15 in lankamycin and C-6 and C-12 in erythromycin A) and the C-13 side-chain corresponding to a starter-unit in their biosynthesis (3-hydroxy-2-butyl in lankamycin and ethyl in erythromycin A) (Figure 38 A). In spite of the structural similarities between lankamycin and erythromycin, the [IC_{50}] values for antibiotic inhibition of translation of lankamycin was lower than of erythromycin (Table 28) [**54**].

Table 28. Comparison of [IC_{50}] values for antibiotic inhibition of translation

Antibiotic	[IC_{50}] (μM)
Lankamycin	275
Lankacidin	1.5
Erythromycin	0.2

It is noteworthy that lankacidin and lankamycin, both are produced by *S. rochei*, inhibit ribosomal function synergistically in bacteria [**53**]. Lankamycin could bind to peptide exit tunnel in ribosome in a similar fashion to erythromycin, however, when in complex with lankacidin, lankamycin could locate at the adjacent to the peptidyl transferase center, which exhibits synergistic effect with lankacidin (Figure 38B). In the case of erythromycin, it showed competition with lankacidin in ribosome, resulting in no

synergistic function. Apparent differences between lankamycin and erythromycin are the nature of the C5-attached deoxy-sugar reside and the location of hydroxyl groups, both of which may contribute hydrogen bond formation and filling of the binding cavity [**52**,**53**]. Engineering of hydroxylation on lankamycin may provide more potent synergistic pair with lankamycin. Synergistic action of the two antibiotics may be related to the findings that the close location of their biosynthetic genes and co-regulation by the same regulatory pathway.

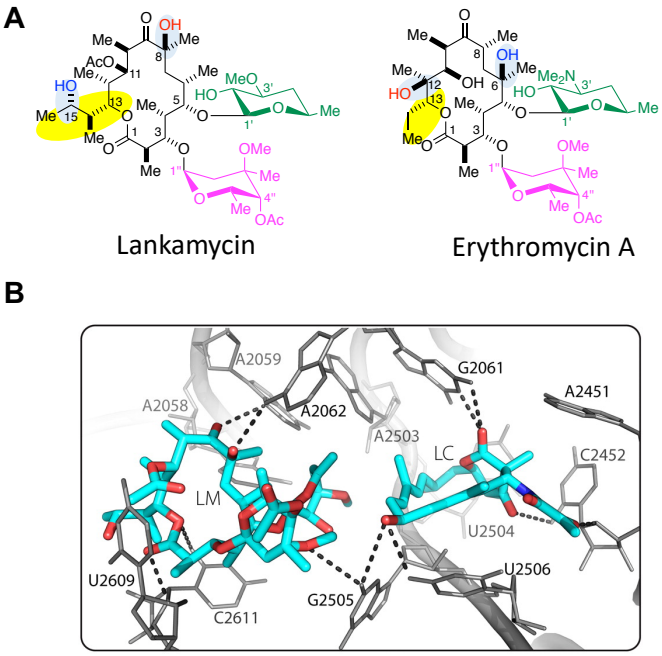

Figure 38. Binding pockets of LM/LC in the 50S subunit. (**A**) Structure of lankamycin and Erythromycin A. (**B**) Interaction network of LM and LC (cyan) with surrounding rRNA (gray).

Biotechnological applications of P450s are widely investigated to create useful chemical substances. For example, Shengying *et al*. reported the substrate engineering of

a macrolide biosynthetic P450 monooxygenase PikC with remarkable substrate flexibility [**68**]. PikC is the cytochrome P450 involved in pikromycin biosynthesis from *Streptomyces venezuelae* to hydroxylate both a 12-membered ring macrolide YC-17 and a 14-membered ring macrolide narbomycin (Figure 39).

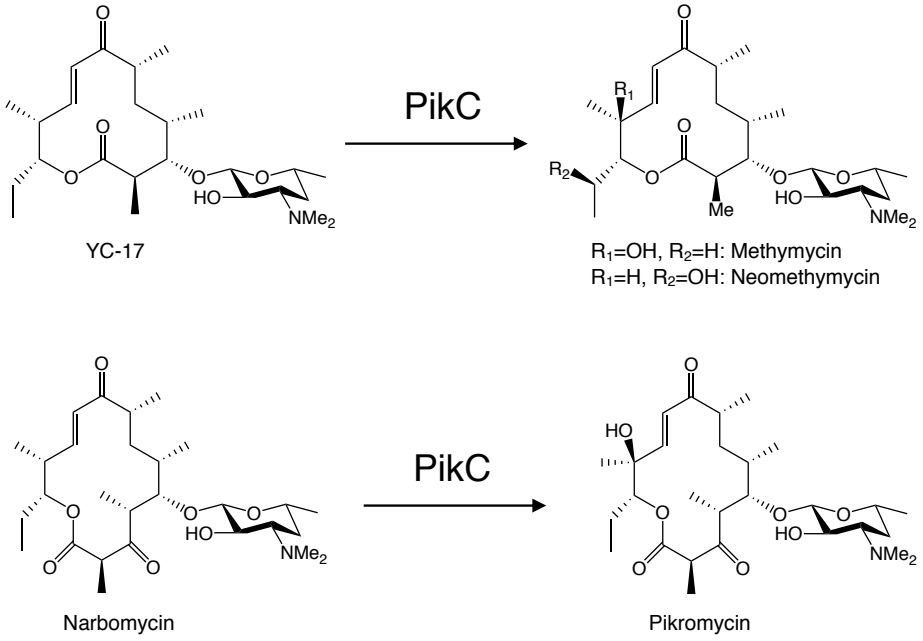

Figure 39. Major hydroxylation reactions catalyzed by PikC

The engineered macrolide P450, $PikC_{D50N}$-RhFRED was exhibited remarkable substrate flexibility, and catalyzed the oxidation of linear or aromatic substrates as shown in Figure 40.

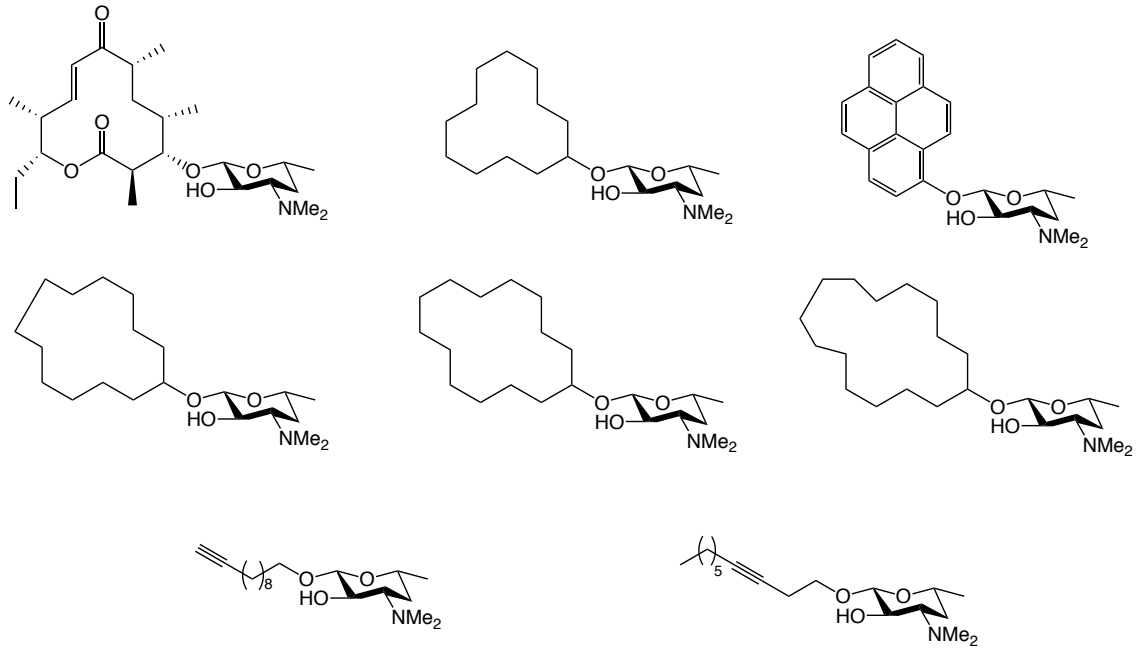

Figure 40. The structure of various substrates recognized by PikC$_{D50N}$-RhFRED

If the detailed functions of P450s can be clarified and substrate recognition can be made more flexibly, they can be applied to use for industrial applications to create bioactive and/or value-added chemicals.

Acknowledgments

This thesis study has been carried out at the Cell Biochemistry Laboratory, Department of Molecular Biotechnology, Graduate School of Advanced Science of Matter, Hiroshima University.

I am deeply grateful to Associate Professor Kenji Arakawa, for his elaborated guidance, considerable encouragement and providing me this precious study opportunity as a Ph.D. student. I also want to thank Prof. Tsunehiro Aki, Prof. Seiji Kawamoto and Prof. Nobukazu Tanaka for their advice on my doctoral thesis. I have a deep appreciation for Prof. Yoshiko Okamura for her encouraging words. I grateful to Ms. Tomoko Amimoto (Natural Scince Center for Basic Research and Development, Hiroshima University) for help her technical support on ESI-MS analysis. I thank Prof. Michihiko Kobayashi and Prof. Yoshiteru Hashimoto (Tsukuba University) for providing constitutive expression vector pHSA81.

I would like to offer my special thanks to all the members of the laboratory of Cell Biochemistry, who give me warm encouragements and support.

Finally, I would like to express my gratitude to my family, who give me a chance to chase my dream.

References

[1] Lewis D. F. V. “Cytochromes P450-Structure, Function and Mechanism.” *Taylor and Francis Ltd.*, 79-113 (1996).

[2] Ōmura T., Ishimura Y. and Fujii Y. “Molecular Biology of P450.” *Kodansha scientific*, (2003) (in Japanese).

[3] Lamb D. C., Zhao B., Guengerich F. P., Kelly S. L. and Waterman M. R. “Genomics of *Streptomyces* cytochrome P450. In *Streptomyces* Molecular Biology and Biotechnology” (P. Dyson, Ed.), *Caister Academic Press,* Norfolk, UK, 233-253 (2011).

[4] Rudolf J. D., Chang C. Y., Ma M. and Shen B. “Cytochromes P450 for natural product biosynthesis in Streptomyces: sequence, structure, and function.” *Nat. Prod. Rep.*, **34**, 1141-1172 (2017).

[5] Hussain H. A. and Ward J. M. “Enhanced heterologous expression of two *Streptomyces griseolus* cytochrome P450s and *Streptomyces coelicolor* ferredoxin reductase as potentially efficient hydroxylation catalysts.” *Appl. Environ. Microbiol.*, **69**, 373–382 (2003).

[6] Matsuoka T., Miyakoshi S., Tanzawa K., Nakahara K., Hosobuchi M. and Serizawa N. “Purification and characterization of cytochrome P450sca from *Streptomyces carbophilus*. ML-236B (compactin) induces P450sca in *Streptomyces carbophilus* that hydroxylates ML-236B to pravastatin sodium (CS-514), a tissue-selective inhibitor of 3-hydroxy-3-methylglutaril coenzyme-A reductase.” *Eur. J. Biochem.*, **184**, 707–713 (1989).

[7] Sasaki J., Miyazaki A., Saito M., Adachi T., Mizoue K., Hanada K. and Ōmura S. “Transformation of vitamin D3 to 1α,25-dihydroxyvitamin D3 via 25-hydroxyvitamin D3 using *Amycolata* sp. strains.” *Appl. Microbiol. Biotechnol.*, **38**, 152-157 (1992).

[8] Takeda K., Asou T., Matsuda A., Kimura K., Okamura K., Okamoto R., Sasaki J., Adachi T. and Ōmura S. “Application of cyclodextrin to microbial transformation of vitamin D3 to 25-hydroxyvitamin D3 and 1α,25-dihydroxyvitamin D3.” *J. Ferment. Bioeng.*, **78**, 380-382 (1994).

[9] Kinashi H., Mori E., Hatani A. and Nimi O. "Isolation and characterization of linear plasmids from lankacidin-producing Streptomyces species." *J. Antibiot.*, **47**, 1447-1455 (1994).

[10] Mochizuki S, Hiratsu K, Suwa M., Ishii T., Sugino F., Yamada K. and Kinashi H. "The large linear plasmid pSLA2-L of *Streptomyces rochei* has an unusually condensed gene organization for secondary metabolism." *Mol. Microbiol.*, **48**, 1501-1510 (2003).

[11] Arakawa K., Mochizuki S., Yamada K., Noma T. and Kinashi H. "γ-Butyrolactone autoregulator-receptor system involved in lankacidin and lankamycin production and morphological differentiation in *Streptomyces rochei*." *Microbiology*, **153**, 1817-1827 (2007).

[12] Yamamoto S., He Y., Arakawa K. and Kinashi H. "Gamma-Butyrolactone-dependent expression of the SARP gene *srrY* plays a central role in the regulatory cascade leading to lankacidin and lankamycin production in *Streptomyces rochei*." *J. Bacteriol.*, **190**, 1308–1316 (2008).

[13] Nindita Y., Cao Z., Fauzi A.A., Teshima A., Misaki Y., Muslimin R., Yang Y., Shiwa Y., Yoshikawa H., Tagami M., Lezhava A., Ishikawa J., Kuroda M., Sekizuka T., Inada K., Kinashi H. and Arakawa K. "The genome sequence of *Streptomyces rochei* 7434AN4, which carries a linear chromosome and three characteristic linear plasmids." *Sci. Rep.*, **9**, 10973 (2019)

[14] Senate L. M., Tjatji M. P., Pillay K., Chen W., Zondo N. M., Syed P. R., Mnguni F. C., Chiliza Z. E., Bamal H. D., Karpoormath R., Khoza T., Mashele S. S., Blackburn J. M., Yu J., Nelson D. R. and Syed K. "Similarities, variations, and evolution of cytochrome P450s in *Streptomyces* versus *Mycobacterium*." *Sci. Rep.*, **9**, 3962 (2019).

[15] Kieser T., Bibb M. J., Buttner M. J., Chater K. F. and Hopwood D. A. "Practical *Streptomyces* Genetics" *The John Innes Foundation*, Norwich, UK (2000).

[16] Zhang H., Shinkawa H., Ishikawa J., Kinashi H. and Nimi O. "Improvement of transformation system in *Streptomyces* using a modified regeneration medium." *J. Ferment. Bioeng.*, **83**, 217–221 (1997).

[17] Sambrook J., Fritsch E. F. and Maniatis T. “Molecular Cloning, A laboratory manual.” *Cold Spring Harbor Laboratory Press*, New York, USA (2001).

[18] Suwa M., Sugino H., Sasaoka A., Mori E., Fujii S., Shinkawa H., Nimi O. and Kinashi H. "Identification of two polyketide synthase gene clusters on the linear plasmid pSLA2-L in *Streptomyces rochei*." *Gene*., **246**, 123-131 (2000).

[19] Hopwood D. A., Wright H. M., Bibb M. J. and Cohen S. N. “Genetic recombination through protoplast fusion in *Streptomyces*.” *Nature*, **268**, 171–174 (1977).

[20] Sambrook J., Fritsch E. F. and Maniatis T. “Molecular Cloning: A Laboratory Manual” *Cold Spring Harbor Laboratory Press*, New York, USA (1989).

[21] Bibb M. J. “Regulation of secondary metabolism in streptomycetes.” *Curr. Opin. Microbiol.*, **8**, 208–215 (2005).

[22] Horinouchi S. and Beppu T. “Hormonal control by A-factor of morphological development and secondary metabolism in *Streptomyces*.” *Proc. Jpn. Acad. Ser. B*, **83**, 277–295 (2007).

[23] Takano E. “Gamma-butyrolactones: *Streptomyces* signalling molecules regulating antibiotic production and differentiation.” *Curr. Opin. Microbiol.* **9**, 287–294 (2006).

[24] Niu G., Chater K. F., Tian Y., Zhang J. and Tan H. “Specialized metabolites regulating antibiotic biosynthesis in *Streptomyces* spp.” *FEMS Microbiol. Rev.*, **40**, 554–573 (2016).

[25] Arakawa K. “Manipulation of metabolic pathway controlled by signaling molecules, inducers of antibiotic production, for genome mining in *Streptomyces* spp.” *Antonie Van Leeuwen.*, **111**, 743–751 (2018).

[26] Kong D., Wang X., Nie J. and Niu G. “Regulation of antibiotic production by signaling molecules in *Streptomyces*.” *Front. Microbiol.*, **10**, 2927 (2019).

[27] Hara O. and Beppu T. “Mutants blocked in streptomycin production in *Streptomyces griseus*–the role of A-factor.” *J. Antibiot.*, **35**, 349–358 (1982).

[28] Kato J., Funa N., Watanabe H., Ohnishi Y. and Horinouchi S. "Biosynthesis of gamma-butyrolactone autoregulators that switch on secondary metabolism and morphological development in *Streptomyces*." *Proc. Natl. Acad. Sci. USA*, **104**, 2378–2383 (2007).

[29] Corre C., Song L., O'Rourke S., Chater K. F. and Challis G.L. "2-Alkyl-4-hydroxymethylfuran-3-carboxylic acids, antibiotic production inducers discovered by *Streptomyces coelicolor* genome mining." *Proc. Natl. Acad. Sci. USA*, **105**, 17510–17515 (2008).

[30] Kitani S., Miyamoto K. T., Takamatsu S., Herawati E., Iguchi H., Nishitomi K., Uchida M., Nagamitsu T., Ōmura S., Ikeda, H. and Nihira T. "Avenolide, a *Streptomyces* hormone controlling antibiotic production in *Streptomyces avermitilis*." *Proc. Natl. Acad. Sci. USA*, **108**, 16410–16415 (2011).

[31] Arakawa K., Tsuda N., Taniguchi A. and Kinashi H. "The butenolide signaling molecules SRB1 and SRB2 induce lankacidin and lankamycin production in *Streptomyces rochei*." *Chem. Bio. Chem.*, **13**, 1447–1457 (2012).

[32] Rodriguez A. M., Olano C., Méndez C., Hutchinson C. R. and Salas J. A. "A cytochrome P450-like gene possibly involved in oleandomycin biosynthesis by *Streptomyces antibioticus*." *FEMS Microbiol. Lett.*, **127**, 117–120 (1995).

[33] Misaki Y., Yamamoto S., Suzuki T., Iwakuni M., Sasaki H., Takahashi Y., Inada K., Kinashi H. and Arakawa K. "SrrB, a pseudo-receptor protein, acts as a negative regulator for lankacidin and lankamycin production in *Streptomyces rochei*." *Front. Microbiol.*, **11**, 1089 (2020).

[34] Arakawa K., Kodama K., Tatsuno S., Ide S. and Kinashi H. "Analysis of the loading and hydroxylation steps in lankamycin biosynthesis in *Streptomyces rochei*." *Antimicrob. Agents Chemother.*, **50**, 1946–1952 (2006).

[35] Suzuki T., Mochizuki S., Yamamoto S., Arakawa K. and Kinashi H. "Regulation of lankamycin biosynthesis in *Streptomyces rochei* by two SARP genes, *srrY* and *srrZ*." *Biosci. Biotechnol. Biochem.*, **74**, 819–827 (2010).

[36] Ishikawa J., Niino Y. and Hotta K. “Construction of pRES18 and pRES19, *Streptomyces-Escherichia coli* shuttle vectors carrying multiple cloning sites.” *FEMS Microbiol. Lett.*, **145**, 113–116 (1996).

[37] Arakawa K., Sugino F., Kodama K., Ishii T. and Kinashi H. “Cyclization mechanism for the synthesis of macrocyclic antibiotic lankacidin in *Streptomyces rochei*.” *Chem. Biol.*, **12**, 249–256 (2005)

[38] Bourguignon J. J. and Wermuth C.G. “Lactone chemistry. Synthesis of β-substituted, γ-functionalized butanolides and butenolides and succinaldehydic acids from glyoxylic Acid.” *J. Org. Chem.* **46**, 4889–4894 (1981).

[39] Feringa B.L., de Lange B. and de Jong J.C. “Synthesis of enantiomerically pure γ-(menthyloxy) butenolides and (*R*)- and (*S*)-2-methyl-1,4-butanediol.” *J. Org. Chem.*, **54**, 2471–2475 (1989).

[40] Ohtani I., Kusumi T., Kashman Y. and Kakisawa H. “High-field FT NMR application of Mosher’s method. The absolute configurations of marine terpenoids.” *J. Am. Chem. Soc.*, **113**, 4092–4096 (1991).

[41] Yamauchi Y., Nindita Y., Hara K., Umeshiro A., Yabuuchi Y., Suzuki T., Kinashi H. and Arakawa K. “Quinoprotein dehydrogenase functions at the final oxidation step of lankacidin biosynthesis in *Streptomyces rochei* 7434AN4.” *J. Biosci. Bioeng.*, **126**, 145–152 (2018).

[42] Tamura M. and Kochi J. “Coupling of Grignard reagents with organic halides.” *Synthesis*, **3**, 303–305 (1971).

[43] Arakawa K., Eguchi T. and Kakinuma K. “Specific deuterium labeling of archaeal 36-membered macrocyclic diether lipid.” *Bull. Chem. Soc. Jpn.*, **71**, 2419–2426 (1998).

[44] Sakuda S., Higashi A., Tanaka S., Nihira T. and Yamada Y. “Biosynthesis of virginiae butanolide, a butyrolactone autoregulator from *Streptomyces*.” *J. Am. Chem. Soc.*, **114**, 663–668 (1992).

[45] Niehs S. P., Kumpfmuüller J., Dose B., Little R. F., Ishida K., Florez L. V., Kaltenpoth M. and Hertweck C. “Insect-associated bacteria assemble the antifungal butenolide gladiofungin by non-canonical polyketide chain termination.” *Angew. Chem. Int. Ed. Engl.*, **59**, 23122-23126 (2020).

[46] Nakou I. T., Jenner M., Dashti Y., Romero-Canelón I., Masschelein J., Mahenthiralingam E., and Challis G. L. “Genomics-driven discovery of a novel glutarimide antibiotic from *Burkholderia gladioli* reveals an unusual polyketide synthase chain release mechanism.” *Angew.Chem. Int. Ed.*, **59**, 23145–23153 (2020).

[47] Ōmura S. “Macrolide Antibiotics: Chemistry, Biology, and Practice.” *Academic Press*, New York, USA (2002).

[48] Trefzer A., Salas J. A., and Bechthold A. “Genes and enzymes of deoxy-sugar biosynthesis.” *Nat. Prod. Rep.*, **16**, 283-99 (1999).

[49] Gäumann E, Hütter R, Keller-Schierlein W., Neipp L., Prelog V. and Zähner H. “Lankamycin und lankacidin.” *Helv. Chim. Acta*, **43**, 601-606（1960).

[50] Harada S., Higashide E., Fugono T. and Kishi T. “Isolation and structures of T-2636 antibiotics.” *Tetrahedron Lett.*, **10**, 2239-2244 (1969).

[51] Ayoub A. T., El-Magd R. M. A., Xiao J., Lewis C. W., Tilli T. M., Arakawa K., Nindita Y., Chan G., Sun L., Glover M., Klobukowski M. and Tuszynski J. “Antitumor activity of lankacidin antibiotics is due to microtubule stabilization via a paclitaxel-like mechanism.” *J. Med. Chem.*, **59**, 9532–9540 (2016).

[52] Ayoub A. T., Elrefaiy M. A. and Arakawa K. “Computational prediction of the mode of binding of antitumor lankacidin C to tubulin.” *ACS Omega.*, **4**, 4461–4471 (2019).

[53] Auerbach T., Mermershtain I., Davidovich C., Bashan A., Belousoff M., Wekselman I., Zimmerman E., Xiong L., Klepacki D., Arakawa K., Kinashi H., Mankin A. S. and Yonath A. “The structure of ribosome-lankacidin complex reveals ribosomal sites for synergistic antibiotics.” *Proc. Natl. Acad. Sci. USA*, **107**, 1983–1988 (2010).

[54] Belousoff M. J., Shapira T., Bashan A., Zimmerman E., Rozenberg H., Arakawa K., Kinashi H. and Yonath A. “Crystal structure of the synergistic antibiotic pair, lankamycin and lankacidin, in complex with the large ribosomal subunit.” *Proc. Natl. Acad. Sci. USA*, **108**, 2717–2722 (2011).

[55] Arakawa K., Suzuki T. and Kinashi H. “Gene disruption analysis of two glycosylation steps in lankamycin biosynthesis in *Streptomyces rochei*.” *Actinomycetol*, **22**, 35-41 (2008).

[56] Arakawa K. “Genetic and biochemical analysis of the antibiotic biosynthetic gene clusters on the *Streptomyces* linear plasmid.” *Biosci. Biotechnol. Biochem.*, **78**, 183–189 (2014).

[57] Agematu H., Matsumoto N., Fujii Y., Kabumoto H., Doi S., Machida K., Ishikawa j. and Arisawa A. “Hydroxylation of testosterone by bacterial cytochromes P450 using the *Escherichia coli* expression system.” *Biosci. Biotechnol. Biochem.*, **70**, 307-311 (2006).

[58] Teshima A., Hadae N., Tsuda N. and Arakawa K. “Functional analysis of P450 monooxygenase SrrO in the biosynthesis of butenolide-type signaling molecules in *Streptomyces rochei*.” *Biomolecules*, **10**, 1237 (2020).

[59] Arakawa K., Cao Z., Suzuki N. and Kinashi H. “Isolation, structural elucidation, and biosynthesis of 15-norlankamycin derivatives produced by a type-II thioesterase disruptant of *Streptomyces rochei*.” *Tetrahedron*, **67**, 5199-5205 (2011).

[60] Andersen J.F. and Hutchinson C.R. “Characterization of *Saccharopolyspora erythraea* cytochrome P-450 genes and enzymes, including 6-deoxyerythronolide B hydroxylase.” *J. Bacteriol.*, **174**, 725-735 (1992).

[61] Haydock S. F., Dowson J. A., Dhillon N. Roberts G. A., Cortes J. and Leadlay P. F. “Cloning and sequence analysis of genes involved in erythromycin biosynthesis in *Saccharopolyspora erythraea*: sequence similarities between EryG and a family of S-adenosylmethionine-dependent methyltransferases.” *Mol. Gen. Genet.*, **230**, 120-128 (1991).

[62] Weber J. M., Leung J.O., Swanson S. J., Idler K. B. and McAlpine J. B. "An erythromycin derivative produced by targeted gene disruption in *Saccharopolyspora erythraea*." *Science*, **252**, 114-117 (1991).

[63] Guengerich F. P. "Common and uncommon cytochrome P450 reactions related to metabolism and chemical toxicity." *Chem. Res. Toxicol.*, **14**, 611-650 (2001).

[64] Ortiz de Montellano P. R. "Cytochrome P450: Structure, Mechanism and Biochemistry, 3rd ed." *Kluwer Academic Press/Plenum*, New York, USA (2005).

[65] Liu G., Chater K. F., Chandra G., Niu G. and Tan H. "Molecular regulation of antibiotic biosynthesis in *Streptomyces*." *Microbiol. Mol. Biol. Rev.*, **77**, 112–143 (2013).

[66] Martín J. F. and Liras P. "Harnessing microbiota interactions to produce bioactive metabolites: Communication signals and receptor proteins." *Curr. Opin. Pharmacol.*, **48**, 8–16 (2019).

[67] Thao N. B., Kitani S., Nitta H., Tomioka T. and Nihira T. "Discovering potential *Streptomyces* hormone producers by using disruptants of essential biosynthetic genes as indicator strains." *J. Antibiot.*, **70**, 1004-1008 (2017).

[68] Li S., Chaulagain M. R., Knauff A. R., Podust L. M.,Montgomery J. and Sherman D. H. "Selective oxidation of carbolide C–H bonds by an engineered macrolide P450 mono-oxygenase." *Proc. Natl. Acad. Sci. USA*, **106**, 18463-18468 (2009).

公表論文

(1) Functional analysis of P450 monooxygenase SrrO in the biosynthesis of butanolide-type signaling molecules in *Streptomyces rochei*
Aiko Teshima, Nozomi Hadae, Naoto Tsuda, and Kenji Arakawa
Biomolecules, **10**(9), 1237 (2020).
DOI : 10.3390/biom10091237

(2) Substrate specificity of two cytochrome P450 monooxygenases involved in lankamycin biosynthesis
Aiko Teshima, Hisashi Kondo, Yu Tanaka, Yosi Nindita, Yuya Misaki, Yuji Konaka, Yasuhiro Itakura, Tsugumi Tonokawa, Haruyasu Kinashi, and Kenji Arakawa
Bioscience, Biotechnology, and Biochemistry, **85**(1), 115-125 (2021).
DOI : 10.1093/bbb/zbaa063

参考論文

(1) The genome sequence of *Streptomyces rochei* 7434AN4, which carries a linear chromosome and three characteristic linear plasmids.
Yosi Nindita, Zhisheng Cao, Amirudin Akhmad Fauzi, Aiko Teshima, Yuya Misaki, Rukman Muslimin, Yingjie Yang, Yuh Shiwa, Hirofumi Yoshikawa, Michihira Tagami, Alexander Lezhava, Jun Ishikawa, Makoto Kuroda, Tsuyoshi Sekizuka, Kuninobu Inada, Haruyasu Kinashi, and Kenji Arakawa
Scientific Reports, **9**, 10973 (2019).
DOI : 10.1038/s41598-019-47406-y